



Alphonsus V. Pocius

# **Adhesion and Adhesives Technology**

An Introduction

3<sup>rd</sup> Edition

Hanser Publishers, Munich

**HANSER**

Hanser Publications, Cincinnati

*The Author:*

Dr. Alphonsus V. Pocius,  
445 Highpoint Curve South, Maplewood, MN 55119-6754, USA

Distributed in North and South America by:

Hanser Publications  
6915 Valley Avenue, Cincinnati, Ohio 45244-3029, USA  
Fax: (513) 527-8801  
Phone: (513) 527-8977  
www.hanserpublications.com

Distributed in all other countries by

Carl Hanser Verlag  
Postfach 86 04 20, 81631 München, Germany  
Fax: +49 (89) 98 48 09  
www.hanser.de

The use of general descriptive names, trademarks, etc., in this publication, even if the former are not especially identified, is not to be taken as a sign that such names, as understood by the Trade Marks and Merchandise Marks Act, may accordingly be used freely by anyone. While the advice and information in this book are believed to be true and accurate at the date of going to press, neither the author nor the editors nor the publisher can accept any legal responsibility for any errors or omissions that may be made. The publisher makes no warranty, express or implied, with respect to the material contained herein.

Library of Congress Cataloging-in-Publication Data

Pocius, Alphonsus V.

Adhesion and adhesives technology : an introduction / Alphonsus V. Pocius.

-- 3rd ed.

p. cm.

Includes bibliographical references and index.

ISBN 978-1-56990-511-1 (hardcover) -- ISBN 978-3-446-43177-5 (e-book)

1. Adhesion. 2. Adhesives. 3. Chemistry, Physical and theoretical. I.

Title.

QC183.P72 2012

668'.3--dc23

2012007729

Bibliografische Information Der Deutschen Bibliothek

Die Deutsche Bibliothek verzeichnet diese Publikation in der Deutschen Nationalbibliografie; detaillierte bibliografische Daten sind im Internet über <<http://dnb.d-nb.de>> abrufbar.

ISBN 978-1-56990-511-1

E-Book ISBN 978-3-446-43177-5

All rights reserved. No part of this book may be reproduced or transmitted in any form or by any means, electronic or mechanical, including photocopying or by any information storage and retrieval system, without permission in writing from the publisher.

© Carl Hanser Verlag, Munich 2012

Production Management: Steffen Jörg

Coverconcept: Marc Müller-Bremer, [www.rebranding.de](http://www.rebranding.de), München

Coverdesign: Stephan Rönigk

Typesetted by Manuela Treindl, Fürth

Printed and bound by CPI buch bücher.de gmbh

Printed in Germany

*This book is dedicated to my wife, Janice,  
to whom I owe everything, including my life which she helped save.  
The book is also dedicated to our children:  
our son Nick, his wife Eliza, our daughter Amanda,  
and our grandson, Vincent James*

# Preface

Adhesion science is a multidisciplinary field, which encompasses aspects of engineering as well as physical and organic chemistry. The breadth of the field is possibly the reason that there have been so few books on the subject written by a single author. The books in this area have tended to be handbooks, treatises, or other compilations by multiple authors. I have attempted to provide a broad view of the field, but with a consistent style, that leads the reader from one step to another in the understanding of the science. This book also includes problems for the student to work in order to help build on the information presented in the text.

The text assumes that the reader has little or no knowledge of the science of adhesion. The bulk of the book is written with the supposition that the reader has had a course in college level calculus as well as college level organic and physical chemistry. The book has also been written in such a fashion that even a person that has a meager knowledge of these subjects can learn something about adhesion science from reading this book. That is, the emphasis is on *understanding* the science rather than a complete and detailed exposition on any part of it. An attempt has been made to describe as much as possible in words and examples rather than in detailed mathematical derivations. That mathematics has been included in those sections where more detail seemed necessary. Each section or chapter starts with a simple view of the subject area, starting at the same point an entry-level textbook would begin. Each section or chapter then builds to a point at which more detail is available for the reader who is or wants to be a practitioner of the art and science of adhesion. Many sections also includes helpful practical suggestions about how measurements can be made, how surfaces can be modified, or how adhesives can be formulated to lead to a useful result. The third edition of this book includes a number of new topics such as the durability of structural adhesive bonds and adhesion in biological systems. The wish of the author is to produce a well-rounded introductory view of each of the fields, which form adhesion science no matter what the technical background of the reader may be. As science progresses, our understanding of natural phenomena changes. This book also includes news aspects of the understanding of adhesion science, in particular the connection between fundamental adhesion and the practical adhesive bond strengths of adhesive bonds is expanded upon.

I would like to acknowledge some of the people at 3M who have assisted me either by reviewing this manuscript or by providing support to pursue my study of the science of adhesion. These people include Sam Smith, Bill Schultz, Dave Wangsness, Ted Valentine, Brian Smillie, Dick Hartshorn, Don Theissen, George Allen, Tom Savereide, Morgan Tamsky, Larry Clemens, Rich Newell, Mike Engel, Ilya Gorodisher, Chris Campbell, Zhong Chen and Terry Smith. Without their friendship and support, it is doubtful that I would have had the opportunity to build the base of expertise necessary to prepare a book this book. I would also like to acknowledge the late Prof. Bob Kooser at Knox College who inspired me to pursue a career in physical chemistry.

*Al Pocius*

# Contents

<b>Preface</b> .....	VII
<b>1 Introduction</b> .....	1
1.1 Introduction and Chapter Objectives .....	1
1.2 Basic Definitions .....	2
1.3 Advantages and Disadvantages of Adhesive Bonding .....	2
1.4 Uses of Adhesive Bonding in Modern Industry .....	6
1.5 Economics of Adhesive Technology .....	12
1.6 Literature and Other Sources of Information .....	12
1.7 Summary .....	14
References .....	15
<b>2 The Mechanical Properties of Materials as They Relate to Adhesion</b> .....	17
2.1 Introduction .....	17
2.2 Definition of Mechanical Stresses for Materials Testing .....	17
2.3 Stress-Strain Plots and the Definition of Materials Property Parameters .....	19
2.3.1 Tensile Forces .....	19
2.3.2 Shear Forces .....	22
2.3.3 Strain Energy Density .....	23
2.4 Introduction to Linear Elastic Fracture Mechanics .....	24
2.5 Introduction to Rheology of Liquids .....	27
2.6 Introduction to Linear Viscoelasticity .....	29
2.7 An Application of Materials Properties and Mechanics: The Bending of Beams .....	35
2.8 Summary .....	43
Bibliography .....	43
Problems and Review Questions .....	44

<b>3 Mechanical Tests of Adhesive Bond Performance</b>	47
3.1 Introduction	47
3.2 Failure Modes and the Definition of Practical Adhesion	48
3.3 Tensile Testing of Adhesive Bonds	49
3.4 Shear Loading of Adhesive Bonds	52
3.4.1 The Standard Lap Shear Specimen	54
3.4.2 Variations on the Lap Shear Specimen	57
3.4.3 Specimen for Determining the True Shear Properties of an Adhesive	60
3.4.4 The Goland-Reissner Analysis of the Lap Shear Specimen	61
3.5 Cleavage Loading of Adhesive Bonds	68
3.5.1 Cleavage or Fracture Specimens	69
3.5.1.1 Double Cantilever Beam Specimens	70
3.5.1.2 Linear Elastic Fracture Mechanics Applied to the Double Cantilever Beam Specimen	71
3.5.2 Blister Test	73
3.5.3 Compact Tension Test	74
3.5.4 Wedge Test	74
3.6 Peel Tests	75
3.6.1 Stress Analysis in a Peel Specimen	78
3.7 Summary	82
Bibliography	82
References	82
Problems and Review Questions	83
<b>4 The Basics of Intermolecular Forces and Surface Science</b>	85
4.1 Introduction	85
4.2 Fundamental Forces	86
4.2.1 Electrostatic Forces	87
4.2.2 van der Waals Interactions	88
4.2.2.1 Dipole–Dipole Interactions	89
4.2.2.2 Dipole-Induced Dipole	90
4.2.2.3 Dispersion Forces	91
4.2.3 Interactions through Electron Pair Sharing	93
4.2.4 Repulsive Forces	93
4.3 Surface Forces and Surface Energy	94
4.4 Work of Cohesion and Adhesion	99
4.5 Methods of Measurement of Surface Energy and Related Parameters	101
4.5.1 Surface Tension	101
4.5.1.1 Drop Weight/Volume Method	102



4.5.1.2	Du Nuoy Tensiometer.....	102
4.5.2	Surface Energy of Solids.....	102
4.5.2.1	Contact Angle Methods.....	103
4.5.2.2	Contact Mechanics and Direct Measurement of Solid Surface Energy.....	105
4.6	Surface Thermodynamics and Predictions of Surface and Interfacial Tensions.....	112
4.6.1	The Good-Girifalco Relationship.....	114
4.6.2	The Fowkes Hypothesis and Fractional Polarity.....	115
4.6.3	The Zisman Plot.....	117
4.6.4	Modern Application of Contact Angle Measurements.....	118
4.7	Modern Methods of Surface Analysis.....	120
4.7.1	Modern Methods for Analysis of the Chemistry of Surfaces.....	120
4.7.2	Topological Methods of Surface Analysis.....	122
4.8	Summary.....	123
	Bibliography.....	124
	References.....	124
	Problems and Review Questions.....	126
<b>5</b>	<b>Basic Physico/Chemical Properties of Polymers.....</b>	<b>129</b>
5.1	Introduction.....	129
5.2	Basic Terminology.....	130
5.2.1	Monomers versus Polymers.....	130
5.2.2	Basic Types of Polymeric Materials.....	130
5.2.3	Molecular Weight.....	132
5.3	Thermal Transitions of Polymers.....	134
5.3.1	Measurement of $T_g$ .....	135
5.4	Dynamic Mechanical Measurements and Viscoelasticity.....	136
5.4.1	Methods of Measurement of Dynamic Mechanical Properties.....	136
5.4.2	Examples of Dynamic Mechanical Data for Polymers.....	138
5.5	Time-Temperature Superposition.....	142
5.6	Summary.....	144
	Bibliography.....	144
	References.....	144
<b>6</b>	<b>The Relationship of Surface Science and Adhesion Science.....</b>	<b>145</b>
6.1	Introduction.....	145
6.2	Rationalizations of Adhesion Phenomena.....	145
6.3	Electrostatic Theory of Adhesion.....	146

6.4	Diffusion Theory of Adhesion.....	149
6.4.1	Diffusive Adhesive Bonding and Block Copolymers at Interfaces .....	152
6.5	Mechanical Interlocking and Adhesion.....	155
6.5.1	Kinetics of Pore Penetration.....	158
6.6	Wettability and Adhesion.....	160
6.7	Acid-Base Interactions at Interfaces.....	163
6.8	Covalent Bonding at Interfaces .....	166
6.8.1	Coupling Agents .....	168
6.9	The Relationship of Fundamental Forces of Adhesion and Practical Adhesion.....	170
6.10	The Weak Boundary Layer.....	175
6.11	Summary .....	176
	Bibliography .....	176
	References .....	177
	Problems and Review Questions .....	178
<b>7</b>	<b>The Surface Preparation of Adherends for Adhesive Bonding.....</b>	<b>181</b>
7.1	Introduction.....	181
7.2	Plastic Surface Preparation.....	183
7.2.1	Corona Discharge Treatment.....	184
7.2.1.1	Corona Discharge Treatment of Polyethylene.....	185
7.2.1.2	Corona Discharge Treatment of Polypropylene .....	188
7.2.1.3	Corona Discharge Treatment of Poly(ethylene terephthalate) .....	189
7.2.1.4	Corona Discharge Treatment of Other Materials.....	190
7.2.2	Flame Treatment.....	191
7.2.3	Plasma Treatment.....	193
7.2.3.1	Plasma Treatment of PE .....	194
7.2.3.2	Plasma Treatment of Other Substrates.....	195
7.2.4	Other Physical Treatment Methods of Polymer Surfaces ....	197
7.2.4.1	Treatments Using Ultraviolet Radiation.....	197
7.2.4.2	Other Vacuum Methods of Surface Preparation.....	197
7.2.5	Wet Chemical Methods of Treatment of Polymer Surfaces...	198
7.2.5.1	Single Surface Chemical Functionalization and Chromic Acid Treatment of PE .....	198
7.2.5.2	Wet Chemical Surface Treatment of Poly(tetrafluoroethylene) .....	200
7.2.6	Priming of Polymer Surfaces .....	201
7.2.6.1	Priming of Polyolefins for Cyanoacrylates.....	201
7.2.6.2	Chlorinated Polyolefins .....	201

7.3	Metal Surface Preparation.....	202
7.3.1	Surface Preparation of Aluminum for Adhesive Bonding ....	203
7.3.1.1	The Forest Products Laboratory (FPL) Etch.....	203
7.4	Anodization Treatments for Adhesive Bonding of Aluminum .....	207
7.4.1	Mechanism of Anodization.....	208
7.4.2	Anodization Media .....	208
7.4.3	Phosphoric Acid Anodization in the Aerospace Industry ....	209
7.5	General Techniques for the Surface Preparation of Metals.....	211
7.5.1	Conversion Coatings.....	211
7.5.2	Abrasion.....	212
7.5.3	Electrochemical Methods for Treating Metals other than Aluminum .....	213
7.6	Summary .....	214
	Bibliography .....	214
	References .....	215
	Problems and Review Questions .....	217
<b>8</b>	<b>The Chemistry and Physical Properties of Structural Adhesives .....</b>	<b>219</b>
8.1	Introduction to Chapters 8–11 and 13.....	219
8.2	Introduction to Structural Adhesives .....	219
8.2.1	Physical Forms of Uncured Structural Adhesives .....	220
8.3	Chemistry of Base Resins Used in Structural Adhesives .....	222
8.3.1	Phenolics .....	222
8.3.2	Proteins .....	225
8.3.3	Epoxy Resins .....	226
8.3.3.1	Time-Temperature-Transformation Diagrams and the Cure of Epoxy Resins .....	230
8.3.4	Urethane Resins .....	232
8.3.5	Acrylics .....	234
8.3.6	High Temperature Performance Structural Adhesives .....	237
8.4	Formulation of Structural Adhesives for Optimum Performance .....	240
8.4.1	Formulation of Phenolic Resins .....	240
8.4.2	Epoxy Resins .....	243
8.4.3	Acrylics .....	250
8.4.4	High Temperature Performance Structural Adhesives .....	253
8.5	Summary .....	255
	Bibliography .....	255
	References .....	255
	Problems and Review Questions .....	257

<b>9 Durability of Structural Adhesive Bonds</b> .....	259
9.1 Introduction .....	259
9.2 Methods of Examining Durability of Structural Adhesive Bonds .....	259
9.3 Mechanisms of Durability Failure of Adhesive Bonds .....	262
9.4 Methods Used to Predict Durability .....	268
9.5 Summary .....	269
References .....	271
<b>10 The Chemistry and Physical Properties of Elastomer-Based Adhesives</b> ...	273
10.1 Introduction .....	273
10.2 Pressure-sensitive Adhesives .....	273
10.2.1 Chemistry of the Base Resins Used in PSAs .....	274
10.2.2 Chemistry of Tackifiers .....	277
10.2.2.1 Natural Product Based Tackifiers .....	277
10.2.2.2 Petroleum Based Tackifiers .....	278
10.2.2.3 Other Tackifiers .....	280
10.2.3 Testing of Pressure-sensitive Adhesives .....	281
10.2.3.1 Measurements of Tack .....	281
10.2.3.2 Measurement of Peel .....	283
10.2.3.3 Measurement of Shear .....	285
10.2.4 Balance of Properties .....	286
10.2.5 PSA Performance Viewed as a Time Scale in Viscoelastic Response .....	287
10.2.6 PSA Viscoelasticity and Tack .....	287
10.2.7 PSA Peel and Viscoelasticity .....	291
10.2.8 Shear and Creep Behavior of PSAs .....	294
10.2.9 Summary .....	295
10.3 Rubber-Based, Contact Bond and other Elastomeric Adhesives .....	296
10.3.1 Formulation of RBAs .....	296
10.3.2 Base Polymers .....	297
10.3.3 Tackifiers .....	299
10.3.4 Pigments and Fillers .....	299
10.3.5 Crosslinking/Vulcanization of RBAs .....	300
10.3.6 Solvents .....	301
10.3.7 Elastomeric Adhesives, Sealants and Release Coatings Based upon Silicone Chemistry .....	302
10.4 Summary .....	305
Bibliography .....	305
References .....	305
Problems and Review Questions .....	306

<b>11 Thermoplastic, Pseudothermoplastic, and Other Adhesives .....</b>	<b>307</b>
11.1 Introduction .....	307
11.2 Hot Melt Adhesives .....	307
11.2.1 Introduction .....	307
11.2.2 Polymer Physical Properties and Hot Melt Adhesives .....	308
11.2.3 Formulation of Hot Melt Adhesives .....	311
11.2.4 Synthetically Designed Hot Melt Adhesives .....	315
11.2.5 Curing Hot Melts .....	319
11.3 Polyvinyl Acetate-Based Adhesives .....	320
11.4 Polyvinyl Acetal Adhesives .....	321
11.5 Thermoplastic or Pseudo-thermoplastic Adhesives based upon Natural Products .....	321
11.5.1 Starches .....	322
11.5.2 Cellulosics .....	322
11.6 Summary .....	323
Bibliography .....	324
References .....	324
<b>12 Adhesion in Biological Systems .....</b>	<b>325</b>
12.1 Introduction .....	325
12.2 Adhesion in Microbiological Systems .....	325
12.3 Biofilm Formation .....	326
12.4 Growth Stages of Biofilms .....	327
12.4.1 Attachment to a Surface .....	327
12.4.2 Irreversible Attachment of Bacteria .....	327
12.4.3 Maturation Phase .....	328
12.4.4 Biofilm Dispersal .....	328
12.5 Maintenance or Elimination of Biofilms .....	329
12.6 Adhesion in the Cling Ability of the Tokai Gecko .....	330
12.6.1 Attempts to Artificially Produce the Gecko Features and Adhesive Ability .....	333
12.7 Summary .....	335
References .....	335
<b>13 The Basis for Adhesive Bond Design .....</b>	<b>337</b>
13.1 Introduction .....	337
13.2 Chemistry and Mechanical Properties of Adhesives .....	337
13.3 Application Criteria .....	340
13.4 Interfaces and Surface Preparations .....	343
13.5 Miscellaneous Concerns .....	344

13.6 Basic Criteria for the Design of an Adhesive Bond ..... 346

    13.6.1 Hart-Smith Design Criteria for Double Lap Joints ..... 347

13.7 Summary ..... 351

References ..... 351

Problems and Review Questions ..... 352

**Answer Key ..... 353**

**Subject Index ..... 365**

# 4

## The Basics of Intermolecular Forces and Surface Science

### ■ 4.1 Introduction

In the previous chapters we have concerned ourselves with the mechanics of adhesive bonds. The discussion assumed that the interface or interphase of the adherend and adhesive was perfectly capable of transferring stress from the first to the second and so on. The phenomenon by which the adhesive takes up stress from the adherend is known as *adhesion*. Adhesion is a physical phenomenon resulting from the same attractive forces which bind atoms together to make molecules and molecules together to make liquids and solids. To understand adhesion, we must first understand the forces existing between atoms or molecules and then apply that knowledge to what occurs at surfaces and within interphases. In this chapter, we first discuss the forces binding atoms and molecules together. These concepts are familiar to those who have taken freshman chemistry and the mathematics employed are understandable to those who have taken college level physical chemistry. Enough explanatory material is provided so that understanding of the mathematics is not necessary to develop an understanding of the phenomena. Observable surface chemical phenomena are described in terms of these basic physical forces. In Chapter 6, surface chemical phenomena are related to adhesion phenomena. Guidelines for good adhesion needed for the design of reliable adhesive bonds are given in Chapter 6, as well.

The objectives of this chapter are to develop or review information on the physical forces binding atoms or molecules together to make liquids and solids. This knowledge should naturally lead to an understanding of the physical basis for surface energy. Methods used to measure surface energy of materials as well as modern methods for determining their surface chemistry are discussed. In particular, contact angle measurements and how they play a role in surface science is emphasized. In addition, thermodynamics, force balances and the measurement of adhesion through the surface forces apparatus are discussed.

## ■ 4.2 Fundamental Forces

A basic tenant of physics is that all natural phenomena can be described when all of the forces between bodies and their energy states are described. Physical forces in nature range from nuclear forces that bind protons and neutrons in an atom's nucleus to gravitational forces that control the motion of celestial bodies. Gravitational forces are, for the most part, unimportant in the study of adhesion. Gravitational forces can play a role in the wetting of an adhesive or in the design of an adhesive bond. However, it is only those forces of a chemical nature that are important in understanding adhesion. The forces binding atoms to make molecules and molecules to make liquids and solids are most relevant in the study of adhesion. These topics are similar to the theory of solutions and the theories of the cohesive strength of materials.

There are several fundamental terms that need to be remembered or learned from basic physics before we can continue. The term *potential energy* has to do with the ability to do work. A rock sitting on a ledge has the *potential* to do work. *Work* is defined as a force times a distance. Thus, the work done by the rock falling off the ledge is the action of the gravitational force over the distance the rock falls. Once the rock has reached its final resting place, we say that the rock has a lower potential energy than it had before its fall and now it has less potential to do work. Mathematically,

$$W = F d \quad (4.1)$$

where  $W$  is work,  $F$  is the force and  $d$  is the distance over which the force acts. The work done is the difference in potential energy between the starting and resting positions of the system. If  $\Phi_1$  is the potential energy of the starting state and  $\Phi_2$  is the potential energy of the final state of the system,

$$W = \Phi_1 - \Phi_2 \quad (4.2)$$

This important equation indicates the relationship between potential energy and work. Throughout the next section we discuss various mathematical functions describing the potential energy of various interactions between molecules and atoms. From Eq. (4.1) and Eq. (4.2), and assuming  $\Phi_1 - \Phi_2$  is an infinitesimally small change such that it is equal to  $\delta\Phi$  and  $F$  is constant, then

$$\delta\Phi = \delta W = F \delta d \quad (4.3)$$

and

$$-\frac{\delta\Phi}{\delta d} = F \quad (4.4)$$



The force in a system can then be determined by differentiating the potential energy function by the distance over which the force acts. Similarly, the potential energy function can be determined by integrating a function describing the force with respect to the distance over which it acts. We use these simple physical concepts repeatedly in the next sections.

We also recall the laws of thermodynamics. The first law of thermodynamics states that the heat added to a system and the work done by a system changes the internal energy in a physical system. Mathematically, this is stated

$$\Delta E = q - w \quad (4.5)$$

where  $E$  is the internal energy in the system,  $q$  is the heat and  $w$  is the work. For our purposes, this means that the energy in a physical system depends upon how much mechanical or thermal energy is put into a system. In particular, it is important to remember that doing work on a system is the addition of internal energy to a system. Alternatively, if a system does work, its internal energy decreases. The second law of thermodynamics has to do with the disorder in a system. Entropy,  $S$ , is the measure of disorder. The second law of thermodynamics says that for a reversible process, the entropy in the universe stays constant. For an irreversible process, the entropy in the universe increases. This law can give us an insight into which physical processes happen spontaneously. In particular, when one combines the concepts of the internal energy,  $E$ , with the entropy,  $S$ , we obtain the free energy of the system. If the free energy of a system is negative, the process that the system is doing is spontaneous. The third law of thermodynamics states that entropy is zero for all pure elements and perfect crystals at the absolute zero of temperature. This provides a reference state for all chemical systems. For the purposes of this book, the laws of thermodynamics tell us that all physical systems tend to states that are lowest in potential energy and highest in entropy.

#### 4.2.1 Electrostatic Forces

The electrostatic force occurs between atoms or molecules that bear a charge. This force is also known as the Coulombic force. Particles bearing like electrical charges repel each other while particles bearing opposite electrical charges attract each other. The potential energy of interaction between atoms or molecules having a charge is given by the following equation:

$$\Phi^{\text{El}} = \frac{q_1 q_2}{4 \pi \epsilon r} \quad (4.6)$$

where  $q_i$  are the charges on the atoms or molecules (the charges have a positive or negative sign),  $\epsilon$  is the dielectric constant of the medium in which the charged

particles are found, and  $r$  is the distance between the atoms or molecules. If the particles have like charges, the energy of interaction is positive or repulsive. If the particles carry unlike charges, the potential energy is negative or attractive. We can calculate the force of interaction by taking the derivative of the potential energy with respect to distance:

$$\frac{d\Phi^{\text{El}}}{dr} = \frac{q_1 q_2}{4 \pi \epsilon r^2} \quad (4.7)$$

The electrostatic force is the strongest force of interaction (other than covalent bonding) between atoms or molecules. This force has been studied as a potential contributor to adhesion phenomena. However, not all adhesion phenomena can be explained by electrostatics. Electrostatic forces play a primary role in the formation of *ionic* bonds and ionic crystals. In an ionic crystal, such as NaCl, an electron has been transferred from sodium to chlorine. The resulting ions attract each other in a manner described by Coulomb's Law, which can (in turn) be used to calculate the lattice energy of ionic crystals. The energy required to break an ionic bond is very large, usually on the order of 100 kcal/mole or more. This number is important for comparison to the other forces of attraction discussed below.

#### 4.2.2 van der Waals Interactions

In standard freshman chemistry textbooks, the ideal gas is normally thoroughly discussed. The ideal gas law is stated as:

$$P V = n R T \quad (4.8)$$

where  $P$  is the pressure,  $V$  is the volume,  $n$  is the number of moles of gas,  $R$  is the gas constant, and  $T$  is the absolute temperature. It was noted early in the study of the physical properties of materials that most gases do not follow the perfect gas law exactly. One of the first attempts to describe the deviation of gases from the perfect gas law was the equation of state developed by J. D. van der Waals, a Dutch physicist who lived 1837–1923:

$$\left( P + \frac{a n^2}{V^2} \right) (V - b n) = n R T \quad (4.9)$$

$P$ ,  $V$ ,  $n$ ,  $R$  and  $T$  are as described above while the constants  $a$  and  $b$  are meant to describe the attractive and repulsive forces between gas atoms or molecules which the perfect gas law neglects. All of the forces leading gases to deviate from the perfect gas law are considered to be “van der Waals forces” [1]. We discuss each of these forces individually in the next sections.

### 4.2.2.1 Dipole–Dipole Interactions

Each element in the periodic table can be characterized by how much it attracts electrons. Thus, elements on the right hand side of the periodic table are said to be *electronegative* in comparison to the elements on the left-hand side of the periodic table. When atoms are bound together to make molecules, the electronegativity of the individual atoms acts to draw electrons towards those that are the most electronegative. Thus, a molecule such as  $\text{CF}_3\text{CH}_3$ , with the very electronegative fluorine atoms on one end of the molecule, has more of the electron density in the molecule residing more on one end than on the other. One could say that there was a partial charge on either end of the molecule. The  $\text{CF}_3$  side has a partial negative charge and correspondingly, the  $\text{CH}_3$  end has a partial positive charge. In terms of quantum mechanics, the probability function for the electron is greater in the region around the fluorine atoms than it is around the hydrogen atoms. This type of molecule, with a partial separation of charge is known as a *dipole*.

The dipole is characterized by the magnitude of the virtual charge on the ends of the molecule as well as by the distance separating the virtual charges. It is usual to draw a dipole as a dumbbell. The charges reside in the “balls” of the dumbbell. The handle of the dumbbell is the length separating the charges. The dipole is able to act in a mechanical way. If an interaction occurs between a singly charged species and a dipole, the opposite charges attract and the negative charges repel according to Coulomb’s Law. The line of action of this force is controlled by the “lever” holding the virtual charges together. A force acting on a lever in this way is a “moment” and for this situation, we can define a *dipole moment*,  $\mu$ :

$$\mu = q l \quad (4.10)$$

where  $q$  is the magnitude of the virtual charge, and  $l$  is the molecular length separating the charges.

Two dipoles can interact. The oppositely charged ends of the dipole attract and the similarly charged ends of the dipoles repel, thus changing the spatial orientation of one with respect to the other. Figure 4.1, shows such a situation. The potential energy of interaction of two dipoles becomes a matter of trigonometric analysis of charges and moments acting upon one another. This dipole-dipole potential energy of interaction is written as follows:

$$\Phi^P = \frac{\mu_1 \mu_2}{r^3} [2 \cos \theta_1 \cos \theta_2 - \sin \theta_1 \sin \theta_2 \cos(\phi_1 - \phi_2)] \quad (4.11)$$

where  $\mu_1$  and  $\mu_2$  are the dipole moments and  $r$  is the distance of separation of the centroids of the two dipole moments [2]. The angles are all shown in Fig. 4.1.

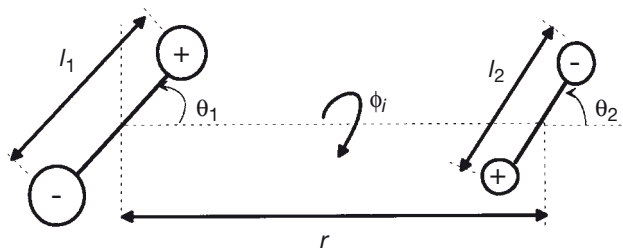


**FIGURE 4.1** Diagram showing the interaction between two dipoles. The interaction is specified by the angles of orientation as well as by the dipole moments of the two molecules

An important advancement concerning the understanding of dipolar species came with the work of Keesom [3]. He surmised that dipoles in a liquid or gas did not exist as species rigidly fixed with one another. Rather, if a liquid or a gas is at a temperature such that its thermal energy is greater than the rotational energy of the dipoles in that material, then the dipoles are free to rotate with respect to one another. The potential energy of interaction must be averaged over all values of  $\theta$  and  $\phi$  to provide a thermally averaged interaction. Keesom derived the following expression for the potential energy of interaction for rotating dipoles with an average thermal energy of  $kT$ , where  $k$  is Boltzmann's constant and  $T$  is the absolute temperature:

$$\Phi^{P,K} = -\frac{2 \mu_1^2 \mu_2^2}{3 k T r^6} \quad (4.12)$$

Other constants in the equation were described previously. An adhesive, when applied, is almost always a liquid and may be described by a Keesom potential, although it is somewhat dubious for us to assume that the interactions that occur between a solid adherend and a liquid adhesive would best be described this way. The Keesom potential may be a reasonable approximation.

#### 4.2.2.2 Dipole-Induced Dipole

In another type of van der Waals interaction between molecules, greater attention is given to the interaction of the electron clouds surrounding molecules. When a molecule with a spherical, symmetrical charge distribution encounters a dipole, we might expect no interaction between these molecules. However, this is not the case. There is a measurable interaction between the two molecules, called the *dipole-induced dipole* interaction. This interaction occurs because of the nature of electron probability distributions around the nuclei in a molecule. We know from atomic theory that electrons move in molecular orbitals and these molecular orbitals can interact with other charges, changing the probability distribution of the

electron in its orbital. Simply stated, the electrons in the spherical, symmetrical molecule see the dipole as two charges. The electrons are attracted to the positive end of the dipole and repelled by the negative end. This creates a dipole moment in the otherwise spherical, symmetrical molecule. We then have a dipole interacting with a dipole that was created by the first dipole's presence, hence the term *dipole-induced dipole interaction* [4]. The expression that describes the potential energy of the dipole-induced dipole interaction is as follows:

$$\Phi^I = -\frac{\mu_1^2 \alpha_2 + \mu_2^2 \alpha_1}{r^6} \quad (4.13)$$

in which the dipole moments,  $\mu_i$ , are as previously described and  $\alpha_i$  are the molecular polarizabilities. This expression is written as if each of the interacting molecules has a dipole moment and these dipoles act upon each other to further increase the dipole strength of the other molecule. If one of the molecules did not have a permanent dipole moment, then the expression is written:

$$\Phi^I = -\frac{\mu_1^2 \alpha_2}{r^6} \quad (4.14)$$

The quantity,  $\alpha$ , the polarizability, is a measure of how tightly the electrons are held by the atom or molecule and is roughly proportional to the molecular or atomic volume.

#### 4.2.2.3 Dispersion Forces

The final energy of interaction is fundamental to the study of adhesion and to the study of polymeric materials. Let us consider a situation in which two atoms or molecules with spherical charge distributions are brought near one another. Noble gases and molecules such as methane have spherical, symmetrical charge distributions. We might think that because they do not have a charge or a virtual separation of charge, that there would be no interaction between these two species. There is, however, a measurable interaction and it is found in all materials. A description of the source of this interaction stems naturally from the discussion on the dipole-induced dipole interaction. In a spherical, symmetrical charge distribution, there is a finite probability, at any one instant in time, that the electrons in an atom or molecule are all on one or the other side of the atom or molecule. If that is the case, then the atom or molecule has a partially unshielded nucleus or nuclei on one side and an excess of electrical charge on the other. This situation forms an *instantaneous dipole*, which can induce an instantaneous dipole in the other atom or molecule with a spherical charge distribution. The result is a net potential energy of interaction that leads to an attraction between these two atoms or molecules.

Because of the instantaneous nature of this interaction, its magnitude can be expected to be small. The expression that describes the potential energy of interaction between two atoms or molecules acting through *instantaneous dipole-induced instantaneous dipole* interaction is:

$$\Phi^D = -\frac{3}{4} \left( \frac{\alpha_1^2 C_1}{r^6} \right) \approx -\frac{3}{4} \left( \frac{\alpha_1^2 I_1}{r^6} \right) \quad (4.15)$$

and

$$\Phi_{12}^D = -\frac{3}{4} \frac{\alpha_1 \alpha_2}{r_{12}^6} \left( \frac{2 C_1 C_2}{C_1 + C_2} \right) \approx -\frac{3}{4} \frac{\alpha_1 \alpha_2}{r_{12}^6} \left( \frac{2 I_1 I_2}{I_1 + I_2} \right) \quad (4.16)$$

The first expression is for the interaction of like atoms or molecules, while the second expression is for unlike atoms or molecules. In the above expressions, the quantities  $\alpha_i$  are the polarizabilities as described above, the  $C_i$  are molecular constants which can be approximated by the  $I_i$ , which are the ionization potentials for atom or molecule  $i$ . This potential energy of interaction is given the symbol  $\Phi^D$  where  $D$  stands for dispersion force interaction. The name dispersion force comes from the relationship of this force to the dispersion of light in the visible and ultraviolet regions of the spectrum. Inherently, “dispersion force” does not accurately describe this phenomenon and may be misleading. However, the literature has adopted this name to describe the instantaneous dipole-induced dipole force.

Upon examination of the equations for the dispersion force potential energy, we can see three things. First, the interaction is directly dependent upon the polarizability of each of the interacting species. Thus, atoms or molecules that have loosely held electrons (loosely held electrons are more easily displaced in an electric field) have large dispersion force interactions in comparison to those molecules that have tightly held electrons. Second, the dispersion force interaction is dependent upon the first ionization potential for the species. Third, the dispersion force interaction is inversely dependent upon the sixth power of the distance separating the two species. The interacting species must be close together for this potential energy of interaction to have any effect. This should be compared to the Coulombic potential energy of interaction which is dependent upon the inverse first power of distance. In charge-charge interactions, the action is over long distances.

The detailed description of the dispersion force interaction between surfaces is based on quantum electrodynamics that is outside of the scope of this book. The theory most often cited is that of Lifschitz [5]. The Lifschitz theory is somewhat difficult and the reader is referred to the useful explanation by Grimley [6]. Israelachvili [7] provides methodology to approximate the measurements needed to calculate the dispersion force interaction between two bodies.

### 4.2.3 Interactions through Electron Pair Sharing

The final interaction that can take place between two atoms or molecules is the formation of a chemical bond through the sharing of an electron pair. We call these “chemical bonds” to distinguish them from “physical bonds” formed by van der Waals interactions or ionic bonds formed by the interaction of two charged species. The types of chemical bonds formed by electron pair sharing fall into two broad categories: *covalent bonding* and *donor-acceptor interactions*. In covalent bonding, molecular species are formed by sharing of electron pairs. The electrons, originally centered on one atom or part of one molecule, are now shared by the atoms in the new molecule. The description of the interaction of atoms or molecules to form new molecules is not a simple one. It requires knowledge of quantum mechanics that is outside the scope of this book.

Covalent bonds are most often described in organic chemistry. Coordinate covalent bonding is a variation of covalent bonding in that a metal atom, usually an ion, acts as an *acceptor*, receiving electron pairs from ligands that are *donor* molecules. Reactions between transition metal ions and amines are examples of coordinate covalent bonding. This form of bonding can also be considered a subset of reactions known as *donor-acceptor* interactions, in which electron pairs are partially shared between atoms or between atoms and molecules.

Another particularly important subset of donor-acceptor interactions is *acid-base* interactions. These interactions include the well-known Bronsted-Lowrey reactions in which a base (e.g., NaOH) reacts with an acid (e.g.,  $\text{H}_2\text{SO}_4$ ) to give a salt (e.g.,  $\text{Na}_2\text{SO}_4$ ) and water. The reactions of Lewis acid-bases, such as antimony pentafluoride (a Lewis acid) with ammonia (a Lewis base), are also examples. The key feature of Lewis acid-base reactions is that Lewis acids are electron deficient and Lewis bases have a non-bonded electron pair. Acid-base interactions have recently become very popular for describing observed adhesion phenomena. It should be clearly noted, however, that acid-base interactions are just one of a set of interactions that can take place between atoms and molecules and are not a fundamental force of nature. We discuss each of these interactions and how they may play a role in the understanding of adhesion phenomena in ensuing sections.

### 4.2.4 Repulsive Forces

We have laid the groundwork describing the interactions between atoms or molecules through the interaction of their electron clouds and nuclei. However, remember that electrons are negatively charged particles. If two electron clouds come close enough together, the electrons see each other for what they are. When atoms or

molecules come very near each other, there is a repulsion of their respective electron clouds and a resulting repulsion of the atoms or molecules. The equations described earlier all show potential energies of interaction which vary with the inverse power of distance to the sixth power or less. In comparison to repulsive forces, these are long range interactions. To describe repulsive forces, the inverse distance must be raised to a much higher power to signify just how short range these interactions are. One of the earliest and most famous potential energy expressions proposed to describe the interactions between atoms or molecules was developed by Lennard-Jones [8], specifically:

$$\Phi^{L-J} = -\frac{A}{r^6} + \frac{B}{r^{12}} \quad (4.17)$$

In this expression,  $A$  is a constant that scales the attractive interactions while  $B$  is a constant that scales the repulsive interactions. The attractive potential is written as the reciprocal sixth power of distance. If we compare this expression with those written above for the various van der Waals interactions, we find that all of them depend on distance to the reciprocal sixth power. The repulsive interaction is very short range in that the reciprocal is raised to the twelfth power of distance. This expression allows us to at least infer the effect of the various attractive constants on things having to do with surfaces. A Lennard-Jones force can also be calculated by taking the derivative of the potential with respect to distance as follows:

$$F^{L-J} = \frac{-d\Phi^{L-J}}{dr} = -\frac{6A}{r^7} + \frac{12B}{r^{13}} \quad (4.18)$$

This expression plays a role in our calculation of the interaction of two surfaces.

### ■ 4.3 Surface Forces and Surface Energy

Surfaces abound in nature. Surfaces and interfaces are the demarcations between various states of matter, between different chemical entities, and between aggregates of those chemical entities, such as materials and living things. Materials, especially liquids, exhibit easily observable surface forces. If you attempt to slowly push a probe through the surface of a pure liquid such as water, you encounter a resistance that is a manifestation of surface forces. In nature, surface forces allow insects to walk on water, for example. Interfacial forces induce the phenomenon of capillary rise which, when accompanied by transpiration, allows fluids to be transported from the roots to the tops of trees. The fact that liquids have a surface energy is



also demonstrated by a simple thought experiment. We know, for example, that all things in nature tend to their lowest available energy state. A finely divided liquid, when suspended in another medium, assumes a spherical shape. Why?

Liquids have an extra energy associated with the surface. Spheres have the lowest possible surface area of any three-dimensional object. Since all things tend to their lowest energy state, liquid droplets tend to be spherical (in the absence of gravitational distortion of shape) so that the energy associated with having a surface is minimized. Understanding surfaces and surface energetics is an important part of understanding adhesion and adhesives. It is the interfacial region that plays a crucial role not only in the forming of the adhesive bond, but also in the transfer of stress once the bond has formed.

Adamson [9] provides a simple molecular view of why liquids have an extra energy associated with their surface. Let us view the molecules in a liquid as a collection of balls interacting with each other by the set of forces described above. A molecule in the bulk of the liquid interacts with all of its nearest neighbors equally. However, a molecule that exists at a surface can interact only with molecules below and to the sides of it. This molecule has “unrequited valences”. To counteract this imbalance of forces at the surface, the molecules tend to be further apart, thus increasing the force acting in the plane of the surface. This leads to the feel that a liquid has a “skin”. In fact, it has been experimentally demonstrated that liquids (at their triple point) have lower density in the surface region [10]. Thus, we could explain the observed phenomena by saying that surface forces result from an imbalance in intermolecular forces for molecules that exist at a demarcation between phases and materials. We use this description to provide a means of estimating surface energy for liquids that have simple (non-directional) interactions between atoms or molecules.

Let us suppose that the energy of interaction between two molecules,  $A$ , is given by the quantity  $\chi$ . In a simple lattice model, the molecule will have  $z_b$  nearest neighbors, where  $z$  stands for the coordination number and  $b$  stands for “bulk” (interior of the liquid.) Thus, the total energy of interaction between the molecule of interest and its nearest neighbors is:

$$X_{A,b} = z_b \frac{\chi_{AA}}{2} \quad (4.19)$$

At a surface, the coordination number will be some number less than  $z_b$ . We call the coordination number at the surface  $z_s$ . Therefore, the energy of interaction of the molecule with its neighbors at the surface is:

$$X_{A,s} = z_s \frac{\chi_{AA}}{2} \quad (4.20)$$

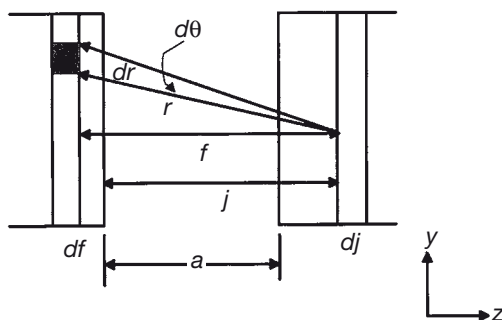


**FIGURE 4.2** Diagram showing the basis of the calculation carried out by Fowler and Guggenheim. The diagram shows the indices over which the integrations are carried out. The basic idea is to sum all the interactions between all elements on one side of the interface with all the elements on the other (redrawn from Fowler and Guggenheim)

In both of these expressions, the interaction energy is divided by two in order to correct for double counting. Thus, the molecules at the surface have a difference from the bulk molecules in their energy as described in the following expression:

$$\frac{1}{\alpha} (X_{A,s} - X_{A,b}) = \frac{\chi_{AA}}{2} \frac{z_s - z_b}{\alpha} = \gamma \quad (4.21)$$

where  $\alpha$  is the area on the surface occupied by molecule A and  $\gamma$  is known as the surface energy.

Another means of calculating the effect of molecular interactions between two surfaces is that described by Fowler and Guggenheim [11]. This type of calculation is similar to others found in the literature and its basis is shown in Fig. 4.2. Two important assumptions are used in this calculation. The first is that the density of the molecules is a constant throughout either side of the interacting surfaces. On a molecular scale, this is incorrect. However, qualitatively it provides a reasonable answer. The second assumption is that each point on either side of the interacting surfaces is acting by means of the Lennard-Jones force described earlier.

The entire integral used in the calculation is as follows:

$$\begin{aligned} F_T^{L-J} &= 2 \pi n^2 \int_{j=a}^{j=\infty} dj \int_{f=j}^{f=\infty} f df \int_{r=f}^{r=\infty} \left[ -\frac{6A}{r^7} + \frac{12B}{r^{13}} \right] dr \\ &= \frac{2 \pi n^2}{a^3} \left[ \frac{A}{12} - \frac{B}{90 a^6} \right] \end{aligned} \quad (4.22)$$

In this expression,  $n$  is the density of molecules on either side of the two surfaces,  $a$  is the distance of separation of the two surfaces and  $A$  and  $B$  are the attractive

and repulsive Lennard-Jones constants, respectively. The calculation starts by determining the number of molecules in an annulus at a distance  $r$  and varying the angle  $d\theta$  and the interaction of all possible annuli on the leftmost surface on a point on the rightmost surface. The calculation then integrates over all possible points in the rightmost surface.

Now look at the total energy,  $\xi_T$ , necessary to separate these two surfaces to an infinite distance. We integrate the total force over all distances from the equilibrium distance,  $r_0$ , out to infinity:

$$\xi_T = \int_{a=r_0}^{a=\infty} F_T^{L-J} da \quad (4.23)$$

A force times a distance is energy. The term,  $r_0$  is the equilibrium distance between the two surfaces. Plugging the result of Eq. (4.22) into Eq. (4.23) gives us the total energy of interaction between these two surfaces:

$$\xi_T = \frac{\pi n^2}{12 r_0} \left( A - \frac{B}{30 r_0^6} \right) \quad (4.24)$$

Realizing that at  $r_0$  (the equilibrium distance), the total force is zero, we have:

$$\frac{A}{12} = \frac{B}{90 r_0^6} \quad (4.25)$$

Substituting this equation into the expression for the total energy we have:

$$\xi_T = \frac{\pi n^2 A}{16 r_0^2} = 2 \gamma \Rightarrow \gamma = \frac{\pi n^2 A}{32 r_0^2} \quad (4.26)$$

This is a crucial equation for this section of this book. Using the method of Fowler and Guggenheim, we have calculated the total energy of interaction existing between two surfaces whose molecules are interacting by means of a Lennard-Jones force. The interaction is found to depend upon the density of molecules in the surface, the equilibrium distance between the two surfaces (which could just as well be taken as an intermolecular spacing, making the assumption that the two surfaces were actually in contact at equilibrium), and the attractive constant  $A$ . The total energy due to the presence of two surfaces in contact is dependent upon the intermolecular forces that exist in the material and upon the intermolecular spacing. Equation (4.26) goes on to define a quantity  $\gamma$  that is one-half of the total energy of interaction. This quantity,  $\gamma$ , is the *surface energy* of the material, as we discussed before. Note that  $\gamma$  depends upon the magnitude of intermolecular forces as demonstrated by

TABLE 4.1 Surface Energies of Familiar Liquids

Liquid	Surface Energy (mJ/m <sup>2</sup> ) at 25 °C
Water	72
Epoxy resin	43
Glycerol	63
Ethylene glycol	47
n-hexane	18
Benzene	28.9
Nitrobenzene	43.9

its dependence on the constant  $A$ . Note that the expression previously derived via coordination number (Eq. (4.21)) has a mathematical form similar to Eq. (4.26).

The surface energy  $\gamma$  plays a crucial role in the understanding of adhesion phenomena. It is important to know that it is just as much a materials parameter as the tensile strength or other descriptors of materials properties. Table 4.1 provides a listing of the measured surface energy for a number of familiar liquids.

We now consider the relationship between surface energy and the stiffness of a material. The isothermal Young’s modulus of a material can be shown to be [12]:

$$E = r_0 \left[ \frac{\partial \Phi^{L-J}(r)}{\partial r} \right]_{T, r=r_0} \tag{4.27}$$

The subscripts indicate that the differential is taken at constant temperature and at  $r = r_0$ . The Lennard-Jones potential can be substituted into this expression and through algebra and the use of the equilibrium distance argument presented earlier, we find that

$$E = \frac{\pi n^2 A}{r_0^3} \tag{4.28}$$

Using Eq. (4.27), we can show that

$$E = \frac{32 \gamma}{r_0} \tag{4.29}$$

This very interesting result shows that the isothermal Young’s modulus is directly related to the surface energy of a material. We find that those materials with the highest stiffness are also those with the highest surface energies. Similar correlations can be drawn with other parameters related to the cohesive properties of materials.

## ■ 4.4 Work of Cohesion and Adhesion

Consider the situation shown in Fig. 4.3. In this thought experiment, the elastic material of unit cross sectional area is subjected to a tensile force. The material breaks, creating two new surfaces. Since the material is completely elastic, the work done on the sample is dissipated only in creating the new surface. Under those assumptions, if both sides of the broken material are of the same composition, then we can say

$$W_{\text{coh}} = 2\gamma \quad (4.30)$$

where  $W_{\text{coh}}$  is defined as the *work of cohesion*. This equation has much the same sense as the result of the Fowler-Guggenheim analysis that resulted in Eq. (4.26). We can understand the origin of Eq. (4.30) if we just realize that the only thing that we have done by the application of work to the imaginary specimen is the creation of two new surfaces, each of unit area. If the new surfaces are each made of the same material, then the total energy expended must have been twice the surface energy of the material.

We have already discussed a similar situation when we discussed the definition of the strain energy release rate. The reader should examine Sections 2.4 and 3.5.1.2. When we derived the equation for the strain energy release rate, we discussed the effect of a crack propagating in a body. What happens when that crack propagates? *Two new surfaces are created!* Thus, in the case of a completely elastic material:

$$\mathcal{G}_{\text{lc}} = W_{\text{coh}} = \frac{F^2}{2w} \frac{\delta C}{\delta a} \quad (4.31)$$

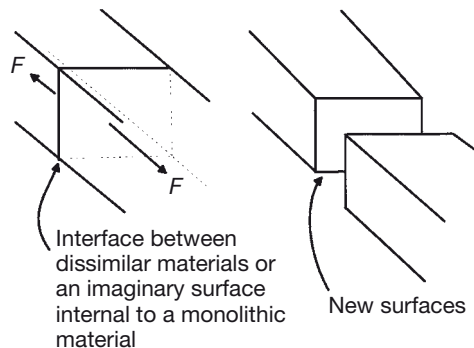


**FIGURE 4.3** Diagram showing the basis for the calculation of the work of cohesion and adhesion. A monolithic material is broken to create two surfaces of unit area. An interface between two materials is separated to create two new surfaces, each of unit area. The materials are assumed to be completely non-energy-absorbing and non-energy-dissipating, that is, entirely elastic

In this equation, the lower case “c” stands for “critical” while the upper case “C” stands for the compliance of the material. The other symbols are defined in Chapters 2 and 3. This equation states that a crack grows in an elastic material, when the strain energy exceeds the surface energy of the material. This criterion is known as the Griffith fracture criterion [13] and was the first of its type. Griffith and his co-workers found that very few materials had a strain energy release rate as low as the work of cohesion, un-sized glass fibers being one of those materials. It is found that most materials do not fail in a brittle, elastic manner, but absorb energy in a number of ways, including viscoelastically. Only a few materials behave according to the Griffith fracture criterion.

Imagine a situation in which two dissimilar materials are in intimate contact. A tensile force splits the materials into two dissimilar materials. If the sample is of a unit cross sectional area, then the energy expended should be the sum of the two surface energies. This is an incomplete description of this imaginary experiment. Because the two dissimilar materials were in contact, there were intermolecular forces present that are now missing since the materials were separated. That is, an *interfacial energy* may have been present before the materials were split apart. As this energy is missing after the two surfaces are separated, we must subtract it from the energy used to create the two new surfaces:

$$W_A = \gamma_1 + \gamma_2 - \gamma_{12} \quad (4.32)$$

where  $W_A$  is the *work of adhesion*,  $\gamma_i$  is the surface energy of the  $i$ th material and  $\gamma_{12}$  is the interfacial energy between the two materials in contact. This equation was postulated centuries ago and is known as the Dupré equation [14]. The interfacial energy can also be considered as the energy necessary to create a unit area of interface. The Dupré equation plays a central role in the study of adhesion. It is important to note that the work of adhesion is a thermodynamic parameter. Therefore, it should not depend upon factors such as rate, thickness of adhesive, or other parameters that could affect the physical properties of the bulk adhesive. However, the work of adhesion is dependent upon temperature as well as the chemical constitution of the adhesive, as would be any chemical system.

We can also describe interfacial energies by means of the same type of simple lattice description used to describe surface energy. Suppose we have materials in contact at an interface, one material containing atoms or molecules of  $A$  and the other atoms or molecules of  $B$ . When either  $A$  or  $B$  is at the interface,  $A$  loses interaction energy with some  $A$  atoms or molecules but gains some interaction energy with  $B$  atoms or molecules. A similar situation occurs for  $B$ . Suppose that there are  $N$  molecules of  $A$  and  $B$  at the interface. We can write:

$$\frac{X_i}{\Omega} = \frac{N(z_b - z_i)}{a} \left( \chi_{AB} - \frac{\chi_{AA}}{2} - \frac{\chi_{BB}}{2} \right) = \gamma_{AB} \quad (4.33)$$

where the  $\chi$ 's are interaction energies between atoms or molecules,  $\chi_{AB}$  is the interaction energy between an A and a B at the interface,  $z_1$  is the coordination number at the interface,  $a$  is the average cross-sectional area per molecular pair at the interface,  $\Omega$  is the total interfacial area and  $\gamma_{AB}$  is the interfacial energy between the liquids A and B. From the form of Eq. (4.33), we can see that it will be likely that interfacial energies are going to be smaller than surface energies since the energy parameters used in this expression are subtracted from one another.

## ■ 4.5 Methods of Measurement of Surface Energy and Related Parameters

### 4.5.1 Surface Tension

If an attempt is made to push a probe through the surface of a liquid, the probe encounters a resistance to the deformation of the surface; known as the *surface tension*. Surface tension and surface energy are numerically identical for liquids. Surface energy is generally given in units of millijoules per meter squared ( $\text{mJ}/\text{m}^2$ ) while surface tension is given in units of dynes/cm or Newtons per meter ( $\text{N}/\text{m}$ ), i.e., the surface tension is given as a force per unit length. Techniques for the measurement of the surface tension of liquids have their basis in two types of measurements: probes and surface area increase. The probe methods generally involve the passage of a probe through the surface and the measurement of the force necessary to accomplish that passage. Such methods include the Wilhelmy plate [15] and the du Nuoy [16] ring.

Surface area increase can be used to measure the surface tension of liquids since the minimization of surface energy is a driving force in nature. We can measure surface area by suspending a drop of liquid on the tip of a syringe and then increasing the volume of the drop until it falls from the syringe under the action of gravity. The drop's shape depends upon the surface tension of the liquid. We could also place a clean capillary tube into a pool of liquid and observe the height to which the liquid travels up the tube under the influence of capillary pressure. The following sections include short descriptions of a few of these methods. When determining liquid surface tensions, the liquids must be in the purest possible state. A double distillation of the liquid in scrupulously clean glassware is recommended. Extremely small quantities of contaminants, especially those materials that are surface active, can cause very large changes in surface tension.

#### 4.5.1.1 Drop Weight/Volume Method

The “Drop Weight/Drop Volume” [17] method is one of the easiest ways to determine both surface and interfacial tensions of liquids. The main piece of equipment necessary to perform this measurement is a hypodermic syringe equipped with a micrometer-driven plunger. A hypodermic needle with a highly polished tip and with known dimensions is applied to the end of the syringe. The liquid of interest is placed in the syringe, which is then placed over a vessel. The micrometer is slowly driven until a drop falls from the tip of the needle. The number of drops is counted and the volume measured. Alternatively, the number of drops is counted and their weight is measured. The weight is converted to volume through knowledge of the density of the liquid. The average volume necessary to cause the drop to fall is used to calculate the surface tension of the liquid. Appropriate geometry factors are applied to arrive at the correct surface tension [18]. Interfacial tensions can be measured by placing the end of the hypodermic needle in another liquid in which the test liquid is not soluble. The liquid of higher density should be in the syringe. With a correction for buoyancy, the interfacial tension between the liquids can be measured.

#### 4.5.1.2 Du Nuoy Tensiometer

Commercial instruments based upon the du Nuoy ring tensiometer [16] are available. The instrument consists of a sensitive force-measuring device, such as a torsion wire, from which is suspended a lever arm and from the lever arm is suspended a harness and ring. The ring is usually made of platinum or another noble metal and is kept scrupulously clean. Normal cleaning procedures are usually followed by firing the ring with a propane torch.

The dimensions and shape of the ring are usually lumped into a “ring factor” supplied by its manufacturer. The shape of the ring is extremely important as any distortion results in incorrect measurements of the surface tension. The ring is placed under the surface of the test liquid. The liquid is slowly moved downward until the ring is near the surface. The force is repeatedly balanced by means of the torsion wire and eventually the ring breaks through the liquid surface. That force is recorded and, by means of appropriate conversion factors, the surface tension of the liquid is calculated.

#### 4.5.2 Surface Energy of Solids

The concept of surface tension is not applicable to solids. Even though it is likely that solid surfaces are under tension, it is not easy to conceive of a method to measure



surface area increases or forces necessary to pass probes through the surface of a solid since both would irreparably damage the solid surface. Since the damage is irreversible, this would not be considered a thermodynamic measurement. However, the concept of a surface energy is certainly applicable to solid surfaces. Because a solid surface contains unrequited bonds, just as those between the molecules in the surface of a liquid do, a solid surface has a surface energy. Unfortunately, none of the methods even remotely similar to the ones we have described earlier are applicable to solids. For the most part, we have only indirect methods for estimating the surface energy of a solid. The easiest ways to estimate the surface energy of a solid are based upon contact angle measurements. These measurements are so fundamental to the study of adhesives and adhesion, that it is appropriate to devote considerable space to their description. In the next section, we also describe a mechanical method for determining the surface energy of solid materials: the surface forces apparatus.

#### 4.5.2.1 Contact Angle Methods

In a contact angle measurement, a drop of a liquid is placed upon the surface of a solid. The liquid is chosen so that it does not swell the surface of the solid nor does it react with the surface. The solid is assumed to be perfectly smooth and rigid. We can often find liquids that do not chemically interact with the solid, but it is difficult to find perfectly smooth solids. In addition, the forces that act at an interface are not only not negligible but in many cases, can distort the surface at a distance considerably remote from the area of contact. This can happen even in substrates that are nominally rigid. Thus, many of the suppositions necessary for the analysis of the contact angle measurement are difficult to achieve in reality. However, the simplicity of the technique, as well as its ability to provide useful data, tends to overshadow these shortcomings.

A diagram of the contact angle measurement is shown in Fig. 4.4. The liquid is placed on the surface so that the effects of gravity to flatten the drop are negligible. Drop size is usually small (tens of microliters). The dispensing instrument is held very close to the surface and the drop of liquid is “laid” on the surface rather than “dropped”. The drop is allowed to flow and equilibrate with the surface. Viscous liquids are allowed a longer time to equilibrate than low viscosity liquids. The measurement is usually done with a goniometer, which is nothing more than a protractor mounted inside a telescope. The table upon which the solid rests should be precisely leveled and that level is used as the baseline of the protractor. Care must be taken to ensure that the cross hairs of the protractor are at the exact drop edge. This can be difficult when contact angles are either very high or very low. Several measurements are made on several drops that are placed in several locations on the surface. Accuracy of  $\pm 1^\circ$  are attainable with careful measurement.

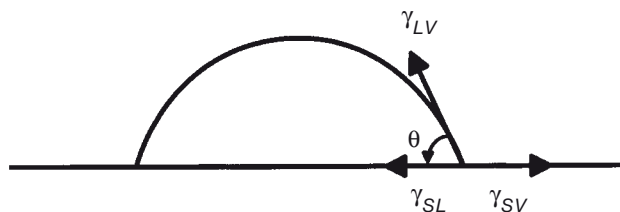


**FIGURE 4.4** Schematic of the contact angle experiment. A drop of liquid is placed on a perfectly smooth, rigid solid. The angle of contact is measured at the three phase point between the solid, the liquid, and the vapor. The “interfacial tensions” between the phases used by Young to generate his equation are shown

Contact angle measurements are dependent upon the direction in which the measurement is made. When a drop is laid down upon a surface and advances over the surface as it spreads, the contact angle in this situation is known as the *advancing contact angle*. If liquid is withdrawn from a drop that has already come into equilibrium with the surface, the contact angle is known as the *receding contact angle*. In general, the advancing angle is larger than the receding angle. The phenomenon of having a different contact angle under advancing and receding conditions is known as *contact angle hysteresis*. Johnson and Dettre [19] have described a number of reasons contact angle measurements are hysteretic, specifically: non-homogeneous surface chemistry, surface roughness, and molecular rearrangement in the solid induced by the liquid and *vice versa*. The hysteretic character of contact angle measurements raises some doubts as to their character as equilibrium measurements of surface energetics.

The importance of the contact angle measurement was established by the analysis originally done by Young [20]. However, his analysis is inherently incorrect because solid surfaces do not have a well-defined “surface tension”. Additionally, the analysis did not take into account the potential distortion of the solid surface by the action of the surface tension of the liquid. Cherry [21] was able to show by thermodynamic arguments that the expression was correct, but not for the vectorial kind of argument originally provided by Young. The Young equation states:

$$\gamma_{LV} \cos \theta = \gamma_{SV} - \gamma_{SL} \quad (4.34)$$

where  $\theta$  is the contact angle (as shown in Fig. 4.4) and the  $\gamma_{ij}$  are the appropriate interfacial tensions between the “S” solid, the “L” liquid and, the “V” vapor. It should be noted the  $\gamma_{SV}$  is the solid-vapor interfacial energy and not the true surface free energy of the solid. The surface free energy is related to  $\gamma_{SV}$  through the following relationship:

$$\gamma_{SV} = \gamma_S - \pi_e \quad (4.35)$$

where  $\gamma_s$  is the true surface free energy of the solid and  $\pi_e$  is a quantity known as the equilibrium spreading pressure. The term,  $\pi_e$ , is a measure of the energy released through adsorption of vapor onto the surface of the solid, thus lowering its surface free energy. The equilibrium spreading pressure is important when the solid surface energy is high and the liquid surface energy is low.

An example of this situation is the wetting of a clean metal by a hydrocarbon. The equilibrium spreading pressure is manifested in the observation that the contact angle of the hydrocarbon on the clean metal surface is not zero even though the metal surface energy is much higher than that of the hydrocarbon. The equilibrium spreading pressure is not important when a high surface energy liquid wets a low surface energy material. Such a situation is exemplified by water on polyethylene. In most of this book, we will ignore  $\pi_e$ . Any quotation of  $\gamma_s$  which has been measured without consideration of the equilibrium spreading pressure should be considered suspect. We know from our discussion of the Dupré Equation that

$$W_A = \gamma_{LV} + \gamma_{SV} - \gamma_{SL} \quad (4.36)$$

Substitution of the Young Equation into the Dupré Equation results in the Young-Dupré Equation that states:

$$W_A = \gamma_{LV} (1 + \cos \theta) \quad (4.37)$$

This deceptively simple equation relates a thermodynamic parameter to two easily determinable quantities: the contact angle and the liquid-vapor interfacial tension. Examination of the data in Table 4.1 provides estimates of the prediction of the work of adhesion between a solid and a liquid. Suppose that an epoxy resin (surface tension of about 43 dynes/cm) completely wets the surface of an aluminum plate. The contact angle would be 0,  $1 + \cos \theta$  would be 2, and the work of adhesion would be 86 mJ/m<sup>2</sup>. This is an exceedingly small quantity. This energy is far lower than the amount needed to break all but the weakest of adhesive bonds. With the substantial difference between the work of adhesion and the actual amount of energy necessary to break an adhesive bond, one would assume that the work of adhesion plays an insignificant role on the practical work of adhesion. In Chapter 6, we find that this is not the case and discuss attempts to relate the thermodynamic work of adhesion to practical adhesion.

#### 4.5.2.2 Contact Mechanics and Direct Measurement of Solid Surface Energy

The above discussion indicates that the direct measurement of the surface energy of solids is a difficult task. In the modern examination of interactions at surfaces, another technique allows us to probe directly the interactions between solid surfaces.

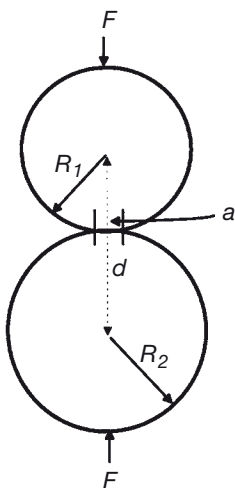


**FIGURE 4.5** Diagram showing the basis for the Hertz analysis. Shown are two elastic spheres in contact. The radii of curvature are shown as well as the distance of separation of the two centers

The technique is the surface forces apparatus (SFA) [22] and the analysis of the experiment was done by Johnson, Kendall, and Roberts (JKR) [23]. Understanding the basis of the JKR theory and the measurement gives insight into many of the basic physical phenomena of adhesion. Energy balance, fracture mechanics, and mechanical properties of materials all play a role in the measurement as well as the analysis of the measurement.

Fig. 4.5 shows a schematic of the meeting of two spheres. Hertz [24] was the first to analyze this situation and made the assumption that the spheres were perfectly elastic and exhibited no adhesion. Hertz was able to show that:

$$a^3 = \left( \frac{3\pi}{4} \right) (k_1 + k_2) \left( \frac{R_1 R_2}{R_1 + R_2} \right) F \quad (4.38)$$

where

$$k_i = \frac{1 - \nu_i^2}{\pi E_i} \quad (4.39)$$

The term,  $\nu_i$ , is the Poisson's ratio of the  $i$ th material,  $E_i$  is its tensile modulus,  $R_i$  is the radius of curvature of the  $i$ th material,  $F$  is the force which is applied to the two materials, and  $a$  is the radius of contact between the two spheres. In addition, the Hertz theory demonstrated that the distance of approach of the centers of the two spheres,  $d$ , would be:

$$d^3 = \left( \frac{9\pi^2}{16} \right) (k_1 + k_2)^2 \left( \frac{R_1 R_2}{R_1 + R_2} \right) F^2 \quad (4.40)$$

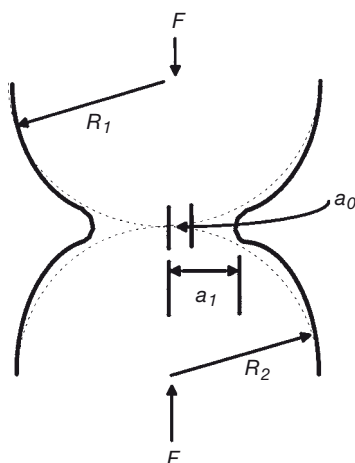


**FIGURE 4.6** Schematic of the situation analyzed by JKR. The Hertz radius of contact is given by  $a_0$  while the radius of contact for two bodies displaying adhesion is given by  $a_1$ . The radii of curvature are as described in Fig. 4.5. The dotted lines show the Hertz situation while the solid lines show the situation in which the two bodies display adhesion to one another

Figure 4.6 shows the situation as analyzed by Johnson, Kendall and Roberts. These workers noted that the force necessary to separate two bodies in contact was not zero as assumed by Hertz and that the radius of contact of the two bodies was not well predicted by the Hertz equation written above. The distance of separation equation was also incorrect. Johnson, Kendall and Roberts made the correct supposition in stating that the deviation of the Hertz equations from experimental observations was due to the forces of adhesion.

The method for examining the contact mechanics of two spheres with forces of adhesion between their surfaces is very similar to the method we used to analyze linear elastic fracture mechanics in Chapters 2 and 3. It involves an *energy balance* approach. That is, the situation is not analyzed in terms of stresses and strains as it was in the case of the Goland-Reissner analysis of lap shear specimens, but rather in terms of energies. For the system shown in Fig. 4.6, we say that the total energy in the system,  $U_T$ , is made up of three parts:  $U_M$ , the mechanical potential energy,  $U_E$ , the elastic energy in the system, and  $U_S$ , the surface energy in the system.  $U_S$  is simply the work of adhesion in the case of spheres made of different materials in contact with one another and the work of cohesion in the case of similar materials in contact with one another. Let's look at the mechanical potential energy next. For this analysis, we need to examine Fig. 4.7.

We first calculate the mechanical potential energy in the system. If a force  $F_0$  is applied to the two spheres and a resultant displacement ( $d_2$ ) occurs, we can easily write the mechanical potential energy in the system as  $F_0 d_2$  (position 3 in Fig. 4.7).

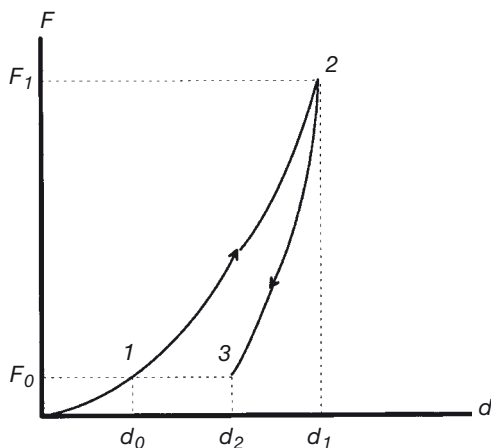


**FIGURE 4.7** Force-displacement plot for the analysis of the contact mechanics of two spheres by means of the energy balance approach

We can calculate the elastic energy by first saying that the spheres are pushed into Hertzian contact by a force  $F_0$ , which results in a Hertz displacement of  $d_0$ . This situation ensues when no surface forces are present and corresponds with position 1 in Fig. 4.7 and with radius  $a_0$  as shown in Fig. 4.6. We can now invoke the presence of surface forces by saying that this is equivalent to having an extra Hertz force applied to the two spheres. This is now the situation at position 2 with force  $F_1$ , displacement  $d_1$  (Fig. 4.7) and radius  $a_1$  (Fig. 4.6). Positions 1 and 2 are not real, but rather virtual situations, which allow us to calculate the energy in the system. We now relax the system to get to the experimentally determined state at position 3 in Fig. 4.7. The total elastic energy in the system is now the amount of energy necessary to attain position 2 minus the energy required to attain position 3. The energy necessary to attain position 2 is easily determined, since we have assumed that the body follows Hertzian mechanics. Rearranging Eq. (4.40), we can find  $d$  and then integrate  $d dF$  from  $F = 0$  to  $F = F_1$ :

$$U_2 = \frac{2}{3} \int_0^{F_1} \frac{F^{\frac{2}{3}}}{K^{\frac{2}{3}} R^{\frac{1}{3}}} dF \quad (4.41)$$

where  $R = \frac{R_1 R_2}{R_1 + R_2}$  and  $K = \frac{4}{3 \pi (k_1 + k_2)}$ .

The calculation of  $U_3$  can be equally straightforward if one knows the relationship between  $F$  and  $d$  for the “unloading” curve. The load-displacement curve for this situation was derived by Johnson [25] and it has the form:

$$d = \frac{2}{3} \frac{F}{K a_1} \quad (4.42)$$

that leads to:

$$U_3 = \int_{F_1}^{F_0} \frac{2}{3} \frac{F}{K a_1} dF \quad (4.43)$$

Combining all of these relationships we have:

$$U_T = \frac{1}{K^{\frac{2}{3}} R^{\frac{1}{3}}} \left[ \frac{1}{15} F_1^{\frac{5}{3}} + \frac{1}{3} \frac{F_0^2}{F_1^{\frac{1}{3}}} \right] - \frac{1}{K^{\frac{2}{3}} R^{\frac{1}{3}}} \left[ \frac{1}{3} F_0 F_1^{\frac{2}{3}} + \frac{2}{3} \frac{F_0^2}{F_1^{\frac{1}{3}}} \right] - W_A \pi \frac{R^{\frac{2}{3}} F_1^{\frac{2}{3}}}{K^{\frac{2}{3}}} \quad (4.44)$$

This complicated algebraic expression can be used to find a relationship between  $F_1$  and  $F_0$  and, more importantly, a relationship between  $F_0$  and  $a_1$ . At equilibrium (here is the energy balance part):

$$\frac{dU_T}{dF_1} = 0 \quad (4.45)$$

Applying this equilibrium condition to the equation for  $U_T$  we find

$$F_1 = F_0 + 3 W_A \pi R + \sqrt{6 W_A R F_0 + (3 W_A \pi R)^2} \quad (4.46)$$

This equation shows that the apparent Hertz force is greater than the actual applied load and that the increase is due to the work of adhesion. This result can also be used to predict other aspects of the contact region when surface forces are taken into account. The radius of the contact area is found to be bigger than the Hertz contact area according to the following equation:

$$a^3 = \frac{R}{K} \left( F + 3 W_A \pi R + \sqrt{6 W_A \pi R F + (3 W_A \pi R)^2} \right) \quad (4.47)$$

Examination of this equation shows that at zero applied force, there is still a finite contact radius that is not predicted by the Hertz analysis and which is one of the possible experimental proofs of the JKR theory. Also, by examination of the equation for the contact radius, we find that if a tensile force is applied to the two spheres (i.e., a  $-F$ ), the radius decreases until the point that

$$F_{JKR} = -\frac{3}{2} W_A \pi R \quad (4.48)$$

An alternative examination of the mechanics of two elastic spheres in contact was presented by Maugis and Barquins [26]. In this situation, the spheres are being unloaded and the situation is modeled as a crack propagating at the interface between the two elastic spheres. The equation provided by Maugis and Barquins states:

$$\mathcal{G}_a = \frac{\left[ \frac{a^3 K}{R} - F \right]^2}{6 \pi a^3 K} \quad (4.49)$$

The notation  $\mathcal{G}_a$  is used in Eq. (4.49) to indicate that it is similar in sense to the strain energy release rate described in Chapter 2. The quantity  $\mathcal{G}_a$  has recently been given the name “adhesion energy”, that is the strain energy inherent in the system in contact that is due to adhesion. This parameter will appear in our discussion of the relationship between adhesion and practical adhesion in Chapter 6.

One can form two elastic spheres and place them in intimate contact. A tensile load is applied until they spontaneously separate. A force can be measured and directly related to the work of adhesion. If the two materials in contact are the same material, then  $W_A = W_C = 2 \gamma_S$  and Eq. (4.48) can be used to measure directly the surface energy of a solid.

Two basic kinds of equipment are used to measure directly the surface energy of solids based on the JKR theory. The first one was described by JKR; a schematic of this apparatus is shown in Fig. 4.8.

The apparatus is remarkably simple. The sample must be optically clear and elastic under the loads of interest. The other half of the sample can also be a sphere but most often is flat and coated either with the same material as the hemisphere is

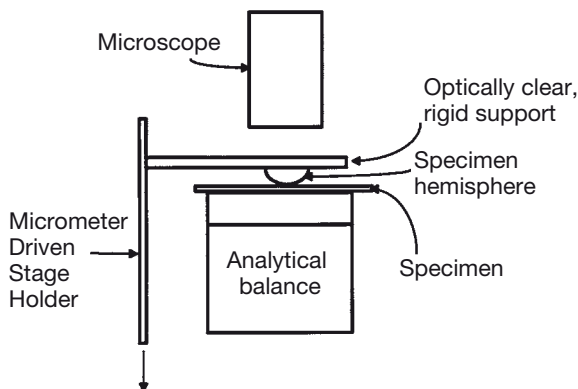


**FIGURE 4.8** Schematic diagram of an apparatus useful for determining surface energy by means of the JKR theory



made or another material of interest (a sphere in contact with a sphere is the same as a sphere in contact with a flat material according to the Derjaguin approximation [27] if the radius of curvature of the sphere is large in comparison to the measurement area). The hemisphere of sample is mounted on an optically clear, rigid support capable of vertical movement. The force is measured by means of an analytical balance and the radius of contact between the sphere and the flat is measured through the optical microscope. Equation (4.47) is used to determine the work of adhesion between the two materials.

The apparatus most often used for direct measurements of the forces of adhesion between solid surfaces is the surface forces apparatus (SFA) [22]. Originally described by Tabor [28], but extensively developed and used by Israelachvili [29] and co-workers, the SFA uses a direct mechanical means to measure the distances between surfaces down to the Angstrom level as well a mechanical means to measure the forces between those surfaces. Figure 4.9 shows a diagram of the surface forces apparatus.

The apparatus measures force by the deflection of a double cantilever of known force constant and the measurement of the distance of separation of the two surfaces through interferometry. The samples need to be almost atomically flat, thin (about 2–5 microns) and optically clear. The back of each sample is silvered to make it partially reflective. The samples are then mounted on the lenses by means of an adhesive. The lenses are mounted into the apparatus so that the apexes of the lenses are crossed with respect to one another, resulting in essentially a point contact. The sample surfaces are brought close together by a motor. Passing white light through the samples allows measurement of the distance separating the sample surfaces. As the samples near each other, interferometric fringes can be observed in the spectrometer. These are known as “Fringes of Equal Chromatic Order” or FECO. The distance between the fringes (as observed in the spectrometer) can be used to measure the distance between the surfaces. The shape of the fringes also corresponds to the shape of the lens’ surfaces.

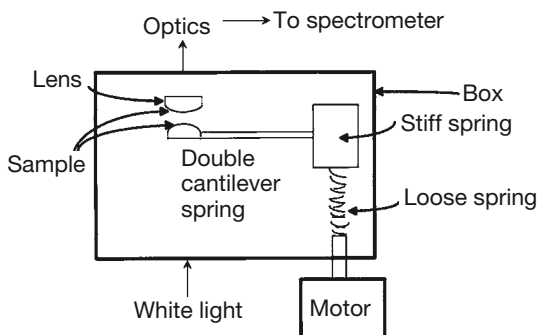


**FIGURE 4.9** Schematic of the Israelachvili Surface Forces Apparatus (SFA)

When the sample surface is not in contact, the FECO are roughly parabolic in shape. At some distance of separation, the forces of attraction between the surfaces overcome the restraining force of the spring, and the samples jump into contact. When the surfaces are in contact, the contact area is flat and the rest of the FECO mirrors the shape of the surfaces outside of the contact zone. The JKR theory predicts such a shape and experiments have shown it to be correct [30]. After contact, compressive force can be applied and Eq. (4.47) can be used to measure the work of adhesion between the two surfaces.

Alternatively, after the jump to contact is made, a tensile force can be applied and the force necessary to remove the samples from contact can be measured using Eq. (4.48). If possible, both measurements should be made and the results should agree. Results of measurements of this type and their implications to adhesion science are discussed in Chapter 6.

## ■ 4.6 Surface Thermodynamics and Predictions of Surface and Interfacial Tensions

In the context of this book, the *understanding* of adhesion and adhesives, it is important to relate contact angle measurements to the basic forces between atoms and molecules. The seminal work in this area was done during the 1950s by Good and Girifalco [31]. To understand this work, we must first realize another important aspect of surface energy, its status as a thermodynamic parameter. If we examine Fig. 4.10, we see an imaginary situation with a section of surface drawn as a free body.

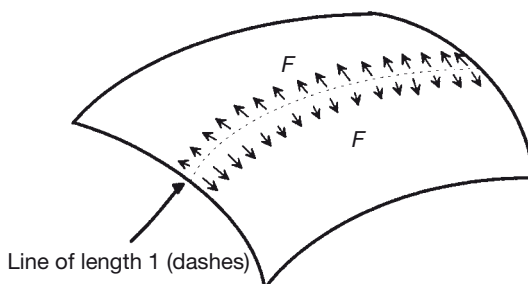


**FIGURE 4.10** A section of surface through which a dashed imaginary line has been drawn. The action of surface tension is to pull in two dimensions across this line.

In a liquid, surface tension and surface energy have the same value as well as the same sense

Imagine that we have a line (indicated by the dashed line) drawn somewhere in that body. We imagine a force acting across the line as shown in Fig. 4.10. We know from our earlier discussion that the surface tends to resist deformation. If the surface is a liquid, the amount of resistance is the “surface tension”. If the surface is deformed, such as by increasing area, work is done on this system. Following Cherry [32], we can describe the internal energy of a system as follows:

$$d\xi = dq - dw + \sum_i \mu_i dN_i \quad (4.50)$$

where  $\xi$  is the internal energy of the system,  $q$  is heat,  $w$  is work,  $\mu_i$  is the chemical potential of the  $i$ th constituent in the system, and  $N_i$  is the number of moles of the  $i$ th component in the system. For the situation of importance to our discussion, the work in the system includes not only the normally considered pressure ( $P$ )-volume ( $V$ ) work, but since the system contains a surface, it also can do work by expanding the surface area. Thus:

$$dw = P dV - \gamma d\Omega \quad (4.51)$$

where  $\Omega$  is the surface area. The change in heat in the system is defined in terms of the entropy ( $S$ ):

$$dq = T dS \quad (4.52)$$

Using the above equations and constraining the system to be at constant temperature, pressure and moles of materials, we can easily show that:

$$d\xi = T dS - P dV + \gamma d\Omega + \sum_i \mu_i dN_i \quad (4.53)$$

The Helmholtz free energy of a system is:

$$A = \xi - T S \quad (4.54)$$

and

$$dA = \gamma d\Omega - P dV - S dT + \sum_i \mu_i dN_i \quad (4.55)$$

which, if we define a system under constraints of constant volume, temperature, and moles of materials, gives:

$$\gamma = \left( \frac{\partial A}{\partial \Omega} \right)_{V, T, N_i} \quad (4.56)$$

The importance of this equation is simply stated in that the surface energy can be described as the change in a thermodynamic system free energy variable with a change in area. A similar derivation can be made for the Gibbs free energy of the system,  $G$ , in that situation:

$$\gamma = \left( \frac{\partial G}{\partial \Omega} \right)_{P,T,N_i} \quad (4.57)$$

The Gibbs free energy and the Helmholtz free energy are related as follows:

$$G = A + P V \quad (4.58)$$

The work of cohesion and adhesion that we have previously described are therefore also thermodynamic variables. This derivation and the definition of the surface energy as a free energy variable sets the stage for the Good-Girifalco derivation.

#### 4.6.1 The Good-Girifalco Relationship

Good and Girifalco define a thermodynamic parameter, usually denoted  $\phi$ , based upon the following ratio:

$$\phi = \frac{W_A}{\sqrt{W_{C,1} W_{C,2}}} \quad (4.59)$$

where  $\phi$  is known as the *interaction parameter*,  $W_A$  is the work of adhesion and the  $W_{C,i}$  are the works of cohesion of the two phases in contact. If we enter the equations for the definitions of the works of cohesion and adhesion, the Dupré equations, we find:

$$\phi = \frac{\gamma_1 + \gamma_2 - \gamma_{12}}{2\sqrt{\gamma_1 \gamma_2}} \quad (4.60)$$

rearranging

$$\gamma_{12} = \gamma_1 + \gamma_2 - 2\phi\sqrt{\gamma_1 \gamma_2} \quad (4.61)$$

This is an interesting equation. It shows that if we have a way to calculate or measure  $\phi$ , we can get the value of  $\gamma_{12}$  by knowing the values of  $\gamma_1$  and  $\gamma_2$ . We know from the thermodynamic derivation we performed above and from the calculations that we did in deriving the basis for the surface energy (Eq. 4.26), we find the following:

$$\phi = \frac{\pi n_1 n_2 A_{12}}{16 r_{0,12}^2} \sqrt{\left( \frac{\pi n_1^2 A_1}{16 r_{0,1}^2} \right) \left( \frac{\pi n_2^2 A_2}{16 r_{0,2}^2} \right)} \quad (4.62)$$

Knowledge of the attractive constants of the materials allows us to calculate  $\phi$ , which in turn allows us to calculate  $\gamma_{12}$ . The attractive constants for a number of liquids are known and thus  $\phi$  can be calculated. Good and Elbing [33] used this relationship to predict interfacial energies of materials. An example is shown in Table 4.2. The results of Good and Elbing are important for a number of reasons. First of all, it gives credence to the idea that molecules can act at interfaces in the same way they interact in their own bulk material. It also shows that we can calculate those forces in a manner familiar to anyone with some knowledge of physical chemistry. The Good and Girifalco relationship and the measurements of Good and Elbing provided the basis for further work, which has added much to the understanding of adhesion. Finally, this work ties together contact angle measurements and basic physical forces leading to further insight into the science of adhesion.

**TABLE 4.2** A Sampling of the Results of Good and Elbing, showing the Relationship Between Measured and Calculated Interfacial Energies

Liquid	Polarizability ( $\text{cm}^3 \times 10^{-23}$ )	Dipole moment (Debye)	Ioniza- tion potential (eV)	Liquid surface tension (dynes/cm)	Interfacial tension with water (dynes/cm)	$\gamma_{\text{calc}}$	$\gamma_{\text{exp}}$
n-hexane	1.15	0.0	10.43	18.0	50.7	0.552	0.55
Chlorobenzene	1.235	1.58	10.5	33.6	37.4	0.697	0.671
Isovaleronitrile	0.991	3.53	10	43.9	25.7	0.973	0.971
Benzene	1.038	0.0	9.24	28.9	33.9	0.739	0.550
Carbontetra- chloride	1.060	0.0	11.1	26.95	45	0.618	0.553

### 4.6.2 The Fowkes Hypothesis and Fractional Polarity

Fowkes [34] proposed a separation of the surface energy of a material into the potential energies of interaction that we described in the first part of this chapter. We know from quantum mechanics that the summation of potential energies is inherently incorrect in that many cross terms are neglected. The Fowkes hypothesis is a first order approximation which, simply stated, is that the surface energy of a material can be divided into component parts. Thus:

$$\gamma = \gamma^d + \gamma^p + \gamma^i + \dots \quad (4.63)$$

where  $\gamma^p$  is the polar contribution to the surface energy,  $\gamma^i$  is the dipole induced dipole contribution to the surface energy and  $\gamma^d$  is the dispersion force contribution to the surface energy. Fowkes also made a fundamental hypothesis important to the study of interfaces and adhesion, namely that materials exhibiting only dispersion force interactions interact with other surfaces by only those interactions. It was also Fowkes' contention that polar force and dipole-induced dipole forces were insignificant when one of the two materials at an interface was non-polar. Mathematically this can be stated:

$$\gamma_{12} = \gamma_1 + \gamma_2 - 2\sqrt{\gamma_1^d \gamma_2^d} \quad (4.64)$$

where  $\gamma_1$  and  $\gamma_2$  are surface energies as we have previously defined them and  $\gamma_1^d$  and  $\gamma_2^d$  are the *dispersion force components* of the surface energy of materials 1 and 2, respectively. Examination of Eq. (4.64) and comparison to Eq. (4.61) show that the Fowkes hypothesis states that in the case of dispersion force interactions, the interaction parameter is essentially 1.

Fowkes provided some ingenious experiments [35] that showed the validity of Eq. (4.64) in which he measured the interfacial energy between a series of liquids. One liquid was an n-alkane (which is purely dispersion force in nature) and the other liquid was mercury. The measured interfacial tensions were remarkably constant from hydrocarbon to hydrocarbon. From these measurements, he was able to calculate the dispersion force component of the surface energy of mercury. Other interfacial tension measurements with mercury then provided the dispersion force components for another series of liquids, including water, which was found to be 17 mJ/m<sup>2</sup>, remarkably close to the value obtained from theoretical calculations [36]. Thus, the Fowkes measurements provide some credence for the equation as well as the separability of the surface energy of materials into their components. This subject is discussed again later in the section on acid base interactions.

The success of the Fowkes hypothesis for dispersion force liquids prompted others to develop what is now called a theory of fractional polarity. That is, each liquid and solid was thought to have both dispersion force as well as polar force character. One such equation was developed by Owens and Wendt [37] who wrote:

$$W_A = 2\sqrt{\gamma_1^d \gamma_2^d} + 2\sqrt{\gamma_1^p \gamma_2^p} \quad (4.65)$$

This equation states that if one knows the polar force and dispersion components to the surface energy of a solid, then the work of adhesion can be determined from the sum of the square roots of their products. This equation has proven useful in the analysis of a number of experimental situations. However, the theory of fractional

polarity cannot be taken to extremes. Erroneous results are obtained if the analysis is taken beyond the Owens and Wendt equation.

### 4.6.3 The Zisman Plot

Another fundamentally important work relating contact angles and estimation of the surface energy of solids was that of Zisman [38]. In an important series of papers, Zisman and his co-workers were able to show that contact angle measurements could be used to determine a criterion for wettability as well as a means for probing the chemistry of surfaces. In these experiments, a series of probe liquids of known surface energy were used to measure contact angles against a series of pure polymeric and non-polymeric solids. For a series of liquids, it was found that a linear or quasi-linear relationship existed between the cosine of the contact angle made by a liquid on a particular surface and the surface energy of that liquid. The linear relationship could be extrapolated to  $\cos \theta = 1$  (or  $\theta = 0$ ), thus predicting the liquid surface tension at which a liquid would spontaneously wet the solid surface. This liquid surface tension was given a special name, the *critical wetting tension of the solid surface* or  $\gamma_C$ .

The mathematical formulation of the Zisman relationship is as follows:

$$\cos \theta = 1 + b (\gamma_C - \gamma_{LV}) \quad (4.66)$$

where  $\theta$  is the contact angle,  $\gamma_{LV}$  is the interfacial tension between the probe liquid and air saturated with the vapor of the liquid,  $\gamma_C$  is the critical wetting tension, and  $b$  is the slope of the line. In general, a linear relationship is obtained only for those liquids that form a homologous series (e.g., n-alkanes) on a non-wetting surface. However, quasi-linear relationships are determined for a wide range of liquids. Kitazaki and Hata [39] have shown that the  $\gamma_C$ , which is measured for a particular surface, is dependent upon the type of liquids used. Thus, these authors proposed that different  $\gamma_C$ s be measured and quoted for different homologous series of liquids. Kitazaki and Hata would have measured and quoted a  $\gamma_C$  for a series of dispersion force liquids, a different  $\gamma_C$  for hydrogen bonding liquids, and a different  $\gamma_C$  for polar liquids. The fact that a different critical wetting tension is measured for each type of liquid series indicates that  $\gamma_C$  cannot be considered a thermodynamic parameter and should not be confused with the true surface energy of a solid, which can only be approximated by contact angle methods. A method by which solid surface energies can be measured was described in a previous section (the surface forces apparatus). The non-thermodynamic character of the critical wetting tension does not diminish its utility, however. In Chapter 6, we examine the critical wetting tension as the basis for a criterion for good adhesion.

**TABLE 4.3** The Relationship between Surface Chemical Composition and the Critical Wetting Tension of a Number of Solids

Surface	Critical Wetting Tension (dynes/cm or Newtons/meter)
Polytetrafluoroethylene	18
Polydimethyl siloxane (silicone)	21
Polyethylene	31
Polystyrene	33
Polyvinyl chloride	39
Cured epoxy resin	43
Polyethylene terephthalate (PET)	43
Nylon-6,6	46

The critical wetting tension of a solid surface can be used to characterize surface chemistry. Zisman and co-workers demonstrated the relationship between  $\gamma_C$  and the chemical structure of a series of polymers. They were able to show that a surface containing a preponderance of  $\text{CH}_2$  groups had a higher critical wetting tension (31 dynes/cm) than a surface containing a preponderance of  $\text{CH}_3$  groups (22 dynes/cm). A similar relationship was found between  $\text{CF}_2$  (18 dynes/cm) and  $\text{CF}_3$  groups (15 dynes/cm). Similar relationships could be found for partially fluorinated hydrocarbons as well as partially chlorinated hydrocarbons. A list of the relationship between surface chemical functionality and critical wetting tension is shown in Table 4.3.

#### 4.6.4 Modern Application of Contact Angle Measurements

Contact angle measurements are the most sensitive of surface characterization tools. Contact angle measurements probe short-range van der Waals forces. The typical “analysis depth” of contact angle measurements is on the order of only five Angstrom units. One example of this type of surface chemical probing is the work by Whitesides and his co-workers [40] on the unique class of materials known as self-assembling monolayers. These materials are long chain hydrocarbons with a reactive surface reactive group at one end and another functionality at the other end. The reactive group provides chemisorption and the crystallizable hydrocarbon group provides the driving force for self-assembly. Whitesides performed a series of unique experiments; two are described here. In the first experiment, a series of mixtures of alkane thiol alcohols were chemisorbed and self-assembled on gold. The series of mixtures ranged from total  $\text{C}_{11}$  hydrocarbon with a hydroxyl terminus to a total  $\text{C}_{19}$  hydrocarbon with a hydroxyl terminus and several compositions



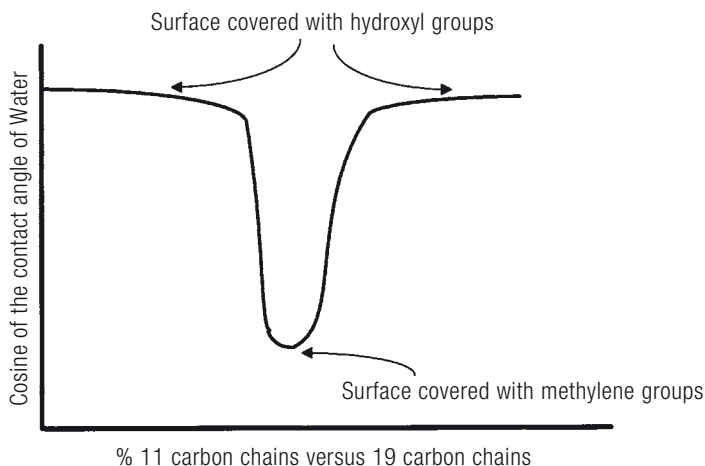


**FIGURE 4.11** Measurements of water contact angle on a series of surfaces in which the surfaces chemical concentration of  $-\text{CH}_2-$  groups was varied by application of varying concentration of  $\text{C}_{11}$  versus  $\text{C}_{19}$  self-assembling monolayers

in between. The contact angle of water was measured on this series of surfaces. A schematic representation of the data is shown in Fig. 4.11.

As can be seen, the contact angle varies from low at full coverage of  $\text{C}_{11}-\text{OH}$  groups to higher at mixed coverage to a once again low contact angle at complete  $\text{C}_{19}-\text{OH}$  coverage. Whitesides and his co-workers ascribed this variation to the change of the surface from one which was entirely covered with OH groups (the terminal group for this series of alkanes) to one in which the layer had folded over, exposing  $-\text{CH}_2-$  groups. The surface covered with  $\text{CH}_2$  groups has lower surface energy than OH groups and is expected to be more poorly wet by water than OH. At the right hand side of the graph, the surface is again entirely covered with OH groups. In another experiment, the Whitesides group designed a self-assembling monolayer that was terminated with carboxyl groups [40b]. They did contact angle measurements on this surface using water of varying pH. They were able to titrate the surface acidity and determine a  $\text{pK}_a$  for the acid groups confined to the surface. This discussion not only amplifies the importance of contact angle measurements in surface and adhesion science, but it also describes a new area of investigation: self-assembling monolayers.

## ■ 4.7 Modern Methods of Surface Analysis

Contact angle measurements provide an extremely sensitive tool by which the gross chemistry of a surface can be examined. The utility of contact angle measurements lies in their simplicity, rapidity of analysis, and economical equipment. Unfortunately, there are any number of surfaces that have equal surface energies and would thus exhibit similar critical wetting tensions. The contact angle measurement provides a “dull edge” to the knife that is cutting into the analysis of surfaces. For an adhesion scientist, it is of importance to know the chemistry of the surface where adhesion or abhesion occurs. In the past four decades, a significant number of new methods of surface analysis have been developed, which allow us to examine several features of surfaces of interest to adhesion scientists. A detailed description of these techniques is not within the scope of this book. Several references are given in the bibliography. These modern techniques yield either chemical or topological information. In the next section, we discuss techniques that probe the chemistry of surfaces.

### 4.7.1 Modern Methods for Analysis of the Chemistry of Surfaces

These techniques use an energetic probe to excite some physical process in a surface that results in the ejection of an energetic species that is analyzed. Table 4.4 provides a listing of some of these techniques, the species used to carry out the measurement, as well as the limitations and the capabilities of these techniques.

Table 4.4 does not list all of the techniques that have been used in surface science nor even in adhesion science. The techniques listed are the ones most commonly used by adhesion scientists. From the descriptions in Table 4.4, one can understand why several of these techniques are practiced in a “hard vacuum”, that is, a vacuum of less than  $5 \times 10^{-7}$  Torr. Since the species analyzed are energetic particles, their mean free path is limited unless there are no other materials in the way. In fact, the surface analytical technique we are about to discuss is dependent upon the short mean free path of an electron in a solid.

Of the techniques listed in Table 4.4, **XPS** is by far the most widely practiced modern surface analysis technique, especially in adhesion science. The technique is based on the Einstein photoelectric effect. X-rays penetrate deeply into a material, usually to a depth of microns or more. For most atoms, the absorption of an X-ray emitted from aluminum or magnesium (materials used in X-ray anode construction) is usually enough to ionize them. The electrons released, however, have a limited mean free path of about 50 Angstrom units and they are reabsorbed by the material, except near the material’s surface. Therefore, the only electrons that can escape the surface

**TABLE 4.4** Modern Surface Analysis Techniques, Capabilities and Limitations

Technique	Probe Species	Species Analyzed	Capabilities	Limitations
X-ray Photo electron Spectroscopy (XPS) or Electron Spectroscopy for Chemical Analysis (ESCA)	X-rays	Electrons (their energy and number)	Quantitative elemental analysis. Chemical information through line shape analysis. Depth profile information through angular dependent measurement. Useful for insulators and conductors. Widely used on polymers. Little spatial information	Chemical information is limited. Depth profile information is limited. Sample can be damaged by too much X-ray exposure
Secondary Ion Mass Spectrometry (SIMS)	Ions or neutrals	Ions (mass to charge ratio and their number)	Semi-quantitative elemental analysis. Excellent elemental depth profiling tool. Useful only for conductors or inorganic insulators	Little chemical information. Sample is severely damaged
Static Secondary Ion Mass Spectrometry (SSIMS)	Ions	Ions (mass to charge ratio and their number)	Non-quantitative tool for polymers. Extensive chemical information. Little sample damage. Excellent tool to use in combination with XPS	Non-quantitative. Spectra are rich in information but are difficult to analyze for unknowns
Auger Electron Spectroscopy (AES)	Electrons	Electrons (their energy and their number)	Quantitative elemental analysis tool for semiconductors and conductors. Excellent profiling tool when used with ion milling. Excellent spatial resolution can be used for mapping	Limited to non-insulators. Little chemical information
Attenuated total reflectance Fourier transform infrared spectroscopy	Infrared light	Infrared light	Detailed chemical information. Real specimens can be used. Non-vacuum method	Specimens must be very flat and capable of intimate contact with the necessary crystal. Depth of analysis is on the order of microns
Infrared reflectance absorbance spectroscopy	Infrared light	Infrared light	Detailed chemical information. Depth of analysis on the order of 100–1,000 Angstrom units. Non-vacuum method	Need special specimens e.g. coatings on a reflective surface

for analysis are those only a few tens of Angstrom units below the actual surface, hence the surface sensitivity of the technique.

The electrons emitted from an atom have a characteristic energy that can be analyzed by an electron spectrometer. Their number can also be counted. Knowing a set of conversion factors, one can determine the surface concentration of any element with the exception of hydrogen and helium. Using a high-resolution electron spectrometer, one can also see a fine structure associated with each emission peak. The fine structure can be analyzed in terms of nearest neighbor effects.

This is particularly true for the XPS peak associated with carbon. Thus, if carbon exists in a state bonded both to carbon as well as to oxygen, a small peak to the higher energy side of the main carbon peak can be detected. If carbon is also bonded to other higher electronegativity atoms such as fluorine, peaks at even higher energy are seen. This provides the basis for the limited chemical information available from XPS. We discuss some XPS experiments in the section on surface preparation of plastics in Chapter 7.

#### 4.7.2 Topological Methods of Surface Analysis

We have already discussed the fact that contact angles can be affected by the presence of surface roughness (contact angle hysteresis). However, the analysis of this effect is not yet complete enough to use contact angles as a measure of surface topology. In Chapter 6, we find that adhesion is definitely affected by surface roughness. It is, therefore, important that we have methods to analyze the topology of surfaces. The primary method for topological analysis used by adhesion scientists is electron microscopy. This technique requires a vacuum environment in which the sample surface is bombarded with electrons and either the transmission of those electrons is measured (**Transmission Electron Microscopy**, TEM), or the secondary emission of electrons is measured (**Secondary Electron Microscopy**, SEM). In the TEM technique, samples are thin-sectioned so electrons can be transmitted through the sample. Contrast is found by means of the electron density of species in the sample. Higher atomic weight species provide dark areas. This technique provides the highest magnification (as high as 80,000 to 100,000X).

SEM analyzes the secondary electrons that are emitted from the sample. Contrast is also provided by means of atomic weights; in this case, high atomic weights appear lighter. SEM is easier to use and understand but is not capable of as high a magnification as TEM. SEM is typically limited to about 50,000X.

In recent years, new techniques known as *probe microscopies* have become available. In these techniques, fine mechanical probes are brought very close to a surface and the interaction of the tip of the probe with the surface is determined. If the sample is a conductor or semiconductor, the probe can be brought near to the sample surface and an electrical bias is applied. This causes electrons to tunnel from the probe tip to the sample surface. The tip can be rastered over the surface and either the current draw or the applied bias can be controlled through a feedback circuit. The level of feedback can be used as a measure of the surface morphology. The applied potential or current draw can be plotted as a function of the raster position and a topological picture can be developed. This technique can provide extremely high resolution pictures of the surface topology, down to atomic levels. This technique is known as **Scanning Tunneling Microscopy** or STM.

An important variation on the STM is the **Atomic Force Microscope** or **AFM**. In this scanning probe technique, a sharp tip, usually made from a ceramic insulator such as silicon nitride, is attached to a cantilever. The back of the cantilever is silvered and a laser is reflected from that mirror. The deflection of the cantilever is monitored by the deflection of the laser beam. If the tip is brought very close to a surface and if the force constant of the cantilever is small, the assembly can sense dispersion forces.

The sample is mounted on a piezoelectric crystal. A feedback circuit is employed to keep the tip at a constant displacement from the surface. A surface topology map can be obtained from the combination of the output of the feedback circuit and the voltages applied to the piezoelectric crystal. Atomic resolution is possible with the AFM on any type of insulator. In the most recent instruments, the tip of the cantilever is not continuously in contact with the surface. Indeed, for soft materials, dragging the tip along the surface can create artifactual damage. In newer instruments, the tip is “tapped” along the surface rather than dragged, thus minimizing damage. In addition, the instrument can be used to measure force-distance profiles between the tip and the surface. In this way, a map can be made of the specific interactions of the surface and the tip. This technique should prove extremely useful in the study of adhesion since it can probe any type of surface.

An additional feature of both AFM and STM is that both techniques can be used under normal atmospheric conditions and even immersed in liquids.

## ■ 4.8 Summary

In this chapter, the basics of surface science necessary for the understanding of the relationship between surface phenomena and adhesion have been described. The chapter began with a review of the fundamental forces between atoms and molecules that give rise not only to the cohesive strength of materials, but also to forces at surfaces. A quantity known as the surface energy was derived and was described in a number of phenomenological as well as theoretical ways. The differences between solid surface energy and liquid surface tension (energy) were highlighted. Methods of measurement of solid and liquid surface energy were described. In particular, two measurements, the surface forces apparatus and the contact angle method were described in detail as a means to probe the surface energetics of solids. The JKR theory, which is used to describe the surface forces measurement, was described to exemplify the energy balance approach to adhesive interactions. Regarding contact angle measurements, the theories of Good and Girifalco as well as that of Fowkes were highlighted. The Zisman critical wetting tension measurement was also described and noted as being of particular importance in the science of adhesion.

The end of the chapter described modern methods of surface analysis. X-ray photoelectron spectroscopy was described as the method most widely used for surface chemical analysis in adhesion science. Electron microscopy was described as the technique most widely used for surface topography determination.

## ■ Bibliography

- Israelachvili, J., *Intermolecular and Surface Forces*, 2nd Ed (1991) Academic Press, London  
 Wu, S., *Polymer Interfaces and Adhesion* (1982) Marcel Dekker, New York  
 Patrick, R. L., (Ed.), *Treatise on Adhesion and Adhesives*, Volume 1: Theory (1969) Marcel Dekker, New York  
 Briggs, D. and Seah, M. P. (Eds.), *Practical Surface Analysis*, Vols. 1 and 2, 2<sup>nd</sup> Ed. (1990) Wiley, New York  
 Stokes, R. J. and Evans, D. F., *Fundamentals of Interfacial Engineering* (1997) Wiley-VCH, New York

## ■ References

- [1] Eggers, Jr., D. F., Gregory, N. W., Halsey Jr., G. D., Rabinovitch, B. S., *Physical Chemistry* (1964) John Wiley and Sons, New York, pp. 168–173
- [2] Hirschfelder, O., Curtis, C. F., Bird, R. B., *Molecular Theory of Gases and Liquids* (1954) John Wiley, New York
- [3a] Keesom, W. H., *Phys. Z.* (1921) 22, p. 126
- [3b] Keesom, W. H., *Phys. Z.* (1922) 23, p. 225
- [4a] Debye, P., *Phys. Zh.* (1920) 23, p. 178
- [4b] P. Debye, *Phys. Zh.* (1921) 22, p. 302
- [5a] Lifschitz, E. M., *Doklady Akademii Nauk. USSR* (1954) 47, p. 643
- [5b] Dzyaloshinskii, I. E., Lifschitz, E. M., Pitaevskii, L. P., *Advances in Physics*, vol. 10 (1961) p. 165
- [6] Grimley, T. B., in: *Aspects of Adhesion*, vol. 7 (1974) Transcripta Books, London, p. 11
- [7] Israelachvili, J. N., *Intermolecular and Surface Forces*, 2<sup>nd</sup> ed. (1991) Academic Press, London, Ch. 6
- [8] Lennard-Jones, J. E., *Proc. Roy. Soc. London, Ser. A* (1924) 196, p. 463
- [9] Adamson, A. W., *Physical Chemistry of Surfaces*, 4<sup>th</sup> ed. (1982) Wiley-Interscience, New York
- [10a] Beaglehole, D., *Phys. Rev. Lett.* (1979) 43 p. 2016
- [10b] Thomas, B. N., Barton, S. W., Novak, F., Rice, S. A., *J. Chem. Phys.* (1987) 86, p. 1036
- [11] Fowler, R., Guggenheim, E. A., *Statistical Thermodynamics* (1952) Cambridge University Press, Cambridge, UK
- [12] Good, R. J., in *Treatise on Adhesion and Adhesives* vol. 1. Patrick, R. L. (Ed.) (1969) Marcel Dekker, New York, p. 50

- [13] Griffith, A. A., *Phil. Trans. Roy. Soc.*, A221 (1920) p. 163
- [14] Dupré, A., *Theorie Mechanique de la Chaleur* (1869) Gauthier-Villars, Paris, p. 369
- [15] Wilhelmy, L., *Ann. Phys.* (1863) 119, p. 177
- [16] du Nuoy, P. Lecounte, *J. Gen. Physiol.* (1919) 1, p. 521
- [17a] Harkins, W. D., Brown, F. E., *J. Am. Chem. Soc.* (1919) 41, p. 499
- [17b] Harkins, W. D., *Physical Chemistry of Surface Films* (1952) Reinhold, New York
- [18] Andreas, J. M., Hauser, E. A., Tucker, W. B., *J. Phys. Chem.* (1938) 42, p. 1001
- [19a] Johnson, Jr., R. E., Dettre, R. H., *J. Phys. Chem.* (1964) 68, p. 1744
- [19b] Johnson, Jr., R. E., Dettre, R. H., in *Surface and Colloid Science*, Vol. 2. Matijevic, E. (Ed.) (1969) Wiley-Interscience, New York
- [19c] Wenzel, R. N., *Ind. Eng. Chem.* (1936) 28, p. 988
- [19d] Cassie, A. B. D., Baxter, S., *Trans. Far. Soc.* (1944) 40, p. 546
- [20] Young, T., *Trans. Roy. Soc.* (1805) 95, p. 65
- [21] Cherry, B. W., *Polymer Surfaces* (1981) Cambridge Univ. Press, Cambridge, pp. 24–25
- [22] Israelachvili, J. N., *Chemtracts: Anal Phys. Chem.* (1989) 1, p. 1
- [23] Johnson, K. L., Kendall, K., Roberts, A. D., *Proc. Roy. Soc. Ser. A.* (1971) 324, p. 301
- [24] Hertz, H., *Miscellaneous Papers*, Jones, Schott (Eds.) (1896) Macmillan, London
- [25] Johnson, K. L., *Brit. J. Appl. Physics* (1958) 9, p. 199
- [26] Maugis, D., Barquins, M., *J. Phys D.: Appl. Phys.* (1978) 11, p. 1989
- [27] Derjaquin, B. V., *Kolloid Zh.* (1934) 69, p. 155
- [28] Tabor, D., Winterton, R. H. S., *Proc. Roy. Soc. Ser. A.* (1969) 312, p. 435
- [29a] Israelachvili, J. N., Tabor, D., *Proc. Roy. Soc. Ser. A.* (1972) 331, p. 19
- [29b] Israelachvili, J. N., Adams, G. E. J., *J. Chem Soc. Faraday Trans. I* (1978) 74, p. 975
- [30a] Merrill, W. W., Pocius, A. V., Thakker, B. V., Tirrell, M., *Langmuir* (1991) 7, p. 1975
- [30b] Mangipudi, V., Tirrell, M., Pocius, A. V., *J. Adhesion Sci. Technol.* (1994) 8, p. 1
- [30c] Mangipudi, V., Tirrell, M., Pocius, A. V., *Langmuir* (1995) 11, p. 19
- [30d] Falsafi, A., Tirrell, M., Pocius, A. V., *Langmuir* (2000) 16, p. 1816
- [31a] Girifalco, L. A., Good, R. J., *J. Phys Chem.* (1957) 61, p. 904
- [31b] Good, R. J., *J. Phys Chem.* (1958) 62, p. 1418
- [31c] Good, R. J., Girifalco, L. A., *J. Phys. Chem.* (1960) 64, p. 561
- [31d] Good, R. J., Hope, C. J., *J. Coll. Interface Science* (1971) 35, p. 171
- [32] Cherry, B. W., *Polymer Surfaces* (1981) Cambridge University Press, Cambridge UK, pp. 2–4.
- [33] Good, R. J., Elbing, E., *Ind. Eng. Chem.* (1970) 62(3), p. 54
- [34a] Fowkes, F. M., *J. Phys. Chem.* (1962) 66, p. 382
- [34b] Fowkes, F. M., *J. Phys. Chem.* (1963) 67, p. 2538
- [35] Fowkes, F. M., *Ind. Eng. Chem.* (1964) 56(12), p. 40
- [36] Israelachvili, J. N., *J. Chem. Soc., Faraday Trans., II* (1973) 45,, p. 69
- [37] Owens, D. K., Wendt, R. C., *J. Appl. Polymer Sci.* (1969) 13, p. 1740
- [38a] Fox, H. W., Zisman, W. A., *J. Colloid. Sci.* (1950) 5, p. 514
- [38b] Fox, H. W., Zisman, W. A., *J. Colloid. Sci.* (1952) 7, p. 109
- [38c] Fox, H. W., Zisman, W. A., *J. Colloid. Sci.* (1952) 7, p. 428
- [38d] Zisman, W. A., in: *Advances in Chemistry Series*, No. 43. Gould, R. F. (Ed.) (1964) American Chemical Society, Washington, DC, pp. 1–51
- [38e] Zisman, W. A., in: *Polymer Science and Technology*, Vol. 9 A. Lee, L. H. (Ed.) (1975) Plenum Press, New York, pp. 55–91
- [39] Kitazaki, Y., Hata, T., *J. Adhesion* (1972) 4, p. 123

- [40a] Whitesides, G. M., Ferguson, G. S., *Chemtracts- Organic Chemistry* (1988) 1, pp. 171–187  
 [40b] Bain, C. D., Whitesides, G. M., *Langmuir* (1989) 5, p. 1370  
 [40c] Bain, C. D., Whitesides, G. M., *Science* (1988) 240, p. 62

## ■ Problems and Review Questions



1. Polyethylene and polypropylene are both purely hydrocarbon polymers. Why is the critical wetting tension of polypropylene less than that of polyethylene?
2. Using the following data and the concept of fractional polarity due to Fowkes, calculate the dispersion force contribution to the surface energy of water.

Hydrocarbon	$\gamma_{\text{Hydrocarbon}}$ (mJ/m <sup>2</sup> )	$\gamma_{\text{Hydrocarbon,mercury}}$ (mJ/m <sup>2</sup> )	$\gamma_{\text{Mercury}}^d$ (mJ/m <sup>2</sup> )	$\gamma_{\text{Hydrocarbon,water}}$ (mJ/m <sup>2</sup> )	$\gamma_{\text{water}}^d$ (mJ/m <sup>2</sup> )
n-hexane	18.4	378	210	51.1	?
n-heptane	20.4			50.2	?
n-octane	21.8	375	199	50.8	?
n-decane	23.9			51.2	?
n-tetradecane	25.6			52.2	?
Cyclohexane	25.5			50.2	?

3. Using the expression for the Lennard-Jones potential, show that

$$E = \frac{32 \gamma}{r_0}$$

- 4a. Using the expression for the total force between two surfaces (under a Lennard-Jones potential energy of interaction), derive an expression for the maximum force between two surfaces. This is also the ultimate (theoretical) strength of a material.
- 4b. An equation can be derived for the relationship between the Young's modulus and the "ideal tensile strength" of a van der Waals solid. That equation is:  $F_{\text{max}} = 0.064 E$ . Complete the following table

Material	Tensile modulus (MPa)	Calculated ultimate strength (MPa)	Measured ultimate tensile stress (MPa)
Epoxy resin	3500		90
Polycarbonate	2400		65
Polystyrene	4100		83



- 4c. Compare the calculated and measured strengths of these materials. Which is larger? What does this tell us about the strength of materials and what controls it?
5. Given the following data, determine the critical wetting tension of the surface.

Liquid	$\gamma_L$ (mJ/m <sup>2</sup> )	Contact angle between the liquid and the surface
Dimethylsulfoxide	44.2	38
Diiodomethane	50.8	29.5
Formamide	58.3	56
Glycerol	63.4	70
water	72.8	77
Tricresyl phosphate	41	7

# 5

## Basic Physico/Chemical Properties of Polymers

### ■ 5.1 Introduction

In Chapter 2, we discussed fundamental properties of all materials. The tensile, shear, and fracture properties of materials were described. In Chapter 3, we discussed test methods that probed these properties for adhesives. The adhesives of interest are based upon organic materials. In particular, we are concerned with those materials that are polymeric or become polymeric in nature during the formation of an adhesive bond. It is important to discuss and to develop at least a basic understanding of the physico/chemical properties of polymers and how these properties affect the polymers' performance in an adhesive bond. In this chapter, we describe those physico/chemical characteristics causing a polymer to be different from non-polymeric materials. The parameters describing these differences are discussed. In addition, we discuss the materials properties particular to polymers. These properties include thermal transitions as well as the response of polymers to temperature and rate of application of stress. Linear viscoelasticity plays an important role in this chapter. Some discussion of methods for measuring these properties is given.

It is the goal of this chapter to lay the basis for relating surface science and polymer physical properties to the understanding of adhesion phenomena. Molecular weight and the thermal transitions of polymeric materials are discussed. Relations are made between graphs of dynamic mechanical properties and the chemical structures of polymers. Basic discussions of the time-temperature superposition principle as well as the meaning and use of the shift factor from the Williams-Landel-Ferry (WLF) equation are provided.

## ■ 5.2 Basic Terminology

### 5.2.1 Monomers versus Polymers

The word *polymer* comes from the Greek “poly” meaning “many” and “mer” meaning part. Thus, polymers are made of many parts. The “mers” (or “monomers”) are the individual units of molecules that have been linked together to form the polymer chain. In layman’s terms, plastics are polymers, although it must be stated that not all polymers behave plastically under all conditions. It may be gathered from this discussion that the main differentiating feature of polymers from monomers is that they are long chains with the monomer units being the links in the chain. One parameter characterizing these long chains is their molecular weight, and that subject forms a portion of this discussion.

### 5.2.2 Basic Types of Polymeric Materials

Polymers can be classified according to their response to heat and also to the application and rate of application of stress. Polymers can be classified as either *thermoplastics* or *thermosets*. Thermoplastic materials melt upon heating and return to their original chemical state upon cooling. Thermoset materials become infusible and insoluble upon heating and, after heating, do not return to their original chemical state upon cooling. Thermosets, in general, chemically degrade upon continued heating.

Thermoplastics can be further classified as *amorphous* or *semi-crystalline*. Amorphous thermoplastics have no long-range order on the supermolecular level. Semi-crystalline thermoplastics have at least some portion of their bulk (and surface) in a state exhibiting long range order. If an amorphous thermoplastic is examined crystallographically, only amorphous halos are observed in the diffraction experiment. Semi-crystalline polymers exhibit both an amorphous halo as well as well-defined crystal patterns. The degree of crystallinity in a semi-crystalline polymer determines its physical properties to a great degree. Thermoset materials can be amorphous or semicrystalline. In general, thermoset materials are in the monomeric or *oligomeric* state when applied as an adhesive. An oligomer is a monomer that has been polymerized to only a low molecular weight.

Polymers are also classified by the arrangement of the monomers used to synthesize the polymer. If a single monomer is used to make a polymer, the result is a *homopolymer*. If one or more monomers are used to make a polymer, the result is a *co-polymer*. The way in which a copolymer is formed is also important.

If the monomers react with each other in a totally random manner, the result is a *random copolymer*. If the monomers are A and B, but B can react with only A and vice versa, the result will be an *alternating copolymer*. Finally, if we have two monomers C and D, and we react them such that we polymerize C only with C, and then form a terminal group that is reactive with D and then we polymerize D from that point, we have a *block copolymer* whose structure can be written as  $-[C]_x-[D]_y-$ , where  $x$  and  $y$  are the number of monomers reacted in each block.

We can also classify polymers according to their response to stress. Figure 5.1 shows tensile stress-strain curves for three distinct types of polymers. The curves should be examined according to two criteria. First, look at how much strain is induced in the material at a near ultimate stress. Second, examine the curves for their strain energy density. Curve 1 represents a polymer having a high Young's modulus (stiffness) but low elongation at break, resulting in a relatively small strain energy density at break. This type of polymer is called *brittle*. As discussed in the previous chapter, the term "brittle" means inability to absorb mechanical energy. Curve 3 represents a polymer that has a low Young's modulus and a very long strain to break. This type of polymer is classified as an *elastomer*. Note that the strain energy at break is moderately high for this type of polymer. Curve 2 corresponds to a "tough" or leathery type of polymer. Note that the stiffness is relatively high and the strain at break is at least intermediate between the other two types. A tough material is capable of a high strain energy density. Joining materials should have a high strain energy density capability as this indicates that the material can absorb a lot of energy before breaking. In later chapters, we discuss the chemistry of materials that enable the formulator to generate adhesives with a high strain energy density capability.

One of the unique features of polymeric materials is that a single high molecular weight polymer can exhibit all three of the stress strain curves shown in Fig. 5.1.

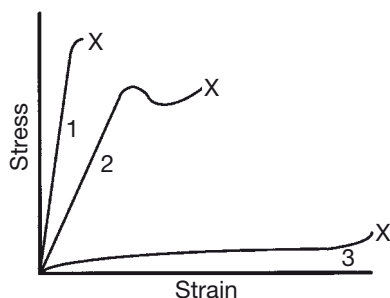


**FIGURE 5.1** Stress-strain curves for three distinct types of polymers. The "X" marks the ultimate property of the polymer. Curve 1 corresponds to a brittle polymer, curve 3 corresponds to an elastomeric polymer, while curve 2 corresponds to a tough or leathery polymer

However, a single high molecular weight polymer does not exhibit all of these characteristics at a single temperature or at a single rate of extension. A non-thermosetting, high molecular weight polymer is elastomeric at high temperatures, brittle at low temperatures, and can exhibit tough or leathery character at intermediate temperatures. In addition, at a single temperature and at high strain rates, polymers will behave as if they are at low temperatures, i.e., brittle. At a single temperature and low strain rates, a high molecular weight polymer behaves as if it were at high temperatures, i.e., elastomeric. This unique property of polymers is known as *time-temperature equivalency*, which forms the basis for much discussion in this and later chapters.

### 5.2.3 Molecular Weight

The primary characteristic that differentiates polymers from other materials is their chain-like structure. Essentially all of the processes used to manufacture polymers produce materials with a distribution of chain lengths and therefore, a distribution of molecular weights. With the exception of genetically engineered polymers, most polymers have a multitude of molecular weights, rather than a single molecular weight. As a result, *distributions* rather than a single number, characterize the molecular weight of a polymer. Figure 5.2 shows a schematic molecular weight distribution curve for a polymer.

The molecular weight distribution shown in Fig. 5.2 could be considered either broad or narrow depending upon the range of the abscissa. Two average molecular weights are shown in Fig. 5.2. If  $N_i$  is the number of molecules at a certain molecular weight  $M_i$ , then

$$\bar{M}_n = \frac{\sum_i N_i M_i}{\sum_i N_i} \quad (5.1)$$

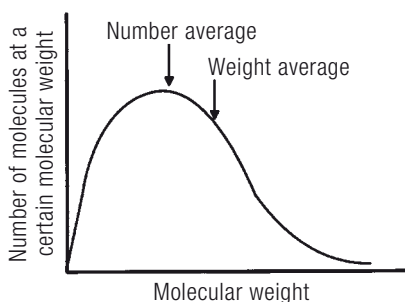


**FIGURE 5.2** Schematic molecular weight distribution curve. The curve shows that a polymer has a wide range of molecular weights. Two average molecular weights are shown as well as their relative position on the molecular weight curves

and

$$\bar{M}_w = \frac{\sum_i N_i M_i^2}{\sum_i N_i M_i} \quad (5.2)$$

The two average molecular weights are just the first and second moments of the molecular weight distribution. The number average molecular weight,  $\bar{M}_n$ , tends to be near the maximum in the molecular weight distribution curve. The weight average molecular weight,  $\bar{M}_w$ , tends toward the high molecular weight side of the distribution curve. A parameter for describing the breadth of the distribution is the *polydispersity* that is defined as

$$\text{polydispersity} = \frac{\bar{M}_w}{\bar{M}_n} \quad (5.3)$$

A high polydispersity means a broad molecular weight distribution while a small polydispersity denotes a narrow molecular weight distribution. The molecular weight of a polymer and its polydispersity control many of its properties, including its properties as an adhesive.

A particularly important molecular weight is known as the *entanglement molecular weight*,  $M_e$ , see Fig. 5.3. This parameter is determined by measuring the melt viscosity of a polymer as a function of average molecular weight. As shown in Fig. 5.3, the log of the melt viscosity of a polymer as a function of the log of its weight average

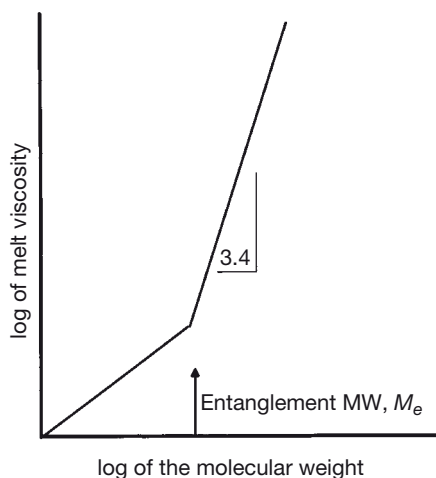


**FIGURE 5.3** Plot of the log of the melt viscosity versus molecular weight for a polymer.

At low molecular weights, the log of the melt viscosity varies approximately linearly with the log of the molecular weight. At some point, this relationship changes drastically and the log of the viscosity varies as the 3.4 power of the molecular weight. The break point is known as the entanglement molecular weight,  $M_e$ .

molecular weight, the curve shows an abrupt change in slope at a certain molecular weight. After the abrupt change, the slope is about 3.4. The point at which the slope changes is known as the entanglement molecular weight,  $M_e$ . As discussed above, polymers are long chain molecules. Below the entanglement molecular weight, the polymer chains are fairly free to move past each other. Above  $M_e$ , the molecular weight has become so high and the polymer chains have become so intertwined that one cannot pull on one chain without pulling on a substantial number of them. Thus, above  $M_e$  the polymer has substantially different flow characteristics than below  $M_e$ , and the polymer also has substantially different ability to absorb strain.  $M_e$  is a characteristic describing amorphous or semi-crystalline thermoplastics.

Thermoplastic materials are normally pictured as long chains that can move past each other to some degree. Thermoset materials are molecules of essentially infinite molecular weight and they do not flow when heated after they have set. The chemical basis for the thermosetting character of some adhesive materials is described in later chapters. At this point, we say that there are chemical means through which one can tie together many long molecular weight chains at various points along their lengths. If every chain is chemically linked to every other chain, the polymer is thought to have infinite molecular weight. The characteristic molecular weight of thermosets is  $M_c$  or the *molecular weight between crosslinks*. A crosslink is a tie point between two polymer chains. There are various chemical and physical means by which the molecular weight between crosslinks can be determined. Some of these are discussed below.

## ■ 5.3 Thermal Transitions of Polymers

We are all familiar with the fact that low molecular weight materials undergo phase changes as a function of temperature. For example, water is a solid below 0 °C and is a gas above 100 °C at atmospheric pressure. The temperatures that characterize water are thus the  $T_m$  or melt point (0 °C) and the boiling point  $T_{bp}$  (100 °C). In a similar manner, polymers have thermal transitions. Semi-crystalline thermoplastic polymers exhibit a  $T_m$  just as low molecular weight solids do. Amorphous thermoplastics do not exhibit a  $T_m$ . Thermoset polymers do not flow or melt and hence do not have a  $T_m$ . Because of their high molecular weight, no polymers exhibit a  $T_{bp}$ . Some *oligomers* will exhibit a boiling point and can be distilled.

Polymers also exhibit a number of other thermal transitions that are not primary transitions such as those described above. In spite of their high molecular weight, polymer chain motion can take place at temperatures far below  $T_m$ . For example, the backbone of the polymer chain can vibrate and, in fact, can move in restricted

crankshaft motions if enough thermal energy is available to the system. If a polymer chain has side groups, these can vibrate and rotate if enough thermal energy is available to them. If we take a polymer down to 0°K and warm it up, we find that the polymer goes through several transitions until its decomposition temperature is reached. These transitions are usually given Greek letters with the higher letters representing transitions at lower and lower temperatures. In addition to the melt temperature, the transition that is of most concern to adhesion scientists is the alpha transition or the *glass transition temperature*,  $T_g$ . The glass transition temperature is the temperature at which a polymer's physical properties change from that of a glass to that of a tough or leathery material. It is usually associated with the onset of long range motion in the polymer backbone.

### 5.3.1 Measurement of $T_g$

One of the more straightforward methods of measuring  $T_g$  that may be easily related to adhesive properties, is dynamic mechanical analysis. We discuss this method later. There are several other methods that can also be used. A simple method is differential scanning calorimetry (DSC). In this method, a small sample of polymer is placed in a sealed metal pan that is placed in a calorimeter capable of measuring small heat flows in the sample. The temperature is increased. At the glass transition temperature, the rate of heat flow into the sample increases, causing a change in slope as the thermal motions in the polymer are excited. The  $T_g$  is not a first order thermodynamic transition and is therefore rate dependent. It is important to know the rate at which the measurement is carried out. DSC is capable of measuring  $T_g$  at very slow rates. Another means of measuring  $T_g$  is through the determination of the refractive index as a function of temperature. The refractive index of a polymer decreases with temperature. The slope of such a plot exhibits a substantial change at the glass transition temperature.

The physical properties of a polymer also exhibit a rather substantial change at the glass transition temperature. Below the glass transition temperature, a polymer acts as though it is a glass and has high stiffness. It is interesting to note that essentially all polymers have similar glassy moduli of about  $3 \times 10^9$  Pascal. Above the glass transition temperature, the material first behaves tough or leathery and at higher temperatures, behaves as an elastomer. The modulus of the material decreases substantially above the  $T_g$ . Another way of determining the glass transition temperature of a polymer is to measure the stress-strain properties as a function of temperature. Although effective, this set of data is quite tedious to collect. For many adhesive materials, the maximizing of adhesive properties in the temperature range between  $T_g$  and  $T_m$  or the decomposition temperature of a thermoset is the goal of the adhesive formulator.



## ■ 5.4 Dynamic Mechanical Measurements and Viscoelasticity

In Chapter 2, we defined the complex modulus of a viscoelastic material as well as the storage and loss moduli. That description provided the basis for linear viscoelasticity, but it did not provide a discussion of the means by which we measure these properties. In this section, methods through which these properties can be measured are described. The measurement of the viscoelastic properties of polymers by the application of a sinusoidal stress is known as *dynamic mechanical spectroscopy*.

### 5.4.1 Methods of Measurement of Dynamic Mechanical Properties

A schematic diagram of an instrument for the measurement of dynamic mechanical properties is shown in Fig. 5.4. The diagram is an extremely simple version of the many complicated devices of this type now available. A sample of polymer is firmly clamped between two pieces of metal that are much stiffer than the sample. One of the clamps is connected to a sinusoidal driving device while the other is connected to a force transducer. The instrument should be capable of measuring both the frequency and the amplitude of the driven and transduced signals. The resulting data can then be analyzed as described in Chapter 2. An important feature (which was not emphasized in Chapter 2) is that dynamic mechanical measurements are done as a function of temperature (at a single frequency) or frequency (at a single temperature). The most versatile instruments of this type can carry out the measurement both of these ways. The reasons for the importance of this statement are made clear in this and later chapters.

The sample configuration shown in Fig. 5.4 is analogous to the lap shear specimen discussed in Chapter 3. The measurement done in this mode provides the shear storage and loss moduli. The measurement can be carried out so that the sample is

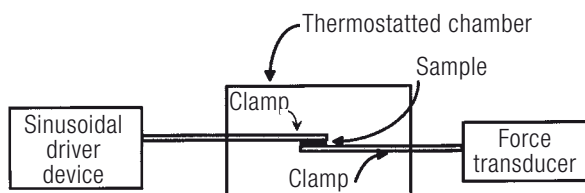


**FIGURE 5.4** Diagram of a simple dynamic mechanical spectrometer used to measure the shear properties of a material. Note that a sinusoidal driver device is used. Frequency and temperature are controlled. The stiffness of the device must exceed that of the sample for the measurements to be valid

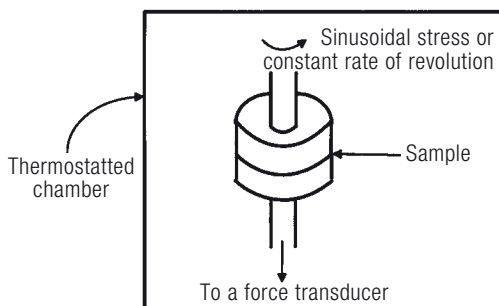


**FIGURE 5.5** Simplistic diagram of the sensor head in a rotating viscometer.

Note that in this configuration the sample is in pure shear

suspended between the two clamps. The measurement is then in tension and the corresponding Young's moduli are determined. The sample must be stiff enough at the temperature and frequency range of interest, so that it does not slump or change shape during the measurement.

Another important means to make dynamic measurements is by a rotating or oscillating rheometer. A schematic of a sample configuration for such a rheometer is shown in Fig. 5.5. The sample is placed in a state of shear. The complex shear modulus can be determined by the application of an oscillating sinusoidal stress. This instrument is also useful for determining the viscosity of a material as a function of shear rate, which is controlled by the rate of revolution of the upper spindle. Yield stresses of fluids can be measured as a function of temperature as well. This last measurement is important in the design of materials with non-sag characteristics.

The last dynamic mechanical spectrometer discussed here is the torsion pendulum. This spectrometer was well researched by Gilham and his group at Princeton University [1]. A schematic of the apparatus is found in Fig. 5.6. A device that provides the spin also holds the sample. The spin is transmitted through the sample and the specimen rotates. When the spin is abruptly released (analogous to the wind-up and release of a mainspring), the response of the specimen to the initial perturbation is determined by watching the decay of the resulting oscillation.

The oscillation can be observed in any one of a number of different ways. For example, on the bottom of the pendulum, a disk can be placed upon which is a digital code for position. A bank of lights and photodiodes can read the digital code. An exponentially damped sinusoidal curve results. The measured quantities are the frequency of oscillation and the decrease in the amplitude of the oscillation as a function of time (damping). This is not a direct measurement of modulus. The frequency of the oscillation is related to the stiffness of the material and the decrease in amplitude per cycle is related to the energy lost by the sample. The  $\tan \delta$  can be determined from this measurement. If  $G'$  or  $G''$  has been determined independently, the other

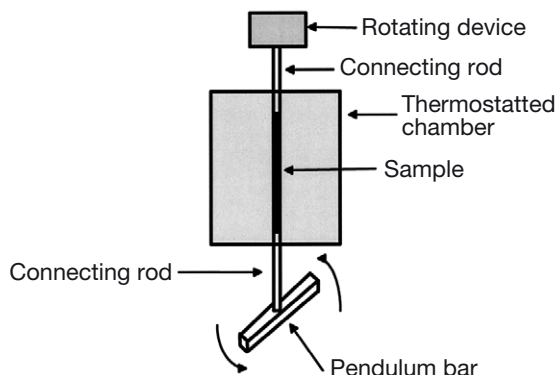


**FIGURE 5.6** Schematic diagram of a torsion pendulum device used to measure dynamic mechanical properties of a polymer. If the sample is generated using a braid into which a thermoset polymer has been impregnated, the device can be used to measure the cure rate and the change in physical properties as a function of cure time

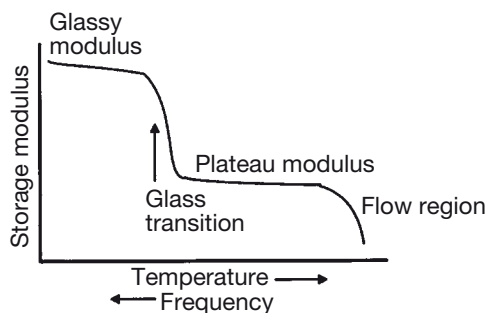
can be determined with  $\tan \delta$ . The apparatus shown in Fig 5.6 has not found as much use as the other instruments described earlier because the actual Young's or shear moduli cannot be determined directly. The apparatus is, however, very useful for the study of the cure processes of thermosetting materials.

A glass braid can be impregnated with a thermosetting polymer. The braid is then placed in a thermostatted compartment in the torsion braid analyzer. The sample is heated and the stiffness of the sample is determined as a function of time. Gilham has made good use of this type of analysis in his description of T-T-T plots (Time-Temperature-Transformation plots) for thermosetting materials which we discuss later in this book [2].

#### 5.4.2 Examples of Dynamic Mechanical Data for Polymers

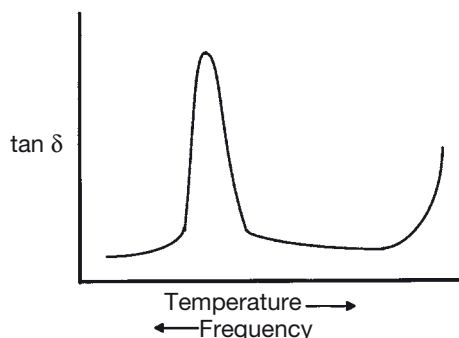
In this section we do not differentiate between the Young and shear moduli but describe the parameters determined as the storage modulus, loss modulus, and  $\tan \delta$ . A typical dynamic mechanical spectrum for the storage modulus of an amorphous polymer is shown in Fig. 5.7. The absolute value of the temperature axis is not shown, as this is a generic curve. It should be noted that a similarly shaped curve is obtained for all amorphous polymeric materials, regardless of type. The curves shift along the temperature axis or vertically along the modulus axis, but the general features are very much like Fig. 5.7.

A plot of the loss modulus of this generic amorphous polymer has a shape similar to that of Fig. 5.7 except that the plot is inverted, i.e., the material has a higher loss modulus at those temperatures or frequencies when the storage modulus is low.

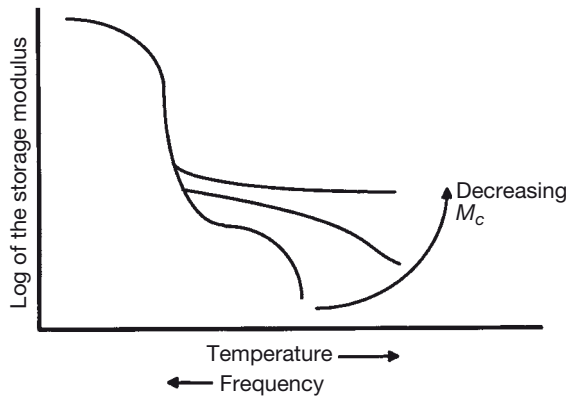


**FIGURE 5.7** Generic dynamic mechanical spectrum for an amorphous thermoplastic. Note that the modulus drops sharply as the glass transition temperature is reached. Note that the abscissa can be either temperature or frequency. Similar curves are obtained for either variable, except that they act inversely to one another

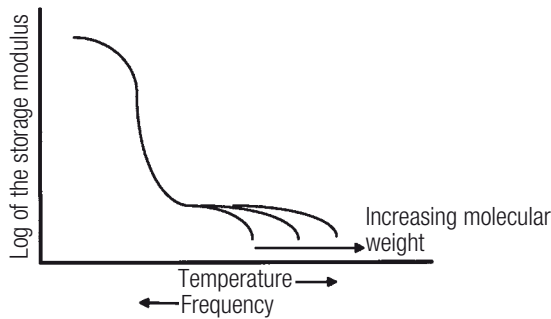
The plot for  $\tan \delta$  of the same generic amorphous polymer looks similar to that shown in Fig. 5.8. Note that the  $\tan \delta$  curve displays a peak at about the same point that the storage modulus curve exhibits the maximum change in slope. Researchers have often designated the maximum in the  $\tan \delta$  curve as the glass transition temperature. It is important to note, however, that the position of the maximum change in slope or the position of the peak in the loss modulus curve is not only dependent upon temperature, but also dependent upon frequency. Thus, if one determines dynamic mechanical spectra for a polymer at a single temperature but at various frequencies, a similar curve to that shown above is obtained, with the exception that the abscissa would be changing frequency instead of temperature. It is important to not only quote the glass transition temperature, but also the frequency at which the measurement was made when reporting such data. This property of viscoelastic materials is known as *time-temperature superposition*.



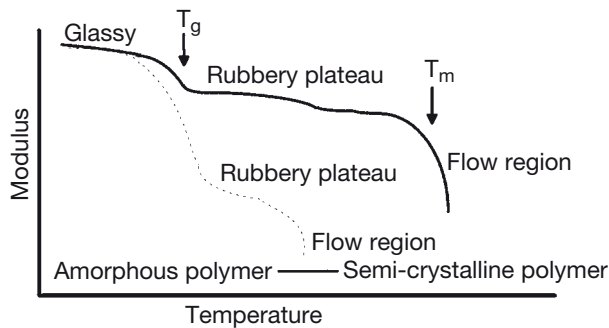
**FIGURE 5.8** Plot of the log of the loss modulus as a function of either frequency or temperature. Note that the frequency and the temperature are inversely related. The peak in the curve corresponds closely with the position of the glass transition at the measurement frequency



**FIGURE 5.9** Dynamic mechanical spectra for a thermoset showing the effect of variation in the crosslink density or  $M_c$



**FIGURE 5.10** Dynamic mechanical spectra for an amorphous thermoplastic showing the effect of increasing the molecular weight



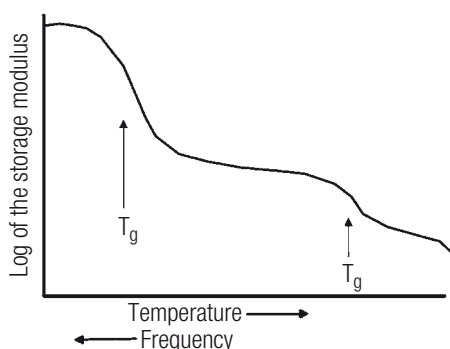
**FIGURE 5.11** Dynamic mechanical spectra showing the difference in response between an amorphous thermoplastic and a semi-crystalline thermoplastic

Fig. 5.9 shows the dynamic mechanical spectra determined for a thermosetting polymer as a function of the degree of crosslinking.  $M_c$  is the molecular weight between crosslinks. As can easily be seen, the value as well as the extent of the plateau modulus is dependent upon  $M_c$ . Note that as  $M_c$  decreases, the flow region of the polymer begins to disappear. This behavior can be expected for a thermosetting material. Note also that the amount of decrease in the storage modulus decreases as the  $M_c$  decreases. This is also to be expected since an increase in crosslink density means a decrease in chain mobility.

We have described the effect of molecular weight on melt viscosity and the entanglement molecular weight,  $M_e$ . We would expect that the dynamic mechanical spectrum would also show some effect of the increase in molecular weight. Figure 5.10 shows that increasing the molecular weight of a polymer increases the temperature at which flow occurs. This has the effect of increasing the extent of the rubbery plateau. The features shown in the figures in this chapter are important in our discussion of structural adhesives, hot melt adhesives, and particularly pressure sensitive adhesives.

Figure 5.11 shows the dynamic mechanical spectrum of a semi-crystalline polymer. The crystallites have the effect of being a “physical cross-link”. That is, the mobility of the polymer is inhibited by the presence of the crystallites. This results in an increase in the value of the plateau modulus as well as its extent.

Finally, Fig. 5.12 shows a dynamic mechanical spectrum for a polymer blend that has separated into two phases. Such a situation can occur for block co-polymers. That is, instead of forming one continuous homogenous phase of material, the material forms two co-existing phases, each of which has its own properties. In such a case, we would expect two glass transition temperatures.



**FIGURE 5.12** Dynamic mechanical spectrum for an amorphous block co-polymer in which the portions of the co-polymer have phase-separated is shown. Note the presence of two glass transition temperatures

## ■ 5.5 Time-Temperature Superposition

In Figs. 5.8–5.12, the abscissa was labeled as increasing temperature or decreasing frequency. For polymers, the effect of changing these variables is identical. A significant amount of the knowledge of the molecular basis for polymer properties has come from the experimental and theoretical study of the time-temperature superposition.

In any dynamic mechanical experiment, one typically varies either the temperature or the frequency over a specific range and measures the modulus of the material. The range of frequencies over which one can do experiments easily is limited, since extremely low frequencies are hard to maintain and are difficult to measure. If we measure the response of a polymer to a small range of easily accessible frequencies (such as 0.1 to 100 Hz) and measure these responses over a wide range of temperatures (which are more easily variable, measurable, and maintainable) we can get the family of curves shown in Fig. 5.13. The temperatures are in the order  $T_1 < T_2 < T_3 < T_4 < T_5 < T_6$ . Examination of this generic data says that by shifting the curve for  $T_6$  to the left and the curves for temperatures  $T_1$  through  $T_4$  to the right by some amount, then all of the curves would form a smooth curve in the shifted frequency space. This is found to be the case for most polymeric materials. The result is known as a *master curve* and the amount by which a segment is shifted is known as a *shift factor*. Thus, a master curve is a plot of the log of the storage modulus (or other modulus) as a function of a reduced rate variable. The reduced variable is obtained by multiplying the frequency by the shift factor. Thus, a set of curves such as that shown in Fig. 5.13 can be reduced to a single curve such as that shown in Fig. 5.14.

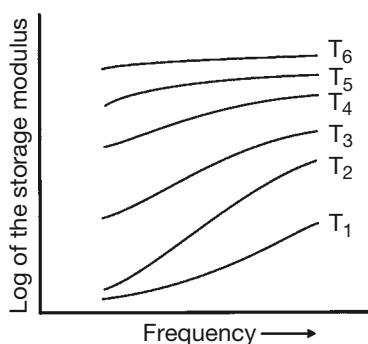


**FIGURE 5.13** Plot of the log of the storage modulus of an amorphous thermoplastic measured as a function of frequency at six temperatures  $T_1 < T_2 < T_3$  etc.

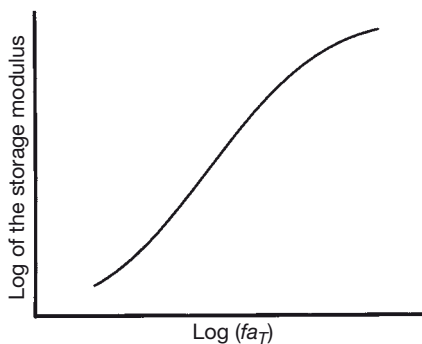


**FIGURE 5.14** A “master curve” which could have been constructed from the data presented in schematic form in Fig. 5.13

In Fig. 5.14,  $f$  is the frequency and  $a_T$  is the shift factor. The shift factors can be determined solely from overlapping the curves in each plot. Care must be taken that enough overlap is obtained with each curve, so that confidence in the measured  $a_T$  is high. One could also make a plot of  $a_T$  versus temperature that would lead to the determination of  $a_T$  values at intermediate temperatures.

A significant advance in the understanding of the viscoelastic properties of polymers occurred with the publication of the work of Williams, Landel and Ferry [3]. They were able to show that for a substantial number of polymers, the shift factors could be determined from a rather simple set of equations:

$$\log a_T = -\frac{8.86(T - T_S)}{101.6 + T - T_S} \quad (5.4)$$

is the Williams-Landel-Ferry (WLF) equation for the shift factor with respect to some standard temperature  $T_S$ . Alternatively, if the standard temperature is chosen to be the glass transition temperature, then

$$\log a_T = -\frac{17.5(T - T_g)}{51.6 + T - T_g} \quad (5.5)$$

The existence of such apparently useful universal equations for the shift factor has formed the basis for many experiments and theories regarding viscoelasticity of polymers.



## ■ 5.6 Summary

In this chapter, we have defined a number of important parameters used to describe the characteristics of polymers. The definition of various molecular weights was presented. The entanglement molecular weight and the molecular weight between crosslinks are both important parameters for understanding adhesives and adhesion. The thermal transitions of polymers were also discussed. Of primary importance here is the glass transition temperature and the melt temperature. The glass transition temperature marks the point at which the polymer changes from a glassy to a rubbery material. The inverse relationship between frequency and temperature was emphasized and related to the measurement of dynamic mechanical properties. Finally, the generation of master curves was described and the WLF equations were presented.

## ■ Bibliography

- Barnes, H. A., Hutton, J. F., Walters, K., *An Introduction to Rheology* (1980) Elsevier, Amsterdam
- Nielsen, L. E., *Mechanical Properties of Polymers* (1962) Reinhold, New York
- Boyer, R. F., *Polym. Sci. Eng.* (1968) 8, p. 161
- Boyer, R. F., *Polymer* (1976) 17, p. 996
- Ferry, J. D., *Viscoelastic Properties of Polymers*, 3<sup>rd</sup> ed. (1980) Wiley, New York
- Aklonis, J. L., MacKnight, W. J., *Introduction to Polymer Viscoelasticity*, 2<sup>nd</sup> ed. (1983) Wiley, New York

## ■ References

- [1] Gillham, J. K., *AIChE J.* (1974) 20, p. 1066
- [2] Gillham, J. K., in *Developments in Polymer Characterization* - 3. Dawkins, J. V. (Ed.) (1982) Applied Science, Essex, UK, pp. 159-227
- [3] Williams, M. L., Landel, R. F., Ferry, J. D., *J. Am. Chem. Soc.* (1955) 77, p. 3701

# 6

## The Relationship of Surface Science and Adhesion Science

### ■ 6.1 Introduction

In Chapter 4, some of the basic aspects of surface science were described, especially as they relate to liquid surfaces and the interaction of liquids with solids. The interaction of liquids and solids forms the basis for the attachment of adhesives to adherends. In Chapter 5, some of the physico-chemical characteristics of polymeric materials forming the basis for most adhesives were described. In this chapter, we describe rationalizations of adhesion phenomena based upon some of the concepts in Chapters 4 and 5. This chapter is central to this book and to the understanding of adhesion phenomena.

The rationalizations used to explain observed adhesion phenomena and their relative importance in adhesion science are assessed in this chapter. An appreciation for the connection between surface science, polymer physics, and observed adhesion phenomena should be developed. Finally, guidelines for generating an adhesive bond to meet the expectations of the adhesive user are provided.

### ■ 6.2 Rationalizations of Adhesion Phenomena

Normally, one would call this section “The Theory of Adhesion”. Unfortunately, there is no unifying theory relating basic physico-chemical properties of materials to the actual physical strength of an adhesive bond. There are theories attempting to predict the strength of an adhesive bond, assuming that adhesion is perfect. There are also theories predicting the strength of interactions at interfaces. However, there are no theories making the complete connection among adhesion, the physical properties of the adhesive and adherend, and the practical strength of an adhesive bond. Rather, the literature on adhesion consists of many articles addressing specific areas of adhesion phenomena. A number of theories that are specifically related to

certain observed phenomena are used to explain them. In this chapter, we discuss some of the more prevalent rationalizations of adhesion phenomena along with experimental evidence for those rationalizations. It is reasonable to conclude that all of the rationalizations have merit. In fact, the physical bases for these rationalizations contribute to one degree or another to the strength of an adhesive bond. The goal of adhesion science is to predict adhesive bond strength from first principles. The goal is likely to be reached by the proper combination of the rationalizations of adhesion (described below) coupled with proper descriptions of how strain energy is dissipated in the adhesive and the adherend.

## ■ 6.3 Electrostatic Theory of Adhesion

We know from elementary physical chemistry that all atoms have a property known as *electronegativity*, which is a measure of the strength of attraction between a certain atom and an electron. We have already discussed how electronegativity causes the formation of dipolar molecules. The periodic table of elements is arranged in approximate order of electronegativity, with the more electronegative atoms to the right and the more electropositive atoms to the left. Thus, fluorine is very electronegative while sodium is more electropositive. Assemblies of atoms and molecules can also have electronegative character. Solid surfaces also can be characterized as being electropositive or electronegative. In a familiar experiment, an amber rod is rubbed with fur and the rod accumulates a surface charge, which can be detected easily. A familiar child's birthday party trick is to take a latex rubber balloon and rub it on a wool sweater. The rubber balloon accumulates a surface charge and the balloon adheres to a number of non-conductive surfaces. In terms of recent adhesion science literature, one could say that surfaces electropositive in character are bases and surfaces electronegative in character are acids.

A primary proponent of the electrostatic theory of adhesion is Derjaguin [1] who proposed that essentially all adhesion phenomena could be explained by electrostatics. He generated a theory predicting the strength of adhesive bonds due to electrostatic forces and also attempted to prove the theory experimentally. Schematically, Fig. 6.1 shows the basis for the theory. An electropositive material donates charge to an electronegative material, thus creating an electrostatic bi-layer at the interface. According to the Derjaguin theory, the strength of the adhesive bond comes from the force necessary to move the charged surfaces away from one another overcoming Coulombic forces. The result of the Derjaguin theory is:

$$W_b = 2 \pi \sigma_0^2 h_b \quad (6.1)$$

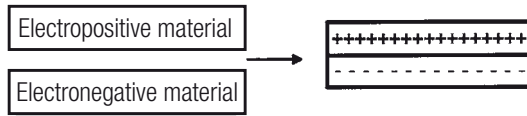


**FIGURE 6.1** Schematic of the formation of an adhesive bond due to transfer of charge from an electropositive material to an electronegative material. The strength of the adhesive bond is thought to be due to the attraction between the charges on the opposite sides of the interface

In this equation,  $W_B$  is the work to break the adhesive bond;  $\sigma_0$  is the surface charge density; and  $h_B$  is the distance of separation at electrical breakdown in the air gap formed when the two materials are separated. Derjaguin and his co-workers used an ingenious method to determine the surface charge and separation distance required by this equation by incorporating Paschen's law for the breakdown of a gas under an electrical potential. Paschen's Law relates the breakdown potential of a gas to the ambient pressure and the distance of separation between two electrodes. Derjaguin and his co-workers assumed that the materials in contact acted as a capacitor and that the voltage across the capacitor was given by the following expression:

$$V^2 = \frac{8 \pi E_C p h}{p} \quad (6.2)$$

where  $V$  is the voltage;  $p$  is the ambient gas pressure;  $E_C$  is the energy stored in the capacitor; and  $h$  is the distance of separation of the two planes of charge. As described by Huntsberger [2], the primary erroneous assumption these workers made was that  $E_C = W_B$ . Using this erroneous assumption, they measured the work to peel adhesive bonds away from glass. The measured  $W_B$  was equated with  $E_C$ , which was then used to plot  $\log V$  versus  $\log ph$  on a Paschen plot. From this plot they could calculate the charge density and separation distance described above by using the equation of the charge density in a capacitor. Unfortunately, their assumption was erroneous because it does not take into account energy dissipated in peeling that was not interfacial energy. Plastic deformation of the adhesive and the adherend was ignored. The only situation where the interfacial energy is the total energy to break an adhesive bond is when the adherends and adhesive are completely elastic. As a result of this erroneous assumption, the Derjaguin experiments and the electrostatic theory of adhesion have gone into disrepute. We see repeatedly in this book that much of the work to break an adhesive bond goes into plastic deformation of the adherend and the adhesive.

However, despite the shortcomings of the Derjaguin work, there are some examples indicating that the electrostatic component to adhesion cannot be ignored entirely. Dickinson and co-workers [3] at Washington State University have studied *fracto-emission*. In these studies, adhesive bonds are placed in high vacuum under conditions where the emission of light, charged and neutral particles, as well as other

electromagnetic emanations can be sensed. The adhesive bond is opened and the various emissions are measured. In the breakage of an epoxy/aluminum adhesive bond, for example, charged particles and light are emitted. If a pressure-sensitive adhesive tape is applied to a photographic emulsion and then stripped from that emulsion, development provides photographic evidence of light emitted in the debonding process. In an enlightening experiment, a piece of tape is applied to an AM transistor radio. When the tape is stripped off, the sound can be heard amplified through the radio, indicating the emission of radio frequency radiation during the debonding operation. These experiments indicate the possibility of the presence of an electrostatic component to adhesion, because discharges are found. Dickinson makes no claim that his work supports or detracts from the electrostatic theory, but indicates that his findings could also be explained by breaking of covalent bonds.

Perhaps the most definitive work detecting the presence of an electrostatic component to adhesion is reported by Smith and Horn [4]. These investigators used the surface forces apparatus (SFA) described in Section 4.5.2.2. The sample surfaces were glass and mica. The investigation was meant to provide JKR measurements of the interfacial energy. The means by which the interfacial distance is determined in the SFA is through interferometric fringes known as *Fringes of Equal Chromatic Order* or FECO [5]. Figure 6.2(a) shows schematically, how the FECO look in an SFA measurement between two surfaces as they are separated. Figure 6.2(b) shows Smith and Horn's observation for surfaces of mica and sapphire that had been brought into contact and then separated. Much to the surprise of these investigators, the shape of the debonded spot, which is usually roughly parabolic in shape, was not parabolic at all. Rather, the contact spot was pointed and the forces seemed to extend over a long distance. In addition, the measured forces between the separated surfaces did not exhibit van der Waals behavior. Rather, the long-range force seemed to change in a discontinuous fashion. Smith and Horn attached an electrometer to the samples and found that a charge had formed during contact. The discontinuous jumps corresponded to discharges from the surfaces, which was direct evidence of the presence of electrostatic forces in a direct adhesion experiment.

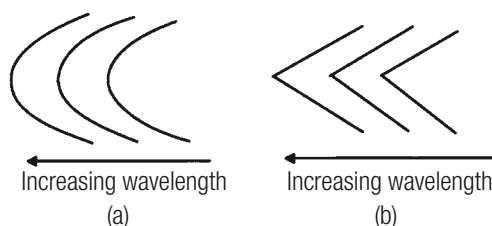


**FIGURE 6.2** Schematic diagram of the FECO (Fringes of Equal Chromatic Order) that can be observed in a “normal” SFA experiment (a) and that observed for a mica-sapphire contact (b). The parabolic shape in the normal experiment is expected from the optics of the interferometer

The Smith and Horn measurements indicate that charge had been transferred between silica and mica. Their results also show that the force of attraction better follows Coulomb's law rather than a van der Waals force-distance law. It is likely that the reason why this could be detected is the large electronegativity difference between silica and mica. Similar measurements of contact between dissimilar polymers do not show this effect [5]. We conclude that electrostatics can play a role in bond-making and can control the strength of an adhesive bond but only when substantial differences in electronegativity exist between the materials brought into contact.

## ■ 6.4 Diffusion Theory of Adhesion

The diffusion theory of adhesion is shown schematically in Fig. 6.3. Two materials, A and B, are brought into close contact. If the two materials are soluble in one another, they form a solution. As a result of diffusive bonding, we no longer have a true interface, but rather an *interphase* in which the properties of material A change gradually into the properties of material B. Diffusive bonding is the ultimate in adhesive bonding. In a “normal” adhesive bond, the adhesive and adherend are not soluble in one another and, at best, there is a microscopic morphology (see Section 6.5) which “diffuses” the interphase. In this “normal” situation, there is usually a substantial mismatch between the properties of the adhesive and the adherend. As such, the contact between the adhesive and adherend acts as a discontinuity providing a stress concentration. The interphase formed in a diffusive adhesive bond does not lead to a stress concentration plane, as there is no discontinuity in physical properties.

Situations in which the adherend and adhesive are soluble in one another are relatively rare. Therefore, the diffusion theory of adhesion can be applied in only a limited number of cases. We can provide some simple criteria for the mutual solubility of materials based upon the theory of simple solutions developed by Hildebrand [6]. The basis of this theory is the *cohesive energy* of a material,  $E_{\text{coh}}$ ,

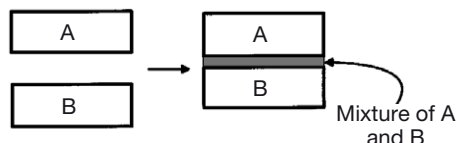


**FIGURE 6.3** If material A and material B are at all soluble in one another, they dissolve in one another and form an interphase which is a solution of material A in material B and vice versa. This schematically shows diffusive bonding

which is the amount of energy necessary to take all of the atoms or molecules in a mole of material and separate them to an infinite distance. The cohesive energy is, in itself, an important parameter since it provides a sense of how strongly the atoms or molecules in a solid or liquid are attracted to one another. The definition of  $E_{\text{coh}}$  is:

$$E_{\text{coh}} = \Delta H_{\text{vap}} - R T \quad (6.3)$$

where  $\Delta H_{\text{vap}}$  is the enthalpy of vaporization;  $R$  is the gas constant; and  $T$  is the absolute temperature. We get a sense of the magnitude of intermolecular forces from the fact that the enthalpy change due to vaporization is the central factor in the equation for the cohesive energy. It takes a lot more energy to vaporize steel than it takes energy to vaporize acetone. Therefore, steel has a much higher cohesive energy than acetone. We define the cohesive energy density of a material as:

$$\text{C.E.D.} = \frac{E_{\text{coh}}}{V} \quad (6.4)$$

where C.E.D. is cohesive energy density and  $V$  is the molar volume. An important parameter in simple solubility theory is the solubility parameter, defined as:

$$\delta = \sqrt{\frac{E_{\text{coh}}}{V}} \quad (6.5)$$

where  $\delta$  is the solubility parameter and  $\delta^2$  is the cohesive energy density. In a solution in which there are no specific chemical interactions, the enthalpy of solution is given by

$$\Delta H_{\text{soln}} = \phi_1 \phi_2 (\delta_1 - \delta_2)^2 \quad (6.6)$$

where  $\delta_i$  is the solubility parameter of component  $i$  and  $\phi_i$  is the mole fraction of component  $i$ . This is an interesting equation since it predicts that there are no exothermic solutions and, in fact, the best one can do is to get no endotherm. There are many solutions that are exothermic, but remember that we had assumed a situation in which there were no specific chemical interactions. In that case, the solutions would have no exotherm. The criterion for the spontaneous formation of a solution is the sign and magnitude of the Gibbs free energy of mixing given by:

$$\Delta G_{\text{mix}} = \Delta H_{\text{soln}} - T \Delta S_{\text{soln}} \quad (6.7)$$

where  $\Delta G_{\text{mix}}$  is the change in the Gibbs free energy of mixing,  $\Delta H_{\text{soln}}$  is the enthalpy of solution;  $T$  is the absolute temperature; and  $\Delta S_{\text{soln}}$  is the change in the entropy in the system. For a regular solution as defined by the equation above, the enthalpy of solution is either positive or zero. We rely on the entropy change to provide a nega-

tive Gibbs free energy of mixing. For low molecular weight materials, the change in entropy is always positive, and usually large, due to the increase in the disorder of a system when two materials are mixed. However, in polymeric materials, the entropy change is usually very small because the number of states in which a polymer can exist is limited by the high molecular weight. That is, all pieces of the polymer are connected to one another and the number of possible configurational states is limited. Since the entropy change is small and the enthalpy change is either 0 or positive, high molecular weight polymers are not likely to dissolve in one another. This is found to be the case in many, if not most, polymeric systems. Polymer pairs that are soluble in one another exhibit some enthalpy of mixing. For example, polymethyl methacrylate is soluble in polyvinylidene fluoride. This solubility is thought to be due to an exothermic acid-base reaction in which the basic methacrylate ester interacts with the acidic vinylidene fluoride group.

The above discussion leads us to one of the criteria for good adhesion. In a situation in which one polymer dissolves in another, one obtains ultimate adhesion. The criterion for obtaining solubility of one polymer in another is the solubility parameter. The most negative value of  $\Delta H_{\text{soln}}$  that we can have is 0 or the point at which the solubility parameter of the two materials is the same. Thus, one criterion for good adhesion is that *the adhesive and adherend should have the same solubility parameter*.

There are numerous examples in which this concept has been put to use. Iyengar and Erickson [7] carried out a series of simple experiments in which a range of adhesives was used to make peel specimens between sheets of polyethylene terephthalate (PET). The solubility parameters of the adhesives were known. The solubility parameter of PET is about 10.3. Figure 6.4 is a drawing similar to that of Iyengar and Erickson in which the salient features of their data are presented.

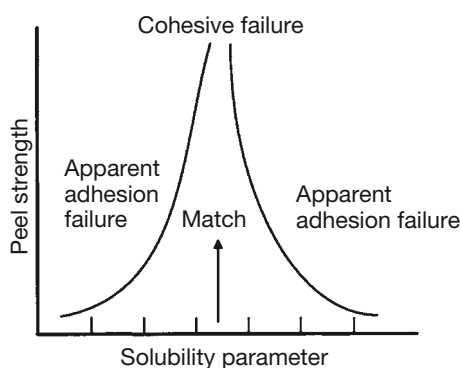


**FIGURE 6.4** Diagram showing the features of the experiment of Iyengar and Erickson for PET (poly(ethylene terephthalate)) bonded to PET by a variety of adhesives. The maximum in adhesive bond strength was found to be at the point when the solubility parameter of the adhesive is matched to the solubility parameter of PET (redrawn from Iyengar and Erickson)



Figure 6.4 shows a plot of peel strength versus the solubility parameter of the adhesive used. There is a strong dependence of practical adhesion on the solubility parameter of the adhesive. If the solubility parameter of the adhesive matches that of the substrate, the failure changes from apparent adhesion failure to cohesive failure in the substrate.

The concept of diffusion bonding is not new to those who have worked with adhesive bonding of plastics. For a number of plastics, solvent welding can be used for bonding. A solvent for the plastic is applied to both adherends and they are joined. While the solvent is present, the polymer molecules in the plastic parts can diffuse into one another. When the solvent has evaporated, an assembly that is inherently just the plastic remains. Plastics and solvents must be chosen carefully to avoid adverse effects, such as solvent-induced crazing on the bulk of the plastic. Plastics can be welded by melting the plastic part thermally or ultrasonically against another plastic part. In the melt state, the polymer molecules can intertwine and form the finished part. Once again, care must be taken since many plastic parts can distort dramatically when heated. Both of these examples of diffusive bonding are examples of *autohesion* in which a polymer adheres to itself.

Vinyl adhesives are typically a solution of polyvinyl chloride plus plasticizer in a solvent mixture of tetrahydrofuran and toluene. Tetrahydrofuran is an excellent solvent for vinyl and swells the vinyl surface to be bonded. While the solvent is still present, the vinyl in the adhesive diffuses into the adherends and forms the bond. Such adhesive bonds can even be formed under water.

#### 6.4.1 Diffusive Adhesive Bonding and Block Copolymers at Interfaces

The desire to join dissimilar polymers by means of adhesives has led to a part of adhesion science concerning block copolymers at interfaces. *Block copolymers* are polymeric materials with at least two chemically distinct blocks of polymer that are chemically joined. Blocks of such a copolymer can be made so that they are each soluble in one of two mutually insoluble polymers to be joined. In this section, we describe studies that address block copolymers at interfaces as well as several concepts from this and previous chapters including fracture measurements.

Polymers such as polymethyl methacrylate (PMMA) and polystyrene (PS) are not soluble in one another. Neither are polyisoprene (PI) and PS soluble in one another. If one melt presses PMMA against PS or PI against PS, one obtains a very poor adhesive bond. Application of a thin (on the order of nanometers) layer of a block copolymer of PS and PMMA between PS and PMMA leads to markedly better adhesion. Similarly, application of a thin layer of a block copolymer of PS and PI between PS and PI leads to a similar result. These studies, carried out by Brown,

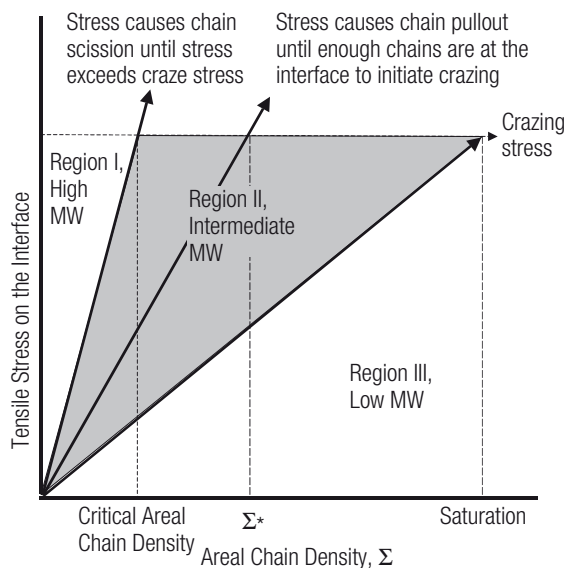
Kramer, Creton et. al. [8], have elucidated the polymer physics in these material combinations.

Brown and co-workers used a modification of the double cantilever beam test to study the effect of the presence of block copolymers at the interface. The double cantilever beam was asymmetric to account for the difference in materials properties between the PS and the PMMA. The thickness of the slabs was set in order to minimize fracture *mode mixity*, which is a term applied to a fracture situation in which more than one fracture mode may be operational due to an asymmetry in the bond or in the loading of the bond. Block copolymers with varying chain lengths of the two blocks were applied at various amounts between PS and PMMA and then annealed. Heat and pressure were used to join the bond. The strain energy release rate was measured by driving a crack down the length of the specimen and measuring the distance ahead of the wedge that the crack traveled.

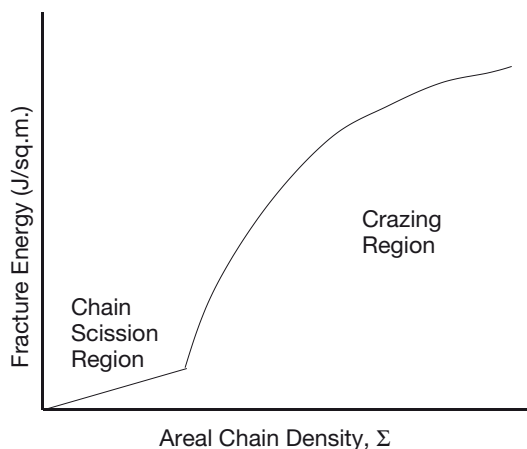
We use several terms to describe the block co-polymers at the interface. The first of these is already known to us, it is the molecular weight. In this case we use the symbol  $N$  to describe the degree of polymerization of the co-polymer halves. The second is the *areal chain density*. We use the symbol  $\Sigma$ . This term describes the cross sectional area occupied by the co-polymer at the interface. Basically, a low areal chain density means that there are fewer chains per unit area than the interface could handle, while  $\Sigma_{\text{sat}}$  is the areal chain density when there is an interface that is fully saturated with the block co-polymer.

Figure 6.5 shows a schematic of what we might expect to happen at the interface as a function of  $\Sigma$  and  $N$ . When a force is applied to propagate a crack along the interface, there are several possibilities as to how the mechanical energy may be dissipated. First, if the  $N$  of the copolymer segments is small such that the co-polymer is not fully entangled with one or both sides of the interface, the chain will likely pull out of one or the other side of the interface and deposit on the other side. Thus, the force necessary to separate the interface should be proportional to the amount of energy necessary for chains to slip past each other multiplied by the number of chains,  $\Sigma$ . If  $N$  is sufficiently high such that both of the arms of the block co-polymer are fully entangled, it is likely that the block co-polymer chain will scission with the force being applied. Thus, the force necessary to separate the interface should be proportional to the number of chains crossing the interface times the energy necessary to break a single chain.

One of the glassy polymers that we have been discussing is polystyrene. The primary energy absorbing mechanism of polystyrene is the formation of a craze. Microscopic examination of a craze in this polymer shows us the formation of a network of strands or microfilaments that have been formed by drawing the polymer chain across the crack. The drawing of these polymer chains into these strands absorbs mechanical energy. There is a specific stress at which this occurs and this is denoted by  $\sigma_{\text{craze}}$ .



**FIGURE 6.5** Plot of interfacial stress as a function of areal chain density. The plot shows three distinct regions. In Region I, where the block co-polymers at the interface are of high molecular weight, the stress can rise quickly to the crazing stress, even at low areal chain density. At very low coverage, the failure mode is chain cleavage. In Region II, where the block co-polymers at the interface are of some intermediate molecular weight, the interface fails by chain pull-out until enough chains at the interface are present that the crazing stress can be reached. In Region III, where the block co-polymers are of low molecular weight, the crazing stress is unattainable. Note that the crazing stress is the ultimate stress that can be attained



**FIGURE 6.6** Schematic representation of the results of a fracture experiment between polystyrene and poly(methyl methacrylate) in which a block co-polymer of the two monomers was placed at the interface. The arms of the block copolymer were long enough that chain scission took place at low areal chain density and crazing was achieved at a low chain density

We return to the interface between PMMA and PS. If the interfacial stress applied to the bimaterial interface exceeds  $\sigma_{\text{craze}}$ , the polymer will begin to form crazes and substantially increase the mechanical energy it absorbs. If the block co-polymer so significantly “stitches together” the interface that  $\sigma_{\text{craze}}$  is exceeded before polymer chains pull out or scission, crazing will be the dominant energy absorbing mechanism. Figure 6.6 shows a schematic representation of the data taken by for the PMMA/PS interface [8 h]. We see that the fracture energy shows an abrupt increase in magnitude when  $\Sigma$  reaches a critical value. It is believed that this is the value at which  $\sigma_{\text{craze}}$  is exceeded.

The physics of this separation process are governed by the phenomenon called *chain pull-out* which can be described by the *reptation theory* of polymer dynamics [9]. Reptation theory describes polymer motion as similar to that of a snake confined to a tube. If the snake is short, little energy is required to move it down the tube. However, if the snake is long, its movement down a tube is convoluted and much energy is required to pull it out. The observations described above seem to follow the physics behind polymer reptation. Indeed, work by Wool and co-workers shows the time dependence of polymer welding to be essentially that predicted by reptation theory [10].

The information in this section shows the intimate relationship between practical adhesion, solubility of polymers at interfaces, and polymer dynamics at the molecular level. We will return to these concepts in a section later in this chapter.

## ■ 6.5 Mechanical Interlocking and Adhesion

The concepts in the previous section were directed towards adhesive bonding situations in which at least one of the adherends is a polymer. This provided an avenue by which a diffuse interphase could form at the junction between the adhesive and the adherend. We now examine a situation in which one or both of the adherends are impermeable to the adhesive. Suppose that the junction between the adhesive and the adherend is in a plane such as that shown in Fig. 6.7. The triangle at the edge of the bond is meant to indicate that a crack opening force is being exerted at the edge of the specimen. Excursions of the crack opening force into the adhesive or the adherend is not necessitated by the force field since the interface acts as a stress concentrator and the crack propagates there.

Let us suppose that instead we have the interface shown in Fig. 6.8 in which the adherend is not smooth but rather has a roughness into which the adhesive can flow. If the adhesive can displace the air in the pockets on the surface, the two

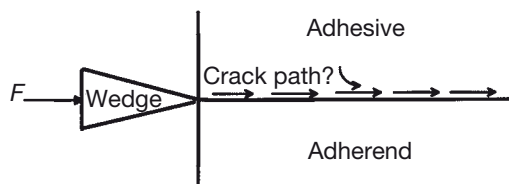


**FIGURE 6.7** A wedge is driven into the edge of a sharp interface between adherends A and B. The loading is known as Mode I (see Chapter 3) and results in crack propagation as shown by the arrows in the figure. Little energy dissipation is required to separate the adherends and clean separation of adherends is possible

materials are in intimate contact along a tortuous path. If a wedge is driven into the edge of this bond, we can see no abrupt plane of stress transfer. Rather, for the crack to propagate across the bond, the lines of force have to take detours. Some of the detours go into the adhesive. In most cases, the adhesive can deform more than the adherend. If either the adhesive (or the adherend) plastically deforms during the debonding, energy is consumed and the strength of the adhesive bond appears to be higher.

Another reason that surface roughness aids in adhesive bonding is the interlocking effect. In Fig. 6.8, arrows indicate a segment of the surface. In this segment, the adhesive has completely filled a pore on the surface. At this pore, the exit of the adhesive is partially blocked by part of the adherend. This place in the interphase will exhibit the so-called “lock and key” effect. A key, when turned into the tumblers of a lock, cannot be removed from the lock because of the physical impediment provided by the tumblers. In the same way, a solid adhesive in a pore such as that shown in Fig. 6.8, cannot move past the “overhang” of the pore without plastically deforming.

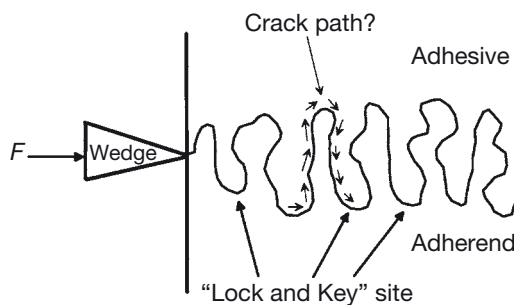









**FIGURE 6.8** Schematic showing a tortuous interface between two adhering materials. When a Mode I loading is applied to this situation, the applied force cannot cleanly follow the path between the two adherends, but rather must make excursions. As excursions are made into the adhesive, energy can be dissipated by plastic deformation. Note also the possibility of “lock and key sites” at which points the adhesive would have to physically pass through the material of the adherend in order for separation to take place

Plastic deformation acts as an energy absorbing mechanism and the strength of the adhesive bond appears to increase.

We are familiar with rubber tires and rubber inner tube repair kits. These usually contain a rubber patch, an adhesive (usually some form of solvent-borne elastomer) and a piece of sandpaper or a serrated tool. The sandpaper is used to roughen the surface of the rubber to be mended, allowing the adhesive to “key” into the substrate.

Another reason surface roughness improves adhesion is purely a matter of physical area of contact. Figure 6.7 illustrates a situation where the contact between the two materials is in a plane, the minimum possible contact area between two rectangular bodies. If we can imagine Fig. 6.8 in three dimensions, we see that the surface area is increased substantially. If we believe that interfacial interactions are the basis for adhesion, we know that the sum of those interactions will scale as the area of contact. If the actual area of contact is increased by a large amount, the total energy of surface interaction increases by an amount proportional to the surface area.

Perhaps the best demonstration of the effect of surface roughness on adhesion is provided by Arrowsmith [11]. He created surfaces of varying roughness by electro-forming the surface of pieces of copper that each had the same thickness. Figure 6.9 is a diagram of some of the shapes he placed on the surface along with adhesive bond strength data. Note that these shapes are all in the range of a micron or so in size.

Surface topography of copper foil		Mean peel load lb/in
Topography	Diagrammatic representation	
Flat		3.75
Flat + 0.3 $\mu$ dendrites		3.8
Flat + 0.3 $\mu$ dendrites + oxide		4.4
3 $\mu$ pyramids (high angle)		5.9
2 $\mu$ low angle pyramids + 0.3 $\mu$ dendrites		7.3
2 $\mu$ low angle pyramids + 0.2 $\mu$ dendrites + oxide		8.8
3 $\mu$ high angle pyramids + 0.2 $\mu$ dendrites + oxide		13.5

**FIGURE 6.9** Experimental results reported by Arrowsmith, relating the surface roughness of electroplated copper to the level of practical adhesion when an epoxy adhesive is removed. Note that as the level of surface roughness increases and the opportunity for mechanical interlocking increases, the level of practical adhesion increases even though the adhesive is identical in all cases (reproduced from Reference 11 by permission of the Institute of Metal Finishing, UK)

He applied the same epoxy adhesive to all of the surfaces and measured the peel strength of the epoxy to the copper. As shown in Fig. 6.9, the peel strength increased, even though the adhesive and the adherend were nominally the same in all cases. We must surmise that the effect of the surface roughness is to increase the plastic deformation of the adhesive in the interphase, resulting in increased peel strength.

### 6.5.1 Kinetics of Pore Penetration

The above discussion is predicated on the notion that the adhesive and the adherend are in intimate contact. It is not obvious that this should be the case since all real adhesives have a viscosity. In normal bonding operations, the adhesive and adherend must come into close contact quickly. We can examine the extent to which adhesives penetrate into pores on a surface by examining the equations describing the wetting of surfaces by polymers and the penetration of liquids into a pore as provided by Packham [12]. Poiseuille's Law describes the penetration of a liquid into a pore:

$$x \frac{dx}{dt} = \frac{r^2 P}{8 \eta} \quad (6.8)$$

where  $x$  is the pore penetration distance;  $P$  is the capillary pressure;  $t$  is the time and  $r$  is the radius of the pore (or capillary, for which Poiseuille's Law is actually derived). The capillary pressure is given by:

$$P = \frac{2 \gamma_{LV} \cos \theta}{r} \quad (6.9)$$

where  $\theta$  is the contact angle and  $\gamma_{LV}$  is the liquid-vapor interfacial tension of the adhesive. The description of the wetting of a surface by a polymer is taken from the work of Schonhorn, Frisch and Kwei [13] and it is described by the following equation which was derived by Newman [14]:

$$\cos \theta(t) = \cos \theta_{\infty} (1 - a e^{-ct}) \quad (6.10)$$

where  $\cos \theta_{\infty}$  is the contact angle at infinite times and  $\theta(t)$  is the time dependent contact angle. Combining these equations, we find the following relationship:

$$x^2(t) = \frac{r \gamma_{LV} \cos \theta_{\infty}}{2 \eta} \left( t - \frac{a}{c} + \frac{a e^{-ct}}{c} \right) \quad (6.11)$$

This equation describes the distance a pore is penetrated by an adhesive, giving an idea of the parameters necessary for expulsion of air from a pore and its replacement by an adhesive.

**TABLE 6.1** Packham's Calculation of Distance Penetrated by Molten Polyethylene into a Microporous Surface

Pore radius (micrometers)	Distance penetrated into pore "x" (micrometers)
1000	220
10	22
1	7
0.1	2.2
0.01	0.7

Let us examine the above equation by introducing parameters associated with the wetting of a surface by polyethylene. Packham assumed that the interfacial tension between the polyethylene and air was  $23.5 \text{ mJ/m}^2$  under the application condition which was  $200^\circ\text{C}$ . He allowed a time of 20 minutes for wetting to take place. Table 6.1 shows results of his calculations.

The table clearly indicates that the amount of penetration of polyethylene into a porous surface is dependent upon the radius of the pore. The depth of penetration is inversely dependent upon the radius of the pore. For a pore radius of 1,000 microns, the depth of penetration is only 220 microns. If the pore were as deep as its radius, the pore would still be mostly empty. In contrast, if the pore radius were 0.1 microns, the depth of penetration could be 2.2 microns, if the pore had that depth available. The calculation clearly says that if we wish to have as complete as possible removal of air from a pore on a surface, the pore radii must be quite small. The approximate radii of the openings of pores that are deeply penetrated are about one micron or less. The ramifications of this correlation become clearer when we discuss surface preparations in the next chapter.

Thus, another criterion for obtaining good adhesion is *provide a surface with a micro-morphology and provide an adhesive with a low enough viscosity to completely fill the surface features.*



## ■ 6.6 Wettability and Adhesion

Examine Fig. 6.10 and imagine a situation in which there is a real adhesive and a real adherend. The importance of wettability to adhesion is apparent. A tortuous surface like that in Fig. 6.8 is not necessarily completely clean. Contaminants are likely to be on the surface, forming a “weak boundary layer” (see Section 6.10). In addition, a real adhesive has a real viscosity (as discussed in the previous section). In many cases, the adhesive will need to cure and the viscosity in these materials increases rapidly as a function of time after application. We can expect that the bottom of the pores may not be filled, leaving voids. The adhesive bond may therefore have vacancies at the interface, each of which acts as a stress concentration point. To understand this problem, re-examine Fig. 1.1. We show two situations, one is a perfect monolithic material in which there are no cracks or voids and the other is of the same material containing a crack.

We can imagine a load being placed on both samples. The load is shown propagating through the unflawed material as continuous lines of force. In the flawed material, the lines of force cannot be continuous because of the flaw. The lines of force, because they must be continuous, gather at the edge of the flaw and increase in intensity. The increase in intensity can be calculated in a simple way for this elliptical crack. If the dimensions of the crack are such that the long axis is 100 times longer than the short axis, the increase in stress intensity is 201. So, a force that is 1 Newton at the ends of the material is more like 201 Newtons at the edges of such a crack. The factor in this discussion is a crude version of the “stress intensity factor” used in fracture mechanics [15]. An adhesive bond with a flawed interface is another example of this situation. Voids or weak boundary materials magnify the remotely applied force at the periphery of the flaw. Very often, this induces propagation of the flaw.

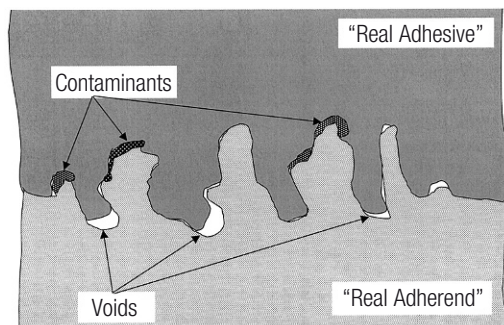


**FIGURE 6.10** Schematic of a “real” bonding situation in which the surface of the adherend has contaminants and in which the adhesive has a finite viscosity. Pore penetration is not complete, leaving voids at the interface. The presence of voids as well as cohesively weak contaminants, decreases the strength of the adhesive bond below its theoretical strength

If the material does not have mechanisms of absorbing the energy, the material fails at loads less (and sometimes even *much* less) than the theoretical strength of that material. Hence, obtaining good wetting of the surface is a matter of eliminating flaws at the interface so that the strength of the bond can be as close to theoretical as possible.

The study of adhesion cannot be separated from the study of wettability and contact angle phenomena. *For good adhesion to take place, the adhesive and the adherend must come into intimate contact.* Obtaining intimate contact of the adhesive with the surface is tantamount to saying that interfacial flaws must be minimized or eliminated. Intimate contact occurs when the adhesive spontaneously spreads over the surface to maximize interfacial contact and minimize contact with other phases. Spreading (spontaneous or not) can be examined by contact angle measurements. In this section we explore the relationship of wetting and adhesion.

A simple view of the relationship of wetting and adhesion is provided in Fig. 6.11. Here, the contact angle of a drop of an epoxy adhesive on a variety of surfaces is shown. The surface energy of a typical epoxy resin is about  $42 \text{ mJ/m}^2$ . The drop has a low profile on materials such as cured epoxy composite or polyvinyl chloride (PVC), although wetting would not be spontaneous on PVC. On polyethylene, which has a critical wetting tension of about  $31 \text{ dynes/cm}$ , the drop has an even higher profile. In our laboratories, we have used sheet polyethylene to line our table-tops because epoxies do not adhere. The adhesive has a very high contact angle on polytetrafluoroethylene (PTFE) with a critical wetting tension of  $18 \text{ dynes/cm}$ . Therefore, we might predict that an epoxy adhesive would have poor adhesion to PTFE and we would be correct. Low surface energy materials such as PTFE have poor adherability and are considered *abhesive* or *release* surfaces. PTFE-like materials form the basis for

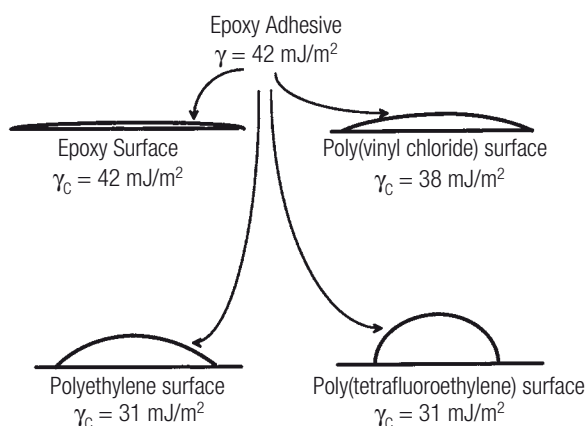


**FIGURE 6.11** Diagram of the observation of the contact angle of an epoxy adhesive (uncured) on four surfaces of varying critical wetting tensions. Note that as the critical wetting tension of the surface decreases, the contact angle of the liquid epoxy on that surface increases

non-stick cookware. When it is demonstrated that eggs do not stick, we have a clear demonstration of the relationship between wettability, the Zisman critical wetting tension, and adhesion. Egg whites are, for the most part, proteinaceous materials. However, the proteins are in aqueous solution and the egg would be expected to have a surface tension of 60–70 dynes/cm. The contact angle between the egg and PTFE is high. Wetting is poor and non-spontaneous and the egg does not adhere.

The ability of an adhesive to spontaneously wet a surface can be codified by means of the Zisman relationship described in Chapter 4. That is, an adhesive spontaneously wets a surface when its surface energy is less than that of the adherend to which it is applied. Thus a corollary to the criterion for good adhesion and wettability is *for spontaneous wetting and good adhesion, choose an adhesive with surface energy less than the critical wetting tension of the surface to which it is applied*. The background for this corollary was described in Fig. 6.11.

One of the clearest experiments relating wettability and adhesion was carried out by Levine, Illka and Weiss [16]. In this work, the experimenters measured contact angles of various liquids on solid polymers. They then measured the butt tensile strength of adhesive bonds made with those plastics and a *single* adhesive. A schematic representation of their results is shown in Fig. 6.12. There is a direct relationship between the butt tensile strength and  $(1 + \cos\theta)$ , as would be predicted if there were a relationship between the thermodynamic work of adhesion and the practical work of adhesion. The Dupré Equation predicts that for a single combination of materials, the thermodynamic work of adhesion decreases as the interfacial energy increases. Figure 6.12 also shows data for the practical work of adhesion as a function of the interfacial tension. The practical work of adhesion does decrease as predicted by the Dupré Equation. Similarly, as the critical wetting tension of the solid surface goes below the surface energy of the adhesive, there is a decrease in butt tensile strength.

Another example of the relationship between the Young-Dupré Equation and adhesion is shown in the work of Barbarisi [17] who carried out a *surface preparation* of polyethylene. Surface preparation is an important technology in adhesion science because it has been found that many surfaces are not amenable to adhesive bonding for a number of reasons, not the least of which is low surface energy. The subject of surface preparation of various adherends is discussed in Chapter 7. The surface preparation used by Barbarisi was chromic acid oxidation. As a function of treatment time, it was found that the contact angle of water with the treated polyethylene surface went down. Therefore,  $(1 + \cos\theta)$  increased, as did the practical adhesive bond strength with the treated polyethylene as adherends. The same epoxy adhesive was used in all of these experiments. A useful reference describing the relationship between wettability and adhesion appears in the book *Adhesion Science and Technology* in the chapter by Mittal [18].

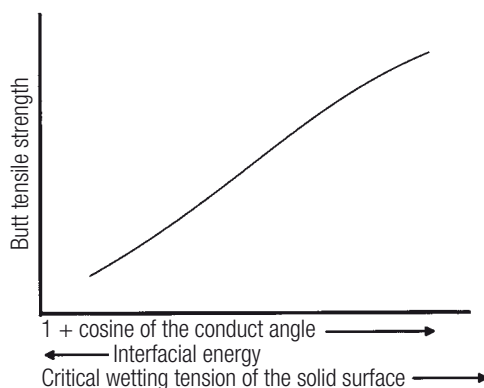


**FIGURE 6.12** Schematic of the data presented by Levine, Illka and Weiss. Butt tensile strength of a range of plastics bonded with a single adhesive is plotted versus several wetting parameters determined from contact angle measurements. This diagram illustrates the relationship between wetting and practical adhesion

## ■ 6.7 Acid-Base Interactions at Interfaces

In Chapter 4, we described various intermolecular interactions that could take place at an interface. In Section 4.2.3, we described generic acid-base interactions including the Bronsted-Lowrey acids and Lewis acids. Acid-base interactions can take place at interfaces as they do in bulk solutions. Work on this subject was done by Bolger and Michaels [19]. They used standard chemical data of acid-base equilibria to examine various interfacial phenomena. Fowkes [20] also used acid-base interactions to describe adhesion phenomena. Fowkes derived the equation that divides the surface energy of a material into its component parts and was known for his belief that polar forces played no role in interfacial phenomena. In his view, the primary interactions taking place at interfaces were due to dispersion forces. He later ascribed the remaining interactions to acid-base interactions. Thus, using the Owens-Wendt equation, in Fowkes' view:

$$W_A = 2\sqrt{\gamma_1^d \gamma_2^d} + W_A^{AB} \quad (6.12)$$

where  $W_A^{AB}$  is the component of the work of adhesion due to acid-base interactions. From a critical point of view, it seems that this analysis just removed a term having to do with polar forces and replaced it with a term having a different designation. Fowkes borrowed from the work of Drago [21] to provide an expression for  $W_A^{AB}$ . He wrote the following expression:

$$W_A^{AB} = k N^{AB} (E_A E_B + C_A C_B) \quad (6.13)$$

where  $k$  is a proportionality constant that corrects for units and  $N^{AB}$  is the number of acid-base pairs which interact in the interphase or at the interface. The  $E_i$  and  $C_i$  are experimentally determined constants obtained from a series of detailed calorimetric experiments in which Drago and his group measured the heat of reaction of a myriad of different acid-base pairs. The purpose of the Drago experiments was to determine the electrostatic ( $E$ ) and covalent ( $C$ ) contribution to the enthalpy of interaction of a large series of acid-base pairs. It was a disappointment to Drago that these experiments did not provide the correlation he wanted but rather yielded a large catalog of data from which enthalpies of reaction could be calculated. Therefore, the Fowkes expression for acid-base interactions is not one that comes from first principles of intermolecular forces, but is obtained from experimentally derived constants. This is not to say that the expression is conceptually incorrect, but it unfortunately gives the impression that acid-base reactions are a fundamental force (like dispersion forces), rather than a combination of electrostatic and covalent interactions, as believed by Drago.

The effect of acid-base interactions at interfaces was examined by Fowkes and Mostafa [22] in a now classic series of experiments and more recently by Whitesides and coworkers (as described in Chapter 4). Fowkes and Mostafa used contact angle measurements to determine the extent of acid-base interactions by creating acidic surfaces by copolymerizing varying amounts of acrylic acid with ethylene. They then used basic liquids such as dimethylsulfoxide and dimethylformamide (basic in the Lewis sense) and sodium hydroxide dissolved in water (basic in the Bronsted-Lowrey sense) as contact angle probe liquids. In addition, they probed the dispersion force contribution to the work of adhesion by using dispersion force-only liquids. Conversely, they generated basic surfaces by using copolymers of vinyl acetate with ethylene and used acidic liquids as probes (vinyl acetate is considered a Lewis base.) The acidic liquids were composed of varying amounts of phenol in tricresylphosphate. Figure 6.13 (a schematic representation of Fowkes' results) shows that as the possibility for acid-base interactions is increased (increasing acidity or basicity of the substrate), combined with the respective increase in acidity or basicity of the probe liquid, there is a resultant increase in the work of adhesion. There are a significant number of other studies in the literature examining the acid-base properties of interfaces including an important set that used *inverse phase gas chromatography*. This type of chromatography determines interfacial interactions because the retention time on the column is directly related to the enthalpy of interaction between the mobile phase and the stationary phase surface.

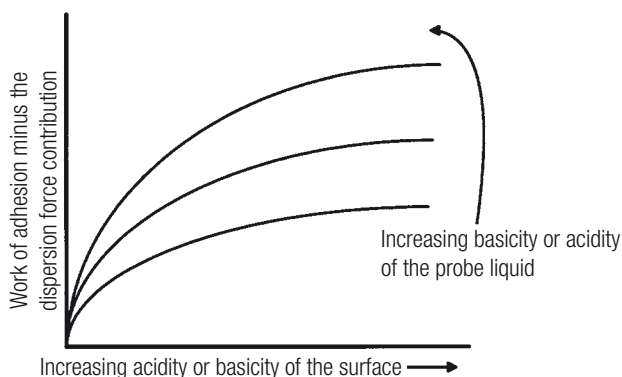


**FIGURE 6.13** Diagram showing the relationship of the work of adhesion due to acid-base interactions versus the increasing acidity or basicity of the substrate and probe liquid. When the substrate is an acid, a basic probe liquid provides results similar to those shown. When the substrate is a base, an acidic liquid provides results similar to those shown. When an acid substrate and an acid probe liquid are used, no effect is seen. The dispersion force contribution is determined by using liquids with only dispersion force character

In addition to the Drago experimentation on acid-base pairs, there have also been a number of other methods proposed to characterize the acidic or basic character of a material. Two of the important classifications are the Gutman donor-acceptor numbers [23] and the hard-soft acid-base principle. The Gutman numbers have been studied by Schreiber and co-workers [24], who have attempted to relate the chemistry of the surfaces (as determined by inverse phase gas chromatography) to those numbers and then to relate those numbers to adhesion phenomena.

Despite all of the interest shown in acid-base interactions at interfaces, there are relatively few detailed studies connecting the acid-base character of interfaces with the actual forces of adhesion between those surfaces. There are experimental results implying the presence or predominance of the acid-base interaction in adhesion. It is known, for example, that silica is acidic and most glasses are basic (due to additives to the glass, such as borate). Materials thought to adhere well to silica are basic and those thought to adhere well to normal glass are acidic. In fact, many industrially useful inorganic surfaces are basic in character because the oxides of most metals (with the exception of tungsten) are either amphoteric or basic in character. Many adhesives are formulated to be acidic in character so that they adhere to a multitude of basic surfaces. From this discussion, we can provide another criterion for good adhesion: *determine the acid or basic character of your substrate and choose an adhesive having the opposite character.*

## ■ 6.8 Covalent Bonding at Interfaces

In Chapter 4, we discussed the potential energy of various intermolecular interactions. In that discussion, we made note of the fact that the deepest potential energy well that is available for the interaction between two atoms or molecules is that formed when they share a pair of electrons. That is, the deepest potential energy well is obtained when a covalent bond is formed. The generation of covalent bonds at interfaces, especially between organics and inorganics, has become an industry of its own.

Assume that we have an area of contact between two dissimilar materials that is one square meter. Let us also assume that the cross sectional area occupied by each member of a large number of carbon-carbon covalent bonds is five square Angstrom units. The number of chemical bonds is then  $2 \times 10^{19}$  bonds/m<sup>2</sup>. Assume that the energy to break a mole of these bonds is 120 kcal. (This is about the amount of energy necessary to break one mole of carbon-carbon covalent bonds.) We can calculate that the total energy at this interface is on the order of 40 J/m<sup>2</sup>. This is a very large number when compared to the values of surface and interfacial energy discussed in Chapter 4. This large number provides background for the reason so much research has been devoted to the generation of interfacial chemical bonds. Indeed, the bond energies described in the work of Brown [9] approach this level. Although it would seem necessary to have covalent bonds at interfaces to have strong adhesive bonds, strong adhesive bonds exist in the absence of any overtly induced interfacial chemical bonds. Indeed, Fowkes [25] has calculated that the strength of a polyethylene/steel butt tensile joint should be in excess of 157,000 psi when one assumes the presence of dispersion forces, exclusively, at the interface. This value is orders of magnitude higher than any experimentally observed adhesive bond strength. This comparison indicates that even though covalent bonds may be useful to have at interfaces, they are not necessary for the generation of strong adhesive bonds.

Why then, is there a desire to generate chemical bonds at interfaces? The primary reason for the need for such chemical bonds can be found in the calculation described by Kinloch [26]. We write the expression for the surface energy of any material as the sum of the polar force and dispersion force contributions, as was proposed by Fowkes [20]. In deference to the work of some adhesion science researchers, we could write the expression substituting acid-base interactions for polar interactions, as:

$$\gamma = \gamma^d + \gamma^p$$

where  $\gamma$  is the surface energy of a material;  $\gamma^d$  is the dispersion force component of that surface energy; and  $\gamma^p$  is the polar (or acid-base) contribution to the surface energy. Using the hypothesis of Owens and Wendt, we have:



$$W_A = 2\sqrt{\gamma_1^d \gamma_2^d} + 2\sqrt{\gamma_1^p \gamma_2^p} \quad (6.14)$$

This expression deals only with a situation where the two materials are in contact and no other material is present. We could have a situation where a third material is present, with its own polar and dispersive character. In that situation, we find that the expression is a bit more complicated but derivable directly from the above relationships:

$$W_A = 2\left(\gamma_l - \sqrt{\gamma_1^d \gamma_l^d} - \sqrt{\gamma_1^p \gamma_l^p} - \sqrt{\gamma_2^d \gamma_l^d} - \sqrt{\gamma_2^p \gamma_l^p} + \sqrt{\gamma_1^d \gamma_2^d} + \sqrt{\gamma_1^p \gamma_2^p}\right) \quad (6.15)$$

where the  $\gamma_i^j$  are the components of the liquid surface energy of the intervening liquid,  $j$  is either  $d$  (dispersive) or  $p$  (polar), and  $i$  is either 1, 2 or  $l$ . If the values of the  $\gamma_i^j$  are known, then the predicted thermodynamic work of adhesion at an interface in the presence of a third material such as the liquid,  $l$ , can be calculated.

Such a calculation was done by Kinloch [26]. Table 6.2 gives values of the polar and dispersive components of the surface energy for a number of familiar materials and shows a listing of the work of adhesion in the presence and absence of a third material, water.

The results in this table provide insight as to the need for interfacial covalent or chemical bonds. In the absence of water, the work of adhesion for epoxy with silica or for epoxy with aluminum oxide are positive. This indicates the stability of this interface in the absence of water. With water present, the calculated values for the work of adhesion are negative. Negative values of the work of adhesion indicate that this system is unstable in the presence of water. That is, the inorganic surface would rather have water present than the epoxy resin.

**TABLE 6.2** Calculation of Work of Adhesion Based upon Polar and Dispersive Components of the Surface Energy

Surface or Interface	$\gamma^d$ (mJ/m <sup>2</sup> )	$\gamma^p$ (mJ/m <sup>2</sup> )	$\gamma$ (mJ/m <sup>2</sup> )	$W_A$ (mJ/m <sup>2</sup> )	$W_{AA}$ (mJ/m <sup>2</sup> )
Epoxy	41.2	5	46.2		
Silica	78	209	287		
Aluminum oxide	100	538	638		
Water	22	50.2	72.2		
Epoxy/silica				178	
Epoxy/aluminum oxide				232	
Epoxy/water/silica					-56.2
Epoxy/water/aluminum oxide					-137



An indication of thermodynamic instability should be a matter of concern here because it is hard to think of many applications where adhesive bonds made with epoxy and these substrates would not, at some time, come into the presence of water. However, an analogy can be drawn with the use of aluminum in various industrial applications. Aluminum is a highly reactive metal that is thermodynamically unstable in ambient atmosphere. If elemental aluminum is exposed to the atmosphere, it explodes. Despite this seemingly dire situation, we use aluminum for frying pans and we fly in airplanes made from aluminum. The reason we can use aluminum for these purposes is that it is insulated from the atmosphere by a thin layer of very stable aluminum oxide. The reaction of aluminum with the atmosphere is kinetically controlled by the formation of an oxide that slows down the degradation of the metal. In a similar sense, if we could place covalent bonds at the interface between organic and inorganic materials, water would first have to hydrolyze those covalent bonds before it could act on the interface. Covalent bonding at interfaces could thus be the kinetic limiter for the action of water. From this discussion, we obtain another guideline for good adhesion: *if one expects to have an adhesive bond in adverse environmental conditions, provide for interfacial covalent bonding.*

### 6.8.1 Coupling Agents

An industry has been built developing, manufacturing and selling agents which “couple” an organic and an inorganic phase. *Coupling agents* are materials with two chemical functions, one that is reactive with the inorganic phase and the other that is reactive with the organic phase. One class of coupling agents, based upon silanes, has found the most utility [27]. The reaction scheme thought to occur when these materials are used is shown in Fig. 6.14.

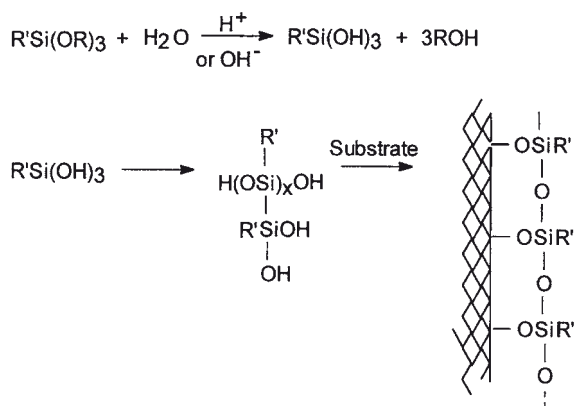


FIGURE 6.14 Diagram showing the proposed action of silanes on inorganic surfaces

Silanes, in the presence of water, hydrolyze to silanols that spontaneously condense to yield silanol oligomers. At low molecular weights, the oligomers are usually soluble in water. If a surface containing a hydroxyl group is nearby, the silanols also condense with the surface, creating the situation shown at the end of Fig. 6.14. There is also an  $R'$  group on each silane which is retained throughout the oligomerization and condensation with the substrate. The  $R'$  group is chosen to be reactive with the matrix material. For example, if the matrix is an epoxy, a propyl amino group could be chosen as  $R'$  or if the matrix is an acrylic, then a propyl acryloyl group could be  $R'$ .

The early image of silanes on a substrate is a monolayer. However, Koenig and Ishida [28] were able to show that to be effective the amount of silane deposited on a surface needed to be substantially in excess of that shown in Fig. 6.14. In fact, they showed that an effective amount was more than hundreds of Angstrom units thick. This data has led to the hypothesis that silane coupling agents form a layer into which the matrix can diffuse and react, creating a diffuse interphasal layer between the inorganic and the organic phases. This physical action occurs in addition to the chemical reaction between the matrix and the  $R'$  groups.

The first application of silanes in industry was in fiberglass. Fiberglass is a material in which a matrix resin, e.g., a styrenated polyester, is filled with glass fiber as a reinforcement. When such materials are fabricated, fiberglass has an increased stiffness over that of the matrix resin. However, with exposure to moisture, the stiffness decreased measurably. The hypothesis was that moisture invaded the composite material and disbonded the matrix resin from the fibers, as was predicted from the equations and analysis described above. If a silane coupling agent was applied to the fibers before they were added to the matrix resin, the fiberglass retained its original modulus longer when the material was exposed to moisture. The presence of covalent bonds in an interphase kinetically inhibited the effect of water on a material whose performance depended on good adhesion between an organic and an inorganic phase.

Although silane coupling agents form the largest and most successful group of such materials, there are other coupling agents. Chrome complexes, with structures shown in Fig. 6.15, are formed by the reaction of chromium oxide with methacrylic acid. The chromium oxide portion of the coupling agent reacts with a substrate while the methacrylic portion reacts with a free-radically-curing overlayer.

Another major class of coupling agent is the titanates [29]. Once again, this material is a combination of an organic and an inorganic material. An example of a titanate ester is also shown in Fig. 6.15. As in the case of the silanes, the material is thought to react with hydroxyls on the surface of inorganics to liberate alcohols. Titanates have been used a great deal in the modification of the viscosity of slurries of organics in inorganics by "compatibilizing" the two materials.

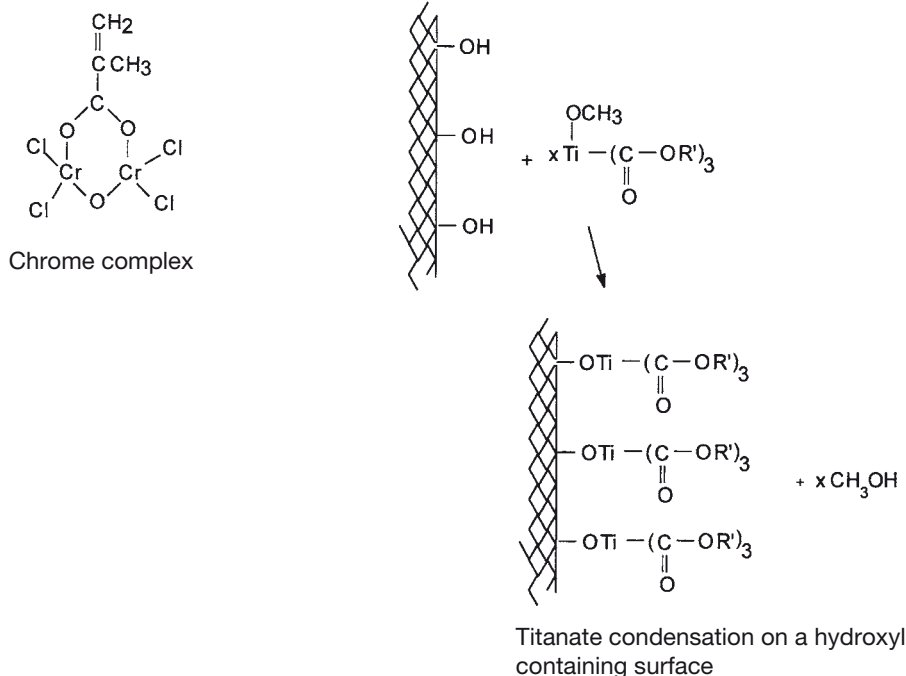


**FIGURE 6.15** The chemistry of a methacrylate/chrome complex.  
Also shown is the action of titanates on an inorganic surface

The R' groups shown in Fig. 6.15 can be any one of a number of chemical functions reactive with a number of different matrices.

## ■ 6.9 The Relationship of Fundamental Forces of Adhesion and Practical Adhesion

Statements have been made as to the lack of a direct relationship between the forces of adhesion and the practical strength of an adhesive bond. In this section, we describe several experiments that have laid the basis for a way to connect interfacial characteristics and the mechanical strength of an adhesive bond.

In the description of silane coupling agents, the effectiveness of the chemistry was described as an increase in the durability of the composite. The modulus of the composite was essentially the same with or without the presence of the silane, but the retention of modulus was improved when a silane was used in the interphase.

There are also descriptions of an increase in the dry bond strength as the result of the presence of a coupling agent. Such an experiment was described by Ahagon and Gent [30]. A glass slide was coated with mixtures of vinyl and ethyl silane, at essentially monolayer coverage. The vinyl silane was available for reaction with a free-radically-curing overlayer, but the ethyl was not. We expect that increasing the percentage of vinyl silane in comparison to ethyl silane provides an improvement in adhesion. An overlayer of polybutadiene was applied to the coated slide and free-radically crosslinked. The strength of the adhesive bond was measured by a  $180^\circ$  peel test, in which the polybutadiene was peeled from the slide at various temperatures and peel rates. The data were superimposed by means of shift factors to create a master curve for the peel tests on each treated surface. Recall the discussion in the previous chapter on master curves and the time-temperature superposition principle for polymers.

A schematic representation of Ahagon and Gent's results is presented in Fig. 6.16. The curve labeled  $W_1$  is for a sample covered entirely with ethyl silane while  $W_4$  is the curve for a surface covered entirely with vinyl silane.  $W_2$  and  $W_3$  are intermediate combinations of vinyl silane in ethyl silane. The symbol  $W$  has been chosen not only for the curves, but also for the asymptotic value of the work to break the adhesive bond. Note that  $W_4 > W_3 > W_2 > W_1$ . The results track well with the amount of vinyl silane in the coating.

Several things can be learned from this plot. First, a plot of peel strength (work to break) as a function of peel rate approaches an asymptotic value, which is tempting to ascribe to the intrinsic work of adhesion. Second, the plots of work to break

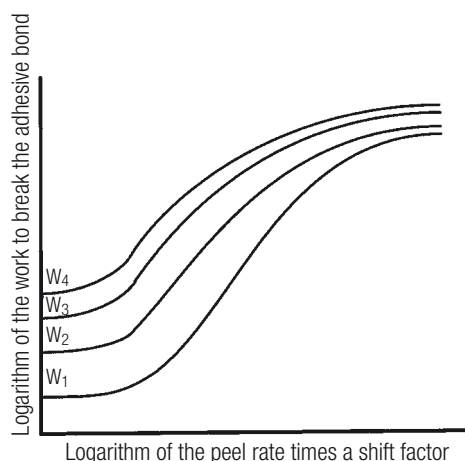


**FIGURE 6.16** Schematic of the data of Ahagon and Gent. The log of the work to break an adhesive bond is plotted versus the reduced rate of peel. The various curves result from a variation in the surface coverage by vinyl silane. Note that the curves seem to tend to an asymptotic adhesion energy that we may call  $\mathcal{G}_0$

versus reduced peel rate seem to have nominally the same shape, but are shifted in the vertical direction with respect to one another. Note that the plot is log-log. For this situation, we write:

$$\log W_B = \log W_i + \log \zeta \quad (6.16)$$

or, taking the antilog:

$$W_B = W_i \zeta \quad (6.17)$$

This equation represents an important relationship between the strength of an adhesive bond and the *multiplication* of some factor describing the intrinsic adhesion by another factor,  $\zeta$ . In Fig. 6.16, the abscissa was described as a shift factor times a rate of peel. This bears a resemblance to the discussion in Chapter 5 and in particular Fig. 5.11, where the log of modulus was plotted versus the frequency times a shift factor. It is reasonable to define  $\zeta$  as a function describing the energy dissipating properties (such as viscoelasticity) of the materials involved in the adhesive bond. The final feature to note here is the value of the work to break the adhesive bond. The intrinsic levels of adhesion were found to be on the order of  $200 \text{ mJ/m}^2$  to about  $2 \text{ J/m}^2$ , which is within an order of magnitude of the intrinsic levels of adhesion that are predicted from the Young-Dupré equation. The above experimental results show a relationship between interfacial bonding, the energy dissipating properties of an adhesive, and the mechanical strength of an adhesive bond.

The polymer molecules in an adhesive can be thought of as a mass of spaghetti noodles placed between two adherends. The noodles are partially cooked so that they stick somewhat to one another and they are intertwined. The spaghetti analogy describes many of the aspects of polymer physics that are important to adhesion science. However, one cannot carry the analogy too far. Spaghetti noodles are static but polymer molecules are constantly in motion. Another analogy that could be more accurate but perhaps less appealing to imagine is that the mass of polymer is a massive collection of wriggling boa constrictors in an oven. They are constantly in motion but constantly intertwined.

First, suppose that the noodles are not attached to the adherend. Pulling on the bond removes the mass of the noodles from the adherend. Therefore, if  $W_A = 0$  then  $W_B = 0$ . Now suppose that the noodles (or snakes) are attached to the two adherends, but the attachment can be much smaller or equal to the attachment of the noodles to one another. If we pull on the adherends, the noodles do not detach from the adherend. Rather, the mechanical energy is placed into stretching the noodles. If the noodles are sufficiently intertwined, the mechanical energy continues to go into stretching and unraveling the noodles. The adhesion of the noodles to the adherend is not tested until at least some of the noodles are fully taut. At that point, however,

the adhesive has absorbed much mechanical energy. Thus, the adhesion that the noodles display to the adherend *activates* the ability of the adhesive to absorb the mechanical energy. The amount of mechanical energy that can be stored depends upon the critical strain energy release rate of the materials in question. Since the adhesion displayed by the adhesive can be considered to be the intermediary that activates energy absorption by the adhesive, it is not difficult to believe that the effect of increasing adhesion should be multiplicative of the energy able to be absorbed by the adhesive.

Let us formulate a more general equation describing the linkage between the practical work of adhesion and the fundamental adhesion. From the discussion of the Griffith criterion for fracture, we know that for a completely brittle material, the energy necessary to break an adhesive bond is  $W_B = W_A$  which is  $2\gamma$  or  $\gamma_1 + \gamma_2 - \gamma_{12}$ , depending upon whether the failure is in cohesion in the adhesive or the failure is in adhesion. This energy can be considered to be the minimum amount of practical adhesion that one can obtain from an adhesive bond. If other modes of dissipating energy are available, then this minimum value increases. The work of Ahagon and Gent (and others) implies that the amount of increase is proportional to  $W_A \zeta$ , in this way:

$$W_B = W_A + f(W_A) \zeta \quad (6.18)$$

This equation says that an unknown function of the work of adhesion  $f(W_A)$  multiplies the function  $\zeta$  which describes how mechanical energy is dissipated in the adhesive and the adherend. This expression fits our reasoning as to the relationship between fundamental adhesion and practical adhesion.

An important question to ask here is if there are any other experimental results lending credence to this equation. In one set of experiments carried out by Gent and Schultz [31], the peel strength of an adhesive/adherend combination was measured under various liquids. Instead of creating surfaces with a single interfacial energy with air, the interfacial energy in this experiment was dependent upon the liquid in which the peeling experiment was done. The work to break was measured as a function of the rate of peel and the rates were shifted in much the same way as described by Ahagon and Gent. A family of curves of approximately the same shape was obtained. However, they were shifted with respect to one another. The shift was dependent upon the interfacial tension between the surfaces and the liquid used for the experiment.

In other work, Andrews and Kinloch [32] made simple fracture specimens in which an adhesive bond was simulated. They measured the crack propagation rate of the flaw as a function of the work of adhesion between the substrate and the adhesive. The crack propagation rate was reduced by a shift factor and the logarithm of the force to propagate the crack was plotted versus the log of the reduced crack propaga-

tion rate. A roughly parallel family of curves was obtained. The curves were shifted from one another by a factor approximately related to the work of adhesion. The work of Gent and Schultz and that of Andrews and Kinloch both lend credence to Eq. (6.18).

Equation (6.18) would also say that if  $\log W_B$  were measured at slower and slower reduced rates (that is, very low rates or high temperatures or both) one eventually comes to the point where  $W_A$  was measured. At very low reduced rates,  $\zeta$  is small. Measurements in the literature indicate that the extrapolated values of  $\log W_B$  to very low reduced rates do not actually attain  $W_A$  from the Dupré equation. Rather, the asymptotic value seems to approach several ranges, depending upon the types of bonds present at the interface. For example, in the work of Brown, et. al. [8], it was found that the asymptotic value for polystyrene in contact with polyisoprene is about  $120 \text{ mJ/m}^2$ , but  $W_A(\text{Dupré}) = 65 \text{ mJ/m}^2$ . With a block copolymer present at this interface, the asymptotic level increases to  $400 \text{ mJ/m}^2$  depending upon both the aerial chain density as well as the length of the block copolymer segments. In other experiments reported by Gent, polybutadiene was partially vulcanized, attached to itself and vulcanization completed. These bonds were then peeled apart as a function of rate and temperature and a log peel force-log reduced rate plot was generated. Extrapolation to low reduced rates provided a value of the intrinsic adhesion energy of  $1 \text{ J/m}^2$ . This value is close to the value we might have expected for an interface composed of carbon-carbon bonds as described in Section 6.8. We conclude from this discussion that the term described as  $W_A$  in Eq. (6.2) should be replaced with another term called  $\mathcal{G}_0$  and which we might call the *threshold adhesion energy* for a particular bonding situation. Thus,  $\mathcal{G}_0$  is about  $50 \text{ mJ/m}^2$  when the forces of adhesion are due entirely to van der Waals type of interactions and about  $400 \text{ mJ/m}^2$  when chain pull-out is a dominant way the interface is held together. However,  $\mathcal{G}_0$  is about one  $\text{J/m}^2$ , or greater, when two surfaces are primarily joined by covalent bonding. We write the equation that relates the fundamental forces of adhesion to practical adhesion as:

$$W_B = \mathcal{G}_0 + f(\mathcal{G}_0)\zeta \quad (6.19)$$

All of these parameters have been defined earlier. It is the goal of adhesion scientists to determine the functional form of  $f(\mathcal{G}_0)$ ,  $\zeta$  and to predict  $\mathcal{G}_0$  from first principles. Maugis [33] has examined the rate dependence of an interfacial crack propagating between a polyurethane sphere and a glass surface using a JKR style measurement (as described in Section 4.5.2.2.) In these measurements, he found that the work to break the adhesive bond formed between these two surfaces was dependent upon the reduced rate of crack propagation to the 0.5 power. Other experiments by Shull, et. al. [34] have provided similar results. These measurements provide our first glimpses at the functional form of  $f(\mathcal{G}_0)$ .

## ■ 6.10 The Weak Boundary Layer

The final rationalization of adhesion phenomena is the weak boundary layer. This view of adhesion was initially proposed by J. J. Bikerman [35], who authored one of the first books about adhesion phenomena. Bikerman's theory, simply stated, is that if a proper adhesive bond is made, the bond fails in either the adherend or the adhesive, whichever is cohesively weaker. Bonds fail at less than their expected strength because materials of low cohesive strength exist at the interface. These low cohesive strength materials form the "weak boundary layer". There is no doubt that if an adhesive bond has low cohesive strength materials at the interface, then the adhesive bond is weaker than expected. In fact, it has been the fallback position of adhesion scientists that any adhesive-bonding situation that cannot be explained by other rationalizations is explained by the presence of a weak boundary layer.

However, it is not always true that in a proper adhesive bond, failure always occurs in either the adhesive or the adherend. For example, in work by Mangipudi, Tirrell and Pocius [5], polyethylene (PE) and polyethylene terephthalate (PET) were co-extruded to generate a multi-layered structure. The materials were mated in the melt and were thus in intimate contact. The surface forces apparatus described in Section 4.5.2.2 was used to measure the interfacial energy between these two materials as  $17 \text{ mJ/m}^2$ . This is a high number. The Dupré equation predicts a low work of adhesion. This is observed in peel results. We examined the failure surface between the PE and the PET, using physical techniques, such as X-ray photoelectron spectroscopy (XPS) and Static Secondary Ion Mass Spectrometry (SSIMS), and we found that the failure between these materials was purely interfacial.

The above discussion notwithstanding, there are many adhesive failures due to a weak boundary layer. It is known that it is extremely difficult to bond to a metal surface from which mill oils have not been removed. It is extremely difficult to bond to a surface that is wet with water. Adhesive bonding to rusty steel is difficult because iron oxide is cohesively weak. Weak boundary layers, however, can also be used to advantage. For example, certain adhesive tape applications would not work without a "release liner", a material to which the adhesive tape lightly adheres and from which it can peel easily. These release liners are often chemically tailored weak boundary layers.

The discussion in this section leads to another criterion for good adhesive bonding: *in order to generate a proper adhesive bond, weak boundary layers need to be removed or modified so that they are cohesively strong*. Chapter 7 provides strategies for assuring this criterion is met.



## ■ 6.11 Summary

In this chapter, we discussed various rationalizations used to describe adhesive bonding phenomena. The rationalizations include the electrostatic theory, the diffusion theory, the mechanical interlocking theory, the wettability theory, covalent bonding at interfaces, and the weak boundary layer theory. Each of these rationalizations has been used to greater or lesser extent in describing various adhesive-bonding phenomena. Of these rationalizations, the wettability/adsorption theory is the most widely used and appreciated. A combination of the salient features of these rationalizations leads to a set of criteria for obtaining a good adhesive bond. These criteria are:

- Choose an adhesive which is soluble in the adherend (diffusion theory), OR
- Choose an adhesive that spontaneously wets the surface (wettability theory)
- Make sure the surface has a microscopic morphology (mechanical interlocking)
- Eliminate all weak boundary layers (weak boundary layer theory)
- Choose an adhesive which has the right viscosity/cure relationship so that pores are completely wetted (wettability + mechanical interlocking)
- If the adhesive bond is to be exposed to adverse environments, provide for covalent bonding in the interphase.

In this chapter, we also related the properties of interphases to the viscoelastic properties of polymers and finally, to the strength of adhesive bonds. Phenomenologically, this relationship is a multiplication of a threshold energy of adhesion with a function that describes the way in which the adhesive bond can dissipate mechanical energy.

## ■ Bibliography

- Wu, S., *Polymer Interfaces and Adhesion* (1982) Marcel Dekker, New York  
Patrick, R. L. (Ed.) *Treatise on Adhesion and Adhesives*, vol. 1 (1968) Marcel Dekker, New York  
Kinloch, A. J., *J. Mater. Sci.* (1982) 17, p. 617  
Kinloch, A. J., *J. Mater. Sci.* (1980) 15, p. 2141

## ■ References

- [1a] Derjaguin, B. V., *Research* (1955) 8, p. 70
- [1b] Derjaguin, B. V., Krotova, N. A., Karassev, V. V., Kirillova, Y. M., Aleinikova, I. N., in *Proc., 2nd. Internat'l Congress on Surface Activity - III* (1957) Butterworths, London
- [1c] Derjaguin, B. V., Smilga, V. P., *Adhesion, Fundamentals and Practice* (1969) McLaren and Son, London
- [2] Hunstberger, J. R., in *Treatise on Adhesion and Adhesives*, vol. 1. Patrick, R. L. (Ed.) (1967) Marcel Dekker, New York
- [3] Dickinson, J. T., Jensen, L. C., Lee, S., Scudiero, L., Langford, S. C., *J. Adhesion Sci. Technol.* (1994) 8, p. 1285
- [4a] Horn, R. G., Smith, D. T., *Science* (1992) 256, p. 362
- [4b] Smith, D. T., *Electrostat.* (1991) 26, p. 291
- [4c] Horn, R. G., Smith, D. T., Grabbe, A., *Nature* (1993) 366, p. 442
- [4d] Smith, D. T., Horn, R. G., in *Proc. Mater. Res. Soc., Symp.*, Vol. 170 (1989) Materials Res. Soc., Pittsburgh
- [5] Mangipudi, V. S., Pocius, A. V., Tirrell, M., *J. Adhes. Sci. Tech.* (1994) 8, p. 1231
- [6] Hildebrand, J., Scott, R., *The Solubility of Non-Electrolytes*, 3rd. Ed. (1950). Reinhold, New York
- [7] Iyengar, Y., Erickson, D. E., *J. Appl. Polymer Sci.* (1967) 11, p. 2311
- [8a] Brown, H. R., *Macromolecules* (1989) 22, p. 2859
- [8b] Creton, C., Karmer, E. J., Hui, C-Y., Brown, H. R., *Macromolecules* (1992) 25, p. 3075
- [8c] Brown, H. R., Char, K., Deline, V. R., Green, P. F., *Macromolecules* (1993) 26, p. 4155
- [8d] Char, K., Brown, H. R., Deline, V. R., *Macromolecules* (1993) 26, p. 4164
- [8e] Brown, H. R., *Macromolecules* (1993) 26, p. 1666
- [8f] Reichert, W. F., Brown, H. R., *Polymer* (1993) 34, p. 2289
- [8g] Brown, H. R., *Science* (1994) 263, p. 1411
- [8h] Creton, C., Brown, H. R., Shull, K. R., *Macromolecules* (1994) 27, p. 3174
- [9] DeGennes, P. G., *J. Chem. Phys.* (1974) 55, p. 572
- [10a] Wool, R. P., *Polymer Interfaces, Structure and Strength* (1995) Hanser Publishers, Munich, Chapters 2 and 3.
- [10b] Russell, T. P., Deline, V. R., Dozier, W. D., Felcher, G. P., Agrawal, G., Wool, R. P., Mays, J. W., *Nature (London)* (1993) 365 (6443), pp. 235-7
- [11] Arrowsmith, D. J., *Trans. Inst. Met. Finish.* (1970) 48, p. 88
- [12] Packham, D. E., in *Adhesion Aspects of Polymeric Coatings*. Mittal, K. L. (Ed.) (1983) Plenum Press, New York
- [13] Schonhorn, H., Frisch, H. L., Kwei, T. K., *J. Appl. Phys.* (1966) 37, p. 4967
- [14] Newman, S., *J. Colloid. Interface Sci.* (1968) 26, p. 209
- [15] Ingliss, C. E., *Proc. Inst. Nav. Archit.* (1913) 55, p. 219
- [16] Levine, M., Ilkka, G., Weiss, P., *Polymer Letters* (1964) 2, p. 915
- [17] Barbarisi, M. J., *Nature* (1967) 215, p. 383
- [18] Mittal, K. L., in *Adhesion Science and Technology*. Lee, L H. (Ed.) (1975) Plenum Press, New York
- [19] Bolger, J. C., Michaels, A. S., in *Interface Conversion for Polymeric Coatings*. Weiss, P., Cheever, G. D. (Eds.) (1968) American Elsevier, New York
- [20] Fowkes, F. M., *Organic Coatings and Plastics Chemistry*, vol. 40 (1979) American Chemical Society, Washington, DC, pp. 13-18

- [21] Drago, R. S., Vogel, G. C., Needham, T. E., *J. Am. Chem. Soc.* (1971) 93, p. 6014
- [22] Fowkes, F. M., in *Microscopic Aspects of Adhesion and Lubrication*. Georges, J. M. (Ed.) (1982) Elsevier, Amsterdam, p. 119
- [23] Gutmann, V., *The Donor-Acceptor Approach to Molecular Interactions* (1978) Plenum Press, New York
- [24a] Schreiber, H. P., Li, Y., in *Molecular Characterization of Composite Interfaces* (1985) Plenum Press, New York
- [24b] Fafard, M., El-Kindi, M., Schreiber, H. P., Dipaola-Baranyi, G., Hor, A. M., *J. Adhesion Sci. and Tech.* (1994) 8, p. 1383
- [25] Fowkes, F. M., *Ind. Eng. Chem.* (1964) 56, p. 40
- [26] Kinloch, A. J., Dukes, W. A., Gledhill, R. A., in *Adhesion Science and Technology*. Lee, L. H. (Ed.) (1975) Plenum Press, New York
- [27] Plueddemann, E. P., *Silane Coupling Agents* (1982) Plenum Press, New York
- [28] Ishida, H., Koenig, J. L., *Polym. Eng. Sci.* (1978) 18, p. 128
- [29] Technical Literature of Kenrich Petrochemical Company, Bayonne, NJ.
- [30] Ahagon, A., Gent, A. N., *J. Polym. Sci., Polym. Phys. Ed.* (1975) 13, p. 1285
- [31] Gent, A. N., Schultz, J., *J. Adhesion* (1972) 3, p. 281
- [32a] Andrews, E. H., Kinloch, A. J., *Proc. Roy. Soc. Lond. A.* (1973) 332, p. 385
- [32b] Andrews, E. H., Kinloch, A. J., *Proc. Roy. Soc. Lond. A.* (1973) 332, p. 401
- [32c] Gent, A. N., Kinloch, A. J., *J. Polym. Sci., Pt. A-2* (1971) 9, p. 659
- [33] Maugis, D., in *Adhesive Bonding*, Lee, L-H. (1991) Plenum Press, New York, p. 303
- [34] Shull, K. R., Ahn, D., Chen, W-L., Flanigan, C. M., Crosby, A. J., *Macromol. Chem. Phys.* (1998) 199, p. 489
- [35] Birkman, J. J., *The Science of Adhesive Joints* (1961) Academic Press, New York

## ■ Problems and Review Questions



1. Examine Figure 6.10, suppose that the drops all have the same volume. What does the figure tell us about the interfacial area formed between the drop and each surface?
2. Suppose that the only interactions occurring across an interface are acid-base interactions. The interacting species each occupy an area of 10 square Angstroms. Also suppose that the interaction energy per mole of bonds is 10 kcal. What is energy necessary to separate the interface in Joules/m<sup>2</sup>?
3. Using the data in the following data, determine whether or not an epoxy adhesive bond to iron is stable in the presence of water.  
  
Using the following data show that an epoxy-steel adhesive bond is thermodynamically unstable under water.

$$\begin{aligned}\gamma^D(\text{iron oxide}) &= 107 \text{ mJ/m}^2 \\ \gamma^P(\text{iron oxide}) &= 1250 \text{ mJ/m}^2 \\ \gamma^D(\text{epoxy}) &= 41.2 \text{ mJ/m}^2 \\ \gamma^P(\text{epoxy}) &= 5 \text{ mJ/m}^2 \\ \gamma^D(\text{water}) &= 22 \text{ mJ/m}^2 \\ \gamma^P(\text{water}) &= 50 \text{ mJ/m}^2\end{aligned}$$

4. In the following table, pick which polymer/adhesive pair is most likely to adhere. Why?

Polymer	Adhesive
Teflon	Epoxy
Polyethylene	Silicone
Polypropylene	Polyethylene

5. A typical epoxy adhesive has a surface energy of about  $44 \text{ mJ/m}^2$ . Would an epoxy adhesive be expected to wet and adhere to the surface examined in Problem 3 in Chapter 4.
6. What type of hole in a material will lead to a minimal stress concentration? How might one apply this knowledge in order to minimize easily the propagation of an existing crack in a structure?
7. Examine the data in the following Table (which is a modified Table 4.3)

The Relationship between Surface Chemical Composition and the Critical Wetting Tension of a Number of Solids

Surface	Critical wetting tension (dynes/cm or Newtons/m)	Solubility parameter ( $\text{cal/cm}^3$ ) <sup>1/2</sup>
Polytetrafluoroethylene	18	6.2
Polydimethyl siloxane (silicone)	21	7.5
Polyethylene	31	7.9
Polystyrene	33	9.1
Polyvinyl chloride	39	9.6
Cured epoxy resin	43	
Polyethylene terephthalate (PET)	43	10.7
Nylon-6,6	46	13.6

From the definition of the solubility parameter and the fact that the critical wetting tension is related to the surface energy of the surfaces listed above, explain why there seems to be a correlation between  $\delta$  and  $\gamma_C$ .